

Long-term aquatic eddy covariance measurements of seagrass metabolism and ecosystem response to warming oceans.

Amélie Cécile Berger
Charlottesville, VA

B.S. Environmental Geosciences, Texas A&M University, 2015

A Dissertation presented to the Graduate Faculty
of the University of Virginia in Candidacy for the Degree of
Doctor of Philosophy

Department of Environmental Sciences

University of Virginia
April 2021

Committee:

Peter Berg (advisor)

Karen McGlathery

Matthew A. Reidenbach

Michael L. Pace

Jonathan L. Goodall

Table of Contents

ABSTRACT	i
ACKNOWLEDGEMENTS	iii
INTRODUCTION.....	1
Seagrass ecosystems.....	1
Aquatic eddy covariance	2
Site description	3
Dissertation outline	4
Literature cited	4
CHAPTER 1: LONG-TERM TRENDS AND RESILIENCE OF SEAGRASS METABOLISM: A DECADAL AQUATIC EDDY COVARIANCE STUDY	8
Abstract	8
Introduction	9
Materials and methods	11
Study site.....	11
Data collection.....	12
Data Analysis	14
Statistical analyses.....	17
Results	18
Aquatic eddy covariance data	18
Long-term record of ecosystem metabolism.....	19
Die-off event	21
Annual oxygen balance in South Bay	23
Discussion	24
Annual net ecosystem metabolism.....	25
Seasonal variations in seagrass ecosystem metabolism	27
Carbon sink capacity	28
Seagrass disturbance and resilience	30
Literature cited	31

CHAPTER 2: TEMPERATURE THRESHOLD FOR SEAGRASS (*ZOSTERA MARINA*) METABOLISM DERIVED FROM IN SITU AQUATIC EDDY COVARIANCE MEASUREMENTS.....37

Abstract37

Introduction37

Methods39

 Study site39

 Seagrass metabolism measurements by aquatic eddy covariance40

 Identifying the temperature stress threshold41

Results43

 Effects of thermal stress on seagrass metabolism43

Discussion44

 Temperature threshold.....45

 Effects of thermal stress on seagrass metabolism46

 Future projections for *Z. marina*47

Literature cited47

CHAPTER 3: OCEAN WARMING EFFECTS ON SEAGRASS (*ZOSTERA MARINA*) AND ITS RESILIENCE TO MARINE HEATWAVES52

Abstract52

Introduction53

Methods55

 Study site55

 Water temperature measurements56

 Seagrass metrics57

 Seagrass resilience and thermal stress metric.....57

 Sulfide presence in the sediment and seagrass tissue.....60

Results61

 Spatiotemporal variations in temperature stress and seagrass growth61

 Thermal stress and die-off events.....64

Sediment temperatures	65
Sulfide	66
Discussion	66
Thermal stress metrics.....	67
Thermal stress effects on seagrass growth	68
The role of sulfide toxicity	69
High temperature-induced die-off events.....	69
Literature cited	70
CHAPTER 4: SEAGRASS MEADOW (<i>ZOSTERA MARINA</i>) LIGHT-USE EFFICIENCY MEASURED BY AQUATIC EDDY COVARIANCE.....	75
Abstract	75
Introduction	76
Methods.....	77
Study Site	77
Data collection and light-use efficiency calculations.....	77
Results	79
Hourly light-use efficiency.....	79
Daily light-use efficiency	79
Seasonal variations in light-use efficiency	80
Discussion	80
Patterns in daily light-use efficiency	82
Patterns in hourly light-use efficiency	83
Seasonal trends in light-use efficiency	83
Conclusion.....	83
Literature Cited	84
CONCLUSIONS.....	87
FUNDING ACKNOWLEDGMENT	91

ABSTRACT

Seagrass meadows are valued globally for their ecosystem services, including their role as a ‘blue carbon’ sink due to high rates of primary production and carbon burial in the sediment. However, seagrasses are threatened by climate change and other natural and anthropogenic stressors, and their ecosystem services risk being lost as well. In some cases, seagrass declines have led to the release of previously stored carbon in the form of greenhouse gases, creating a positive feedback on the climate system. To ensure the success of seagrass conservation and restoration and avoid adverse effects on the climate system, it is essential to better understand the role of seagrass meadows in the global carbon cycle, what drives their metabolism, and their resilience to climate change (e.g. globally increasing temperatures, extreme heating events, sea level rise). These questions have traditionally been addressed via lab, mesocosm, or in situ experiments that do not capture the full range of environmental fluctuations and are difficult to translate to ecosystem-scale dynamics. In this dissertation, I used the relatively novel non-invasive aquatic eddy covariance (AEC) technique in a restored seagrass (*Zostera marina*) meadow at the Virginia Coast Reserve (VCR) to measure seagrass ecosystem metabolism under naturally varying environmental conditions. These measurements have been ongoing since 2007, and captured an eelgrass die-off event during summer 2015, followed by a slow recovery in the following years. This long-term, high-quality AEC dataset presented a unique opportunity to study the long-term trends and resilience of seagrass metabolism, as well as quantify the response of a seagrass ecosystem to extreme heat stress and evaluate its ability to adapt to future changes in water temperatures and light availability.

I found that seagrass metabolism was highly dynamic and variable, with as much variation within a single month as during an entire year, thus indicating rapid internal carbon cycling. Over the 11-year period, however, seagrass metabolism was generally balanced, despite shifts in trophic status during and after the die-off event, with the meadow becoming heterotrophic the summer of the die-off, and autotrophic during its recovery. Long-term water temperature records indicated a warmer growing season in 2015 compared to other years. Using a modeling approach on hourly AEC fluxes, I found that water temperatures above a threshold of 28.6°C negatively impact eelgrass metabolism, causing a 50% decrease in daytime oxygen fluxes when only exceeded by ~2°C. This was the first time this threshold was determined based on in situ data. Based on this threshold and in situ water temperature measurements from 2016–2019, I developed two metrics to quantify thermal stress in seagrass meadows, providing a framework for understanding thresholds for seagrass survival. These

metrics were the cumulative heat stress (as heating degree-hours, HDHs) and thermal stress relief (as cooling degree-hours, CDHs), both relative to the 28.6°C eelgrass thermal tolerance threshold. I compared these metrics to spatiotemporal patterns in summertime seagrass shoot density and length, and found that the healthiest parts of the meadow benefited from greater thermal stress relief (2–3x) from tidal cooling (inputs of cooler ocean water) during periods of heat stress, leading to ~65% higher shoot densities compared to the center of the meadow, which experienced higher heat stress (1.8x) with less relief. I also found that the eelgrass die-off event in 2015 was triggered by heat stress cumulating ~100–200°C-hours in June. This heat stress was later amplified by the effects of sulfide toxicity into seagrass tissues, as indicated by the sulfur isotope signatures of seagrass samples that indicated higher sulfide intrusion into seagrass tissue in 2015 compared to other years. Finally, I estimated the light-use efficiency (LUE) of the eelgrass meadow based on AEC data and in situ light measurements—providing the first ecosystem-scale and in-situ based LUE estimate for eelgrass. LUE was low compared to previous estimates, averaging 0.004–0.005 O₂ photon⁻¹ and potentially reflecting nutrient-limited primary production. Hourly pattern in LUE, however, suggested eelgrasses can regulate photosynthesis in response to changes in light availability, which might aid in their resilience to future environmental change.

Overall, this dissertation leveraged the benefits of long-term AEC measurements to offer new insights on assessing the trophic status of seagrass ecosystems and how it may change in response to disturbance events. We provided the first in situ, whole-ecosystem-based estimates for eelgrass LUE and thermal stress thresholds, further advancing scientific research on ecosystem responses to future climate change scenarios.

ACKNOWLEDGEMENTS

I would like to thank the UVA Department of Environmental Sciences for being a second home to me for 6 years. I have many people to thank for their support during this chapter of my life.

To my advisor, Peter Berg, and unofficial co-advisor, Karen McGlathery, thank you for your scientific wisdom, guidance, and all the opportunities you've given me. I would also like to thank the rest of my committee: Mike Pace, Matt Reidenbach, and Jon Goodall, for being supportive and providing valuable feedback on my work. I have gotten so much help and support from other faculty and staff at UVA, including (but not limited to) Meg Miller, Pat Wiberg, and John Porter. Thank you also to my lab and shoremates for creating such a nice, collaborative, and supportive community: Martin Volaric, Lillian Aoki, Matthew Oreska, Marie Lise Delgard, Alice Besterman, Sara Hogan, Kayleigh Granville, Ieva Juska, Melissa Hey, Ross Palomaki, and Christina Fantasia. Thank you also to Amy Ferguson and Kinsey Tedford for being great friends and officemates.

I am eternally grateful for the staff at the Coastal Research Center: Donna Fauber, Cora Johnston Baird, David Lee, Jonah Morreale, Buck Doughty, and Richard Ayers for their support and help with my fieldwork, without which none of this would have been possible! Donna, thank you for being a great "field mom" and friend. Cora, thank you for all you career, life, and field guidance and your dedication to make the ABCRC a fun and supportive place to be. David, thank you for always having my back, for our low-tide chats, for being a cheerful presence, and for always working with me to make plans happen. Jonah, thank you for all the boat trips and for your undying dedication to finding that one pole we ran over... Buck, I will miss your joyous spirit, amazing cooking, and creative problem-solving. And Richard, thank you for your patience in teaching me how to drive a boat. My parents know how trying of a job that is!

To Berto and Madeline Sales, Vincent Zorn, and Miles Pearce, your amazing personalities, smiles, and music filled my soul with joy and light so many times over the past 6 years. You are one of the parts I'll miss most about Charlottesville.

To my family, thank you for being there for me to lean on more than once over the past 6 years, and thank you for the occasional much-needed boosts!

And finally, to my best friend and roommate, Angelique. Words cannot describe how important you have been to my life in the past few years. You have been such a source of light, comfort, joy, and support, I don't know how anyone could ever go through grad school without someone like you in their life.

INTRODUCTION

Seagrass ecosystems

Seagrasses are marine flowering plants that inhabit shallow coastal water worldwide. While they only cover 0.1–0.2% of the global ocean seafloor, they are highly valued for the ecosystem services they provide (Costanza et al. 1997). Seagrass meadows offer food and habitat to many aquatic organisms important to fisheries and adjacent ecosystems (e.g. Nagelkerken et al. 2000; Beck et al. 2001). They also act as coastal filters by improving water quality and clarity (e.g. McGlathery et al. 2007; Hansen and Reidenbach 2012; Lamb et al. 2017; Aoki et al. 2020). In the past decade, seagrass meadows have been increasingly recognized for their potential as a global ‘blue carbon’ sink, due to high rates of primary production (carbon sequestration) (Duarte et al. 2010) and carbon burial in the sediment (carbon storage) (Fourqurean et al. 2012; Oreska et al. 2017; Aoki et al. 2021). Some studies have even estimated that, when accounting for areal extent, seagrass meadows retain comparable amounts of carbon to forests each year (e.g. Fourqurean et al. 2012).

Unfortunately, seagrass meadows have been declining globally over the past few decades due to climate change, increased coastal development, eutrophication, and other anthropogenic stressors (Orth et al. 2006a; Waycott et al. 2009). These declines result in the loss of seagrass ecosystem services, including their carbon retention capacity (e.g. Marbá et al. 2015; Arias-Ortiz et al. 2018). In some cases, seagrass die-off events have triggered substantial CO₂ emissions through the remineralization of previously buried organic matter (Pendleton et al. 2012; Arias-Ortiz et al. 2018). To better anticipate changes in seagrass ecosystems under future climate change scenarios and avoid adverse feedbacks on the climate system, it is critical to enhance our understanding of the role of seagrass meadows in the global carbon cycle and their response to climate stressors such as warming oceans, extreme heating events (e.g. marine heatwaves), and decreases in light availability (e.g. due to increased storms and sea-level rise). This research is particularly urgent as marine heatwaves are becoming more frequent and are already causing seagrass mortality events worldwide (e.g. Arias-Ortiz et al. 2018; Oliver et al. 2018; Holbrook et al. 2020).

The goal of this dissertation was to answer some of these questions by looking at seagrass ecosystem metabolism, which is a useful measure of ecosystem function and an indicator for

carbon flows in seagrass meadows (Duarte and Prairie 2005). Furthermore, changes in seagrass metabolism can be an indicator of physiological stress due to high temperatures or inadequate light conditions (Staehr and Borum 2011; Ewers 2013). However, most studies have quantified seagrass metabolism using techniques that are difficult to scale up to ecosystem-level processes, and often do not truly replicate in situ conditions. These techniques (benthic chambers, open water oxygen balances, and lab incubations) either scale-up measurements that are made over short time periods (minutes to hours), small spatial scales (from leaf segments to benthic areas $<0.25 \text{ m}^2$), and under altered or controlled light, temperature, and flow conditions (e.g. Martin et al. 2005; Champenois and Borges 2012; Pedersen et al. 2013; Olivé et al. 2016). The aquatic eddy covariance technique (AEC) has recently emerged as a superior way to measure metabolism in benthic environments as it does not alter the natural environment (Berg et al. 2003; Lorrain et al. 2010; Rheuban and Berg 2013). In this dissertation, I used the AEC technique in a restored eelgrass (*Zostera marina*) meadow at the Virginia Coast Reserve (VCR) to quantify eelgrass ecosystem metabolism under naturally varying environmental conditions and investigate its response to high-temperature events and changes in light availability.

Aquatic eddy covariance

The AEC technique is a relatively novel approach to measuring in situ ecosystem-level carbon metabolism using oxygen fluxes as a proxy (Berg et al. 2003). This approach overcomes many of the challenges and shortcomings of other techniques as it does not alter in situ conditions (e.g. Lorrain et al. 2010; Berg et al. 2007) and generates benthic oxygen fluxes at a high temporal resolution (e.g. 15 min or 1 h over several days) and over a large benthic area (10–100 m^2), therefore integrating over landscape heterogeneity (Berg et al. 2007; Rheuban and Berg 2013). The AEC technique has already been successfully used in various environments such as intertidal flats (Volaric et al. 2018), coral reefs (Long et al. 2013), mussel reefs (Attard et al. 2020), and seagrass meadows (Hume et al. 2011; Rheuban et al. 2014; Long et al. 2015; Berg et al. 2019) (Figure 1).



Fig. 1: Aquatic eddy covariance system deployed in South Bay.

The high sampling resolution and noninvasive nature of this technique allow us to simultaneously measure under naturally varying in situ conditions the net effect of seagrass oxygen uptake and production along with environmental parameters such as temperature, photosynthetically active radiation (PAR) and flow velocity. The AEC technique thus offers a unique opportunity to accurately quantify ecosystem-scale seagrass metabolism and its response to changes in environmental conditions, such as high temperatures or decreased light availability.

Site description

The VCR Long-Term Ecological Research (LTER) site is located on Virginia's eastern shore, on the Atlantic side of the Delmarva Peninsula. It is comprised of shallow coastal lagoons between the mainland and barrier islands and is the site of the most successful seagrass restoration project globally (Orth and McGlathery 2012) (Figure 2).

The coastal lagoons of the VCR were previously home to eelgrass (*Zostera marina*) meadows, supporting diverse marine wildlife and prosperous scallop fisheries (Orth and McGlathery 2012). In the 1930s, however, these meadows were decimated by an eelgrass “wasting disease” outbreak followed by a hurricane, and the coastal bays remained unvegetated for decades (Rasmussen 1977; Orth et al. 2006b, 2012). In the late 1990s–early 2000s, the discovery of a natural patch of eelgrass prompted a large-scale restoration effort, with the broadcast-seeding of hundreds of plots in four coastal bays (Orth et al. 2006b, Orth and McGlathery 2012), ultimately restoring over 25 km² of unvegetated seafloor to seagrass meadow

(<http://web.vims.edu/bio/sav>). The research for this dissertation took place in South Bay, which contains the largest of these restored meadows (~20 km² as of 2018, Orth et al. 2020) (Figure 2).

South Bay is connected to the Atlantic Ocean by two inlets north and south of the meadow, which results in a relatively brief water residence time (Safak et al. 2015). The barrier island to its east helps create a low-energy hydrodynamic environment where light conditions are favorable to eelgrass growth (Lawson et al. 2007). South Bay is shallow (mean water depth = 1.2 m) and experiences semi-diurnal tides with a tidal range of 1 m.

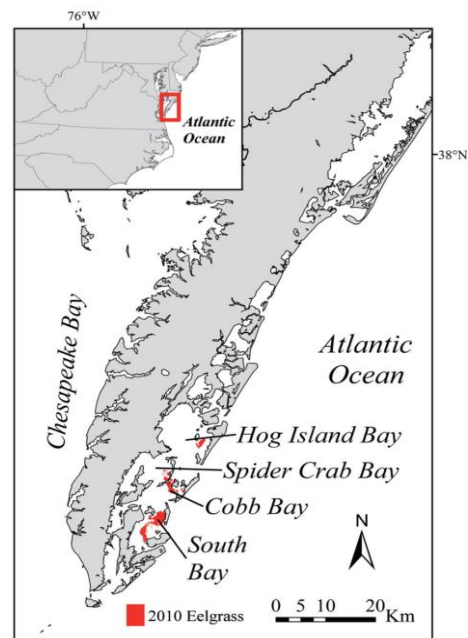


Fig. 2: Delmarva peninsula and sites of eelgrass restoration. From Orth and McGlathery, 2012.

In summer 2015, field observations at the VCR indicated a dramatic (> 90%) decline in seagrass shoot densities at my site. As others and my research indicate, this die-off event was likely caused by high water temperatures early in the season. High water temperatures have been shown to negatively affect eelgrass growth (e.g. Moore and Jarvis 2008; Moore et al. 2012; Raun and Borum 2013), and are very likely in the VCR region, which represents the southern geographical limit for *Z. marina* (Moore et al. 2006).

Dissertation outline

Building on the work of previous students and postdocs, I quantified long-term eelgrass ecosystem metabolism based on 11 years of AEC data, and assessed its variability on multiple timescales (diel to decadal) (Chapter 1). I further investigated the impacts of the 2015 eelgrass die-off event and subsequent recovery on ecosystem metabolism. I then analyzed summer water temperature records from 2012–2017 to assess whether the die-off event was indeed caused by a heating event.

In Chapter 2, I used a modeling approach on hourly AEC and in situ temperature data to determine, for the first time, the eelgrass high-temperature threshold based on ecosystem-scale, in situ measurements. I also quantified the impact of temperature threshold exceedance on eelgrass metabolism on an hourly scale.

In Chapter 3, I developed two metrics to quantify thermal stress in seagrass meadows based on the duration and intensity of heating and cooling. I related these metrics to spatiotemporal patterns of eelgrass density in South Bay and proposed a minimum amount of heat stress capable of triggering an eelgrass mortality event. I also used sulfur isotope analyses of seagrass leaves to assess the role of sulfide toxicity as an additional stressor contributing to the 2015 die-off.

In Chapter 4, I estimated eelgrass ecosystem light-use efficiency (LUE) based on AEC and in situ PAR measurements, to evaluate the performance of eelgrass meadows relative to light availability.

Chapter 1 was published in *Limnology and Oceanography* in January 2020. Chapters 2 and 3 will soon be submitted to *Limnology and Oceanography Letters* and *Global Change Biology*, respectively.

Literature cited

Aoki, L. R., K. J. McGlathery, and M. P. J. Oreska. 2020. Seagrass restoration reestablishes the coastal nitrogen filter through enhanced burial. *Limnol. Oceanogr.* 65: 1–12.

doi:10.1002/lno.11241

- Aoki, L. R., K. J. McGlathery, P. L. Wiberg, M. P. J. Oreska, A. C. Berger, P. Berg, and R. J. Orth. 2021. Seagrass Recovery Following Marine Heat Wave Influences Sediment Carbon Stocks. *Front. Mar. Sci.* 7. doi:10.3389/fmars.2020.576784
- Arias-Ortiz, A., O. Serrano, P. Masqué, and others. 2018. A marine heatwave drives massive losses from the world's largest seagrass carbon stocks. *Nat. Clim. Chang.* doi:10.1038/s41558-018-0096-y
- Attard, K. M., I. F. Rodil, P. Berg, A. O. M. Mogg, M. Westerbom, A. Norkko, and R. N. Glud. 2020. Metabolism of a subtidal rocky mussel reef in a high-temperate setting: Pathways of organic C flow. *Mar. Ecol. Prog. Ser.* **645**: 41–54. doi:10.3354/meps13372
- Beck, M. W., K. L. Heck, K. W. Able, and others. 2001. The Identification, Conservation, and Management of Estuarine and Marine Nurseries for Fish and Invertebrates. *Bioscience* **51**: 633. doi:10.1641/0006-3568(2001)051[0633:TICAMO]2.0.CO;2
- Berg, P., M. L. Delgard, P. Polsenaere, K. J. McGlathery, S. C. Doney, and A. C. Berger. 2019. Dynamics of benthic metabolism, O₂, and pCO₂ in a temperate seagrass meadow. *Limnol. Oceanogr.* Ino.11236. doi:10.1002/lno.11236
- Berg, P., H. Røy, F. Janssen, V. Meyer, B. B. Jørgensen, M. Huettel, and D. De Beer. 2003. Oxygen uptake by aquatic sediments measured with a novel non-invasive eddy-correlation technique. *Mar. Ecol. Prog. Ser.* **261**: 75–83. doi:10.3354/meps261075
- Berg, P., H. Røy, and P. L. Wiberg. 2007. Eddy correlation flux measurements: The sediment surface area that contributes to the flux. *Limnol. Oceanogr.* **52**: 1672–1684. doi:10.4319/lo.2007.52.4.1672
- Champenois, W., and A. V. Borges. 2012. Seasonal and interannual variations of community metabolism rates of a *Posidonia oceanica* seagrass meadow. *Limnol. Oceanogr.* **57**: 347–361. doi:10.4319/lo.2012.57.1.0347
- Costanza, R., R. Arge, R. De Groot, and others. 1997. The value of the world's ecosystem services and natural capital. *Nature* **387**: 253–260. doi:10.1038/387253a0
- Duarte, C. M., N. Marbá, E. Gacia, J. W. Fourqurean, J. Beggins, C. Barrón, and E. T. Apostolaki. 2010. Seagrass community metabolism: Assessing the carbon sink capacity of seagrass meadows. *Global Biogeochem. Cycles* **24**: 1–8. doi:10.1029/2010GB003793
- Duarte, C. M., and Y. T. Prairie. 2005. Prevalence of Heterotrophy and Atmospheric CO₂ Emissions from Aquatic Ecosystems. 862–870. doi:10.1007/s10021-005-0177-4
- Ewers, C. J. 2013. Assessing physiological thresholds for eelgrass (*Zostera marina* L.) survival in the face of climate change. *Biol. Sci.* doi:https://doi.org/10.15368/theses.2013.126
- Fourqurean, J. W., C. M. Duarte, H. A. Kennedy, and others. 2012. Seagrass ecosystems as a globally significant carbon stock. *Nat. Geosci.* **5**: 505–509. doi:10.1038/ngeo1477
- Hansen, J. C. R., and M. A. Reidenbach. 2012. Wave and tidally driven flows in eelgrass beds and their effect on sediment suspension. *Mar. Ecol. Prog. Ser.* **448**: 271–287. doi:10.3354/meps09225
- Holbrook, N. J., A. Sen Gupta, E. C. J. Oliver, A. J. Hobday, J. A. Benthuisen, H. A. Scannell, D. A. Smale, and T. Wernberg. 2020. Keeping pace with marine heatwaves. *Nat. Rev. Earth Environ.* in press. doi:10.1038/s43017-020-0068-4

- Hume, A. C., P. Berg, and K. J. McGlathery. 2011. Dissolved oxygen fluxes and ecosystem metabolism in an eelgrass (*Zostera marina*) meadow measured with the eddy correlation technique. *Limnol. Oceanogr.* **56**: 86–96. doi:10.4319/lo.2011.56.1.0086
- Lamb, J. B., J. A. J. M. van de Water, D. G. Bourne, and others. 2017. Seagrass ecosystems reduce exposure to bacterial pathogens of humans, fishes, and invertebrates. *Science* (80-.). **355**: 731–733. doi:10.1126/science.aal1956
- Lawson, S. E., P. L. Wiberg, K. J. McGlathery, and D. C. Fugate. 2007. Wind-driven sediment suspension controls light availability in a shallow coastal lagoon. *Estuaries and Coasts* **30**: 102–112. doi:10.1007/BF02782971
- Long, M. H., P. Berg, D. De Beer, and J. C. Zieman. 2013. In Situ Coral Reef Oxygen Metabolism : An Eddy Correlation Study. **8**. doi:10.1371/journal.pone.0058581
- Long, M. H., P. Berg, and J. L. Falter. 2015. Seagrass metabolism across a productivity gradient using the eddy covariance, Eulerian control volume, and biomass addition techniques. *J. Geophys. Res. Ocean.* **120**: 3624–3639. doi:10.1002/2014JC010352
- Lorrai, C., D. F. McGinnis, P. Berg, A. Brand, and A. Wüest. 2010. Application of oxygen eddy correlation in aquatic systems. *J. Atmos. Ocean. Technol.* **27**: 1533–1546. doi:10.1175/2010JTECHO723.1
- Marbá, N., A. Arias-Ortiz, P. Masqué, G. A. Kendrick, I. Mazarrasa, G. R. Bastyan, J. Garcia-Orellana, and C. M. Duarte. 2015. Impact of seagrass loss and subsequent revegetation on carbon sequestration and stocks. *J. Ecol.* **103**: 296–302. doi:10.1111/1365-2745.12370
- Martin, S., J. Clavier, J. M. Guarini, and others. 2005. Comparison of *Zostera marina* and maerl community metabolism. *Aquat. Bot.* **83**: 161–174. doi:10.1016/j.aquabot.2005.06.002
- McGlathery, K. J., K. Sundbäck, and I. C. Anderson. 2007. Eutrophication in shallow coastal bays and lagoons: The role of plants in the coastal filter. *Mar. Ecol. Prog. Ser.* **348**: 1–18. doi:10.3354/meps07132
- Moore, K. A., and J. C. Jarvis. 2008. Eelgrass Diebacks in the Lower Chesapeake Bay : Implications for Long-term Persistence. *J. Coast. Res.* **55**: 135–147. doi:10.2112/S155-014.acteristics
- Moore, K. A., E. C. Shields, D. B. Parrish, and R. J. Orth. 2012. Eelgrass survival in two contrasting systems: Role of turbidity and summer water temperatures. *Mar. Ecol. Prog. Ser.* **448**: 247–258. doi:10.3354/meps09578
- Moore, K. A., F. T. Short, R. J. Orth, and C. M. Duarte. 2006. *Zostera* : Biology , Ecology , and Management,.
- Nagelkerken, I., G. van der Velde, M. W. Gorissen, G. J. Meijer, T. Van't Hof, and C. den Hartog. 2000. Importance of Mangroves, Seagrass Beds and the Shallow Coral Reef as a Nursery for Important Coral Reef Fishes, Using a Visual Census Technique. *Estuar. Coast. Shelf Sci.* **51**: 31–44. doi:10.1006/ecss.2000.0617
- Olivé, I., J. Silva, M. M. Costa, and R. Santos. 2016. Estimating Seagrass Community Metabolism Using Benthic Chambers: The Effect of Incubation Time. *Estuaries and Coasts* **39**: 138–144. doi:10.1007/s12237-015-9973-z
- Oliver, E. C. J., M. G. Donat, M. T. Burrows, and others. 2018. Longer and more frequent marine heatwaves over the past century. *Nat. Commun.* 1–12. doi:10.1038/s41467-018-03732-9

- Oreska, M. P. J., K. J. McGlathery, J. H. Porter, H. Asmus, R. M. Asmus, and A. Vaquer. 2017. Seagrass blue carbon spatial patterns at the meadow-scale J. Cebrian [ed.]. *PLoS One* **12**: e0176630. doi:10.1371/journal.pone.0176630
- Orth, R. J., T. I. M. J. B. Carruthers, W. C. Dennison, and others. 2006a. A Global Crisis for Seagrass Ecosystems. *Bioscience* **56**: 987–996. doi:10.1641/0006-3568(2006)56
- Orth, R. J., J. S. Lefcheck, K. S. McGlathery, and others. 2020. Restoration of seagrass habitat leads to rapid recovery of coastal ecosystem services. *Sci. Adv.* **6**: eabc6434. doi:10.1126/sciadv.abc6434
- Orth, R. J., M. L. Luckenbach, S. R. Marion, K. A. Moore, and D. J. Wilcox. 2006b. Seagrass recovery in the Delmarva Coastal Bays, USA. *Aquat. Bot.* **84**: 26–36. doi:10.1016/j.aquabot.2005.07.007
- Orth, R. J., and K. J. McGlathery. 2012. Eelgrass recovery in the coastal bays of the Virginia Coast Reserve, USA. *Mar. Ecol. Prog. Ser.* **448**: 173–176. doi:10.3354/meps09596
- Orth, R. J., K. J. McGlathery, and L. W. Cole. 2012. Eelgrass recovery induces state changes in a coastal bay system. *Mar Ecol Prog Ser* **448**: 173–176. doi:10.3354/meps09522
- Pedersen, O., T. D. Colmer, and K. Sand-jensen. 2013. Underwater photosynthesis of submerged plants – recent advances and methods. **4**: 1–19. doi:10.3389/fpls.2013.00140
- Pendleton, L., D. C. Donato, B. C. Murray, and others. 2012. Estimating Global “Blue Carbon” Emissions from Conversion and Degradation of Vegetated Coastal Ecosystems. *PLoS One* **7**. doi:10.1371/journal.pone.0043542
- Rasmussen, E. 1977. The wasting disease of eelgrass (*Zostera marina*) and its effects on environmental factors and fauna. *Seagrass Ecosyst.*
- Raun, A. L., and J. Borum. 2013. Combined impact of water column oxygen and temperature on internal oxygen status and growth of *Zostera marina* seedlings and adult shoots. *J. Exp. Mar. Bio. Ecol.* **441**: 16–22. doi:10.1016/J.JEMBE.2013.01.014
- Rheuban, J. E., and P. Berg. 2013. The effects of spatial and temporal variability at the sediment surface on aquatic eddy correlation flux measurements. *Limnol. Oceanogr. Methods* **11**: 351–359. doi:10.4319/lom.2013.11.351
- Rheuban, J. E., P. Berg, and K. J. McGlathery. 2014. Multiple timescale processes drive ecosystem metabolism in eelgrass (*Zostera marina*) meadows. *Mar. Ecol. Prog. Ser.* **507**: 1–13. doi:10.3354/meps10843
- Safak, I., P. L. Wiberg, D. L. Richardson, and M. O. Kurum. 2015. Controls on residence time and exchange in a system of shallow coastal bays. *Cont. Shelf Res.* **97**: 7–20. doi:10.1016/j.csr.2015.01.009
- Staehr, P. A., and J. Borum. 2011. Seasonal acclimation in metabolism reduces light requirements of eelgrass (*Zostera marina*). *J. Exp. Mar. Bio. Ecol.* **407**: 139–146. doi:10.1016/j.jembe.2011.05.031
- Volaric, M. P., P. Berg, and M. A. Reidenbach. 2018. Oxygen metabolism of intertidal oyster reefs measured by aquatic eddy covariance. *Mar. Ecol. Prog. Ser.* **599**: 75–91.
- Waycott, M., C. M. Duarte, T. J. B. Carruthers, and others. 2009. Accelerating loss of seagrasses across the globe threatens coastal ecosystems. *Proc. Natl. Acad. Sci.* **106**: 12377–12381. doi:10.1073/pnas.0905620106

CHAPTER 1: LONG-TERM TRENDS AND RESILIENCE OF SEAGRASS METABOLISM: A DECADAL AQUATIC EDDY COVARIANCE STUDY

Amelie C. Berger¹, Peter Berg¹, Karen J. McGlathery¹, Marie Lise Delgard¹

¹Department of Environmental Sciences, University of Virginia, Charlottesville, VA, USA

This chapter was published in Limnology and Oceanography in January 2020:

Berger, A. C., P. Berg, K. J. McGlathery, and M. L. Delgard. 2020. Long-term trends and resilience of seagrass metabolism: A decadal aquatic eddy covariance study. *Limnol. Oceanogr.* 1–16. doi:10.1002/lno.11397

Abstract

Seagrass meadows are valued for their ecosystem services, including their role in mitigating anthropogenic CO₂ emissions through ‘blue carbon’ sequestration and storage. This study quantifies the dynamics of whole ecosystem metabolism on daily to interannual timescales for an eelgrass (*Zostera marina*) meadow using in situ benthic O₂ flux measurements by aquatic eddy covariance over a period of 11 years. The measurements were part of the Virginia Coast Reserve Long-Term Ecological Research study, and covered a relatively stable period of seagrass ecosystem metabolism 6–13 years after restoration by seeding (2007–2014), a die-off event likely related to persistently high temperatures during peak growing season in 2015, and a partial recovery from 2016 to 2018. This unique sequence provides an unprecedented opportunity to study seagrass resilience to naturally occurring stressors. With this extensive dataset covering 115 full diel cycles, we constructed an average annual oxygen budget that indicated the meadow was in metabolic balance when averaged over the entire period, with gross primary production and respiration equal to 95 mmol O₂ m⁻² d⁻¹ and -94 mmol O₂ m⁻² d⁻¹, respectively. On an interannual scale, there was a shift in trophic status from balanced to net heterotrophy during the die-off event in 2015, then to net autotrophy as the meadow recovered. The highly dynamic and variable nature of seagrass metabolism captured by our aquatic eddy covariance data emphasizes the importance of using frequent measurements throughout the year to correctly estimate trophic status in seagrass meadows.

Introduction

Seagrasses are marine flowering plants that inhabit shallow coastal waters worldwide. While they only cover 0.1–0.2% of the global ocean, they are valued for their ecosystem services, which contribute to the ecological and economic prosperity of coastal areas (Costanza et al. 1997). Seagrass meadows improve water quality and clarity (e.g. McGlathery et al. 2007; Hansen and Reidenbach 2012; Lamb et al. 2017) and provide food and habitat for aquatic organisms important to fisheries and adjacent ecosystems (e.g. Costanza et al. 1997; Nagelkerken et al. 2000; Beck et al. 2001). In recent years, they have gained particular recognition for their potential as a ‘blue carbon’ sink, due to high rates of primary production (carbon sequestration) (Duarte et al. 2010) and carbon burial in the sediment (carbon storage) (Fourqurean et al. 2012; Duarte et al. 2013; Oreska et al. 2017). Carbon burial results from direct burial of dead seagrass tissue (e.g. Romero et al. 1994; Greiner et al. 2016) and from flow alteration by the seagrass canopy, which creates a depositional environment for particles in the water column (e.g. Terrados and Duarte 2000; Gacia and Duarte 2001; Hansen and Reidenbach 2012). Global carbon stocks for seagrass meadows have been estimated at 4.2–8.4 Pg C in the top meter of sediment, and 75.5–151 Tg C in above and below-ground biomass (Fourqurean et al. 2012). This carbon retention capacity has given seagrass conservation and restoration efforts merit as climate change mitigation strategies (Duarte et al. 2016).

Seagrass ecosystems rank among the most rapidly declining marine habitats globally due to climate change, increased coastal development, eutrophication, and other anthropogenic factors (Orth et al. 2006a; Waycott et al. 2009). These declines result in the loss of seagrass ecosystem services, including their carbon retention capacity (e.g. Marbá et al. 2015; Arias-Ortiz et al. 2018). The restoration of ecosystem services during seagrass recovery, however, remains largely understudied (McGlathery et al. 2012; Marbá et al. 2015).

Seagrass loss and recovery (natural and through restoration) are typically assessed by quantifying seagrass growth and shoot demography (e.g. Durako 1994; Orth et al. 2006; Macreadie et al. 2014) or areal extent (Robbins 1997; Kendrick et al. 2002; Frederiksen et al. 2004). Ecosystem metabolism (primary production and respiration), however, provides more information about seagrass ecosystem function and resilience, while simultaneously addressing blue carbon sequestration. Respiration (R), gross primary production (GPP), and net ecosystem metabolism (NEM, defined as $GPP - R$) are measures of carbon flows in seagrass meadows (Duarte and Prairie

2005). Autotrophic meadows ($GPP:R > 1$; $NEM > 0$) fix more carbon than they release and may therefore be efficient carbon sinks, while in heterotrophic meadows ($NEM < 0$; $GPP:R < 1$), allochthonous sources of carbon elevate ecosystem respiration. Metabolic balance ($NEM = 0$; $GPP:R = 1$) indicates that all carbon inputs to the meadow (autochthonous and allochthonous) are balanced by losses (autotrophic and heterotrophic respiration, burial, and export). Determining the trophic status of seagrass meadows is therefore crucial to quantifying their role in the global carbon budget and understanding the impacts of their loss (Duarte et al. 2010). It is not surprising that determining seagrass NEM has been the focus of many studies and review papers (Gazeau et al. 2004; Barrón et al. 2006; Duarte 2017). However, net ecosystem metabolism is highly variable between and among species, geographic locations, and seasons (Duarte et al. 2010). The challenge of accurately determining the trophic status of a seagrass meadow is further complicated by the use of different measurement techniques. Net ecosystem metabolism estimates obtained in comparative studies have differed greatly depending on the measurement approach (Long et al. 2015a). Seagrass respiration and primary production have typically been measured using benthic chambers (e.g. Herzka and Dunton 1997), open water oxygen balance approaches (e.g. Champenois and Borges 2012), or core incubations in the lab (e.g. Fourqurean and Zieman 1991). However, these methods may lead to inaccurate estimates of seagrass metabolism by scaling up changes in oxygen concentration resolved over short time periods ($< \text{full diel cycle}$), small spatial scales (individual shoots or benthic areas $< 0.25 \text{ m}^2$) (Martin et al. 2005), at poor temporal resolutions (Long et al. 2015a), and under conditions that often do not mimic in situ light levels and flow rates (Pedersen et al. 2013; Olivé et al. 2016).

Over the last decade, the aquatic eddy covariance technique has emerged as an effective way to integrate in situ metabolism and capture its natural variability (Berg et al. 2003). This technique overcomes many of the aforementioned shortcomings because it is a non-invasive (Lorrai et al. 2010), high temporal resolution (Rheuban and Berg 2013), whole-ecosystem approach that integrates benthic O_2 fluxes over $10\text{--}100 \text{ m}^2$ (Berg et al. 2007). It has already proven successful in seagrass environments (Hume et al. 2011; Rheuban et al. 2014a; Long et al. 2015b; Berg et al. 2019).

The aquatic eddy covariance technique has been used in a restored eelgrass meadow at the Virginia Coast Reserve Long-Term Ecological Research (VCR-LTER) site since 2007, resulting in an extensive dataset of seagrass metabolism during a relatively stable period 6–13 years after

its restoration (Hume et al. 2011; Rheuban et al. 2014b; Berg et al. 2019). Seasonal measurements from the same site in this study captured a seagrass die-off event in 2015 followed by its natural but partial recovery in 2016–2018, thus providing an unprecedented opportunity to study the dynamics and resilience of seagrass metabolism over daily to interannual timescales. The combination of a natural die-off and recovery event with a high-quality long-term dataset of seagrass metabolism allows us to quantify the carbon sequestration capacity of the meadow and the impact of an extreme event on ecosystem function. In this study, we examined the long-term trends in seagrass metabolism (R, GPP, NEM) and the variability of these rates on multiple timescales. Our unique dataset shows the impacts of seagrass loss and recovery on ecosystem-scale metabolism, and the trophic status of the meadow over 11 years through an averaged annual carbon budget for the seagrass meadow, revealing novel information on its carbon retention capacity.

Materials and methods

Study site

South Bay is a restored eelgrass (*Zostera marina*) meadow located in the shallow subtidal coastal bays of the VCR-LTER (Fig. 1a). It is connected to the Atlantic Ocean by two inlets north and south of the meadow, which results in a relatively brief water residence time (Safak et al. 2015). It is also bound by a barrier island to the east and the Delmarva Peninsula to the west, creating a low-energy hydrodynamic environment.

South Bay is part of a landscape-scale eelgrass restoration project at the VCR-LTER that started in 2001 (Orth et al. 2006b; Orth and McGlathery 2012). An eelgrass ‘wasting disease’ outbreak and a hurricane decimated VCR *Z. marina* populations in the 1930s, and the coastal bays remained unvegetated for decades (Rasmussen 1977; Orth et al. 2006b, 2012). In the late 1990s–early 2000s, the discovery of a natural patch of eelgrass at the VCR-LTER prompted a large-scale restoration effort, with the broadcast-seeding of 0.2 to 0.4 ha plots in 4 coastal bays (Orth et al. 2006b), ultimately restoring over 25 km² of unvegetated seafloor to seagrass meadow (<http://web.vims.edu/bio/sav>, accessed 05/2019). The seeded plots in South Bay coalesced and expanded into a 7 km² continuous meadow, now recognized as the largest restored meadow in the world (Orth and McGlathery 2012).

South Bay is a shallow, oligotrophic lagoon where light conditions are favorable for seagrass growth (Lawson et al. 2007). Since 2007, seagrass metabolism has been measured by aquatic eddy covariance at one of the original seeded plots ($37^{\circ} 15'43.6356''$ N, $75^{\circ} 48'54.547''$ W) at the center of the meadow (Figs. 1a, 1b). This site has a mean water depth of 1.2 m and a tidal range of 1 m, and current flow velocities ranging from 0.3 to $21.5 \text{ cm}\cdot\text{s}^{-1}$ (mean: $4.1 \text{ cm}\cdot\text{s}^{-1}$).

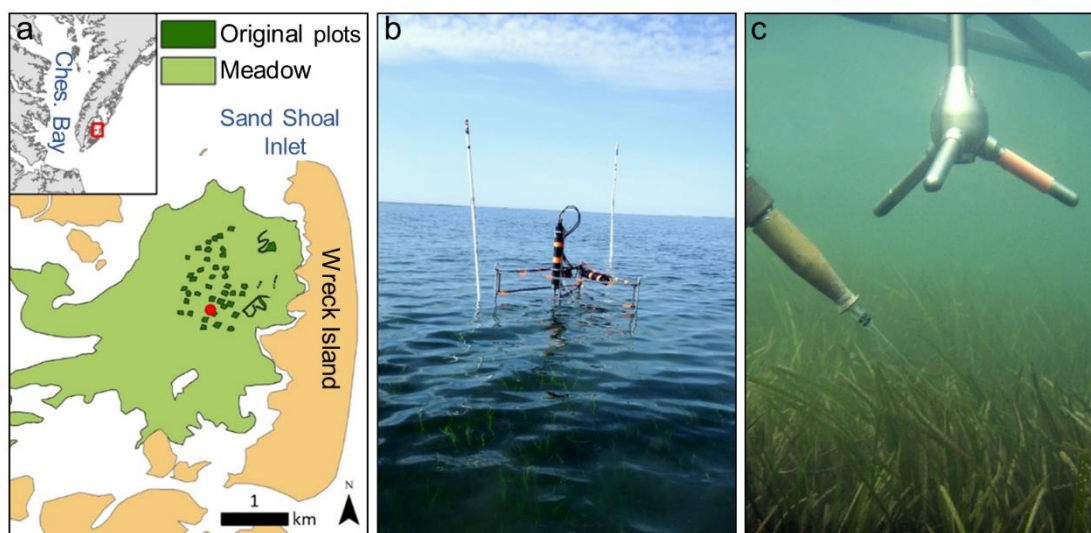


Fig. 1: a) Study site location in the South Bay eelgrass meadow at the Virginia Coast Reserve Long-Term Ecological Research (VCR-LTER) site. Dark green: original seeded plots or tracks. Light green: meadow extent as of 2017. Red marker: long-term study site; b) aquatic eddy covariance system deployed in South Bay; c) Clark-type oxygen microelectrode and Nortek AS Vector[®] acoustic Doppler velocimeter (ADV).

Data collection

The eddy covariance system (Fig. 1b) consists of a Nortek AS Vector[®] acoustic Doppler velocimeter (ADV) coupled to a fast-response ($t_{90\%} \leq 0.4 \text{ s}$) Clark-type oxygen microelectrode (Fig. 1c) and a high-resolution picoamp amplifier (Berg et al. 2003; McGinnis et al. 2011). Velocity measurements (x, y, z), from which current speed and direction were derived, were made continuously by the ADV at 64 or 32 Hz in a $\sim 2 \text{ cm}^3$ measuring volume located $\sim 30 \text{ cm}$ above the sediment surface. The oxygen microsensor had a tip diameter of $10\text{--}100 \mu\text{m}$ and measured oxygen 0.5 cm from the measuring volume so as to not interfere with the velocity measurements. All instruments were mounted on a light and thin stainless steel frame to minimize disturbance of natural flow (Berg and Huettel 2008). We examined our benthic fluxes carefully for any effects of flow direction, including flow across the frame legs. We found no difference in our fluxes when the flow was across the frame legs. We also found no difference based on flow orientation relative

to the oxygen sensor. Oxygen microsensor measurements were calibrated using an oxygen-free reading in a Na-ascorbate/NaOH solution and the maximum dissolved oxygen (DO) concentration measured during each deployment by stable PME miniDOT[®] optodes at 1-min intervals. This two-point calibration was used to transform high-resolution microsensor recordings into oxygen concentrations in $\mu\text{mol L}^{-1}$. Photosynthetically Active Radiation (PAR) was measured at 5 min intervals by planar 2π Odyssey PAR loggers. These loggers were placed 30 cm above the sediment surface to measure PAR at the top of the seagrass canopy. They were replaced every two days to limit the effects of biofouling on light measurements. Seagrass shoot density was obtained for each field campaign by counting seagrass shoots within 10 replicate 0.25 m^2 quadrats thrown randomly within the sampling site.

Eddy covariance measurements were made seasonally to capture a wide range of environmental conditions and stages of seagrass growth (Orth and Moore 1986; Rheuban et al. 2014a). Sampling dates for the 21 field campaigns of this study are shown in Table 1. Each field campaign lasted ~2 weeks and consisted of up to six nearly consecutive deployments, each 1–3 days in duration (Table 1). The oxygen microelectrodes were fragile and sometimes broke mid-deployment, therefore resulting in fewer full 24-hour cycles available for seagrass metabolism calculations. During 2014 and 2015, two eddy covariance systems were deployed in parallel to increase deployment success and to evaluate reproducibility. These systems were deployed 10 m apart with no overlapping footprints. The data collected in this study were added to our existing record of seagrass metabolism from 2007 to 2012 (Hume et al. 2011; Rheuban et al. 2014a). A total of 115 full 24-hour records between 2007 and 2018 were compiled in this study.

Table 1: Sampling months for aquatic eddy covariance field deployments, with the total number of deployments per field campaign, range of deployment duration, and resulting 24-hour periods used in metabolic rate calculations.

Year	Sampled Months	N Deployments	Deployment Duration (d)	N Daily Rates	Reference
2007	July	8	1	5	Hume et al. (2011)
2011	August			5	
	October			4	
2012	February	3–8 (33 total)	1	3	Rheuban et al. (2014b)
	June			5	
	August			1	

2014	April	2	1-2	3	
	May	3	1-2	4	
	June	5	2-3	9	
	July	4	2-3	5	
	August	5	1-2	2	
	October	5	2	6	
2015	January	2	2	2	
	March	1	2	1	
	April	2	2-3	3	
	May	2	2	4	
	June	6	2	6	
	August	5	1-2	4	
2016	April	3	1-2	5	
	June	4	1-3	5	
	July	5	1-2	4	
	August	1	1	1	
	October	2	2	4	
	November	2	2	2	
2017	April	3	1-2	3	
	June	4	2	6	
	August	1	2	2	
	November	2	2	2	
2018	April	3	2	6	
	June	3	2	1	

This study

Data Analysis

The 64 or 32 Hz data were extracted from the ADV and averaged to 8 Hz to reduce unbiased noise in the dataset while still resolving the entire turbulence spectrum carrying the flux signal (Berg et al. 2003). Dissolved oxygen fluxes between the benthic environment and water column were calculated using EddyFlux3.0 software (Peter Berg, unpublished), following the equation:

$$\overline{J_{O_2}} = \overline{w'C'} \quad (1)$$

where the overbars represent time averaging and w' and C' represent the instantaneous fluctuations of vertical velocity (w) and oxygen concentration (C), respectively (Berg et al. 2003).

Dissolved oxygen fluxes were calculated at 15-minute intervals over which velocity and oxygen concentration are determined via linear detrending (Lee et al. 2004; Berg et al. 2009). A storage correction was applied to account for changes in oxygen stored in the water column below the measuring point due to large diel variations in water column oxygen concentration and our relatively large measuring height (~30 cm) (Rheuban et al. 2014a). This correction was applied as:

$$\overline{J_{benthic}} = \overline{J_{O_2}} + \int_0^h \frac{dC}{dt} dz \quad (2)$$

where $\overline{J_{benthic}}$ is the corrected benthic flux, $\overline{J_{O_2}}$ is the measured eddy flux, h is the measuring height, and $\frac{dC}{dt}$ is the temporal change in water column oxygen concentration, obtained by linear detrending. This correction is essential as changes in oxygen storage can distort benthic flux calculations (Rheuban et al. 2014a), and it implicitly assumes that concentration changes in the bottom water below the measuring point are driven primarily by benthic activity (Berg et al. 2019). No data rotation or correction for time lag between the velocity and the oxygen concentration measurements were performed to avoid biases under low flow conditions and in the presence of surface waves (Berg et al. 2015).

Each 15-minute burst was then examined to ensure no fluxes were retained if showing excessive noise or spikes due to interference from debris in the water (Berg et al. 2009; Lorrain et al. 2010). On few occasions, 15-minute bursts were omitted due to the water level falling below the sensors. The remaining bursts were then averaged to obtain hourly fluxes (Fig. 2c). Missing hourly values were interpolated linearly using adjacent oxygen fluxes. Even during extreme low tides, seagrass shoots remained underwater.

Hourly oxygen fluxes were split into sequential 24-hour segments (Fig. 2c) and separated into light fluxes ($PAR > 1.0 \mu\text{mol photons m}^{-2} \text{s}^{-1}$) and dark fluxes ($PAR < 1.0 \mu\text{mol photons m}^{-2} \text{s}^{-1}$) to calculate daily rates of respiration (R), gross primary production (GPP), and net ecosystem metabolism (NEM) using the equations given by Hume et al. (2011):

$$R = \frac{1}{24} \left(\sum \text{flux}_{\text{dark}} + \frac{\sum \text{flux}_{\text{dark}}}{h_{\text{dark}}} h_{\text{light}} \right) \quad (3)$$

$$\text{GPP} = \frac{1}{24} \left(\sum \text{flux}_{\text{light}} + \frac{|\sum \text{flux}_{\text{dark}}|}{h_{\text{dark}}} h_{\text{light}} \right) \quad (4)$$

$$\text{NEM} = \frac{1}{24} \left(\sum \text{flux}_{\text{light}} + \sum \text{flux}_{\text{dark}} \right) \quad (5)$$

where $\text{flux}_{\text{dark}}$ are the hourly DO fluxes during nighttime, $\text{flux}_{\text{light}}$ are the daytime hourly oxygen fluxes, h_{dark} is the number of dark hours, and h_{light} the number of light hours. The rates of R, GPP, and NEM are reported in $\text{mmol O}_2 \text{ m}^{-2} \text{ d}^{-1}$. In June 2018, no full 24-hour record was collected due to oxygen sensor breakage. All existing hourly data for that field campaign ($n = 89$ hours total over 5.5 days) were therefore binned by hour of day to create one dataset representing 24 clock hours. Each hourly bin in that dataset comprised $n = 1\text{--}5$ hours. In cases where parallel

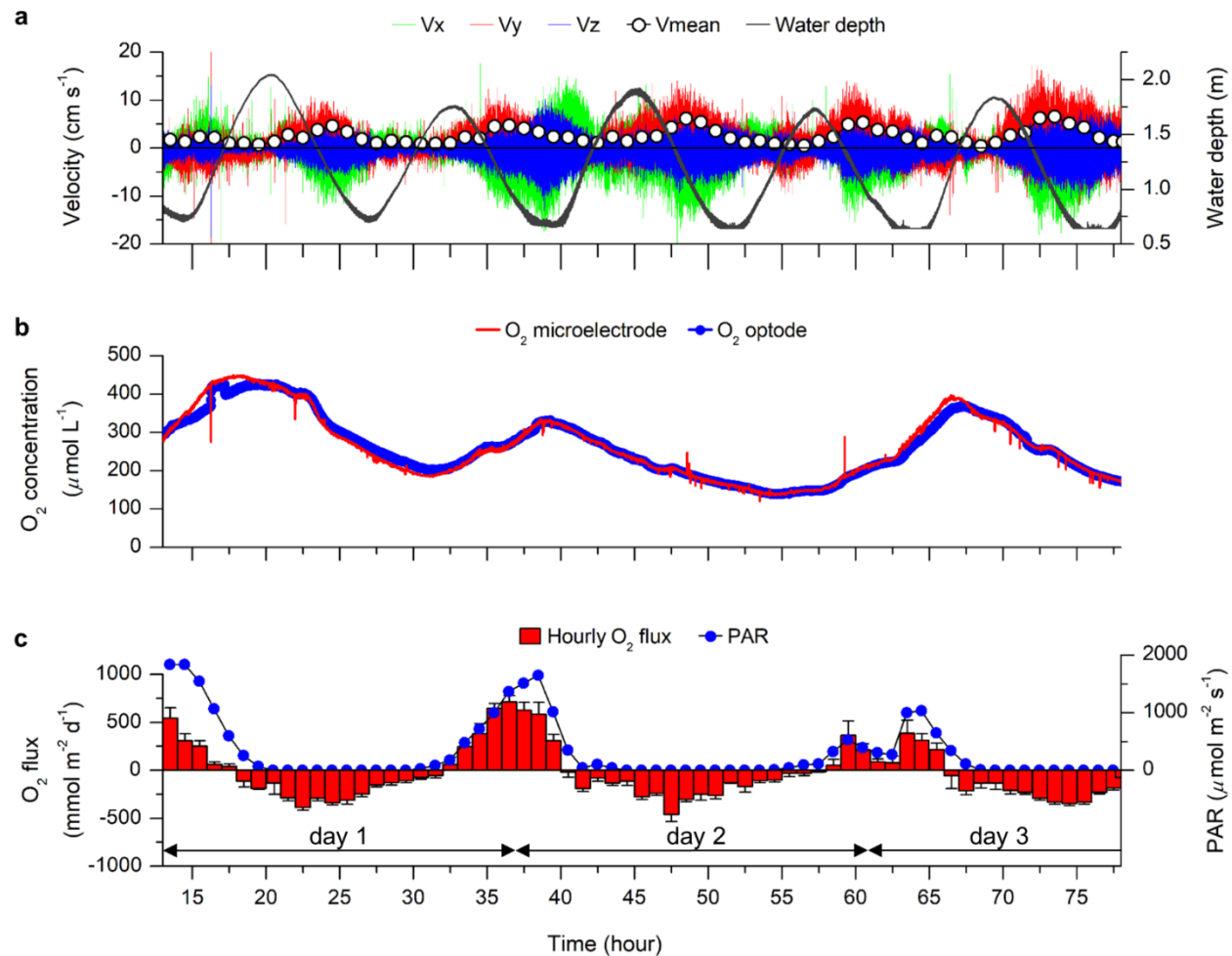


Fig. 2: Example eddy covariance data from one 65-hour deployment in South Bay in June 2014, with a) x, y, z, and mean current speed, water depth, b) oxygen concentration, and c) total hourly oxygen flux and photosynthetically active radiation (PAR). Error bars: SE (based on $n = 3\text{--}4$ averaged 15-min fluxes). Each deployment was separated into 24 hours segments (represented by arrows) from the deployment start time to calculate gross primary production (GPP), respiration (R), and net ecosystem metabolism (NEM).

deployments successfully yielded complete datasets for both systems, the calculated rates of R, GPP, and NEM were averaged together to yield only one value per 24-hr period.

The estimation of metabolic rates is associated with some uncertainties. For example, under occasional conditions of low water, high temperature, and high solar radiation during the summer, we have observed bubbles on seagrass leaves and on the sediment surface. If these bubbles represent oxygen formed by seagrass meadow photosynthesis and if they rise through the water column, this can contribute to an underestimation of GPP (Long et al. 2019). Another—and possibly more significant—source of uncertainty that can also result in underestimating GPP throughout the year is the assumption that nighttime and daytime respiration rates are the same (Glud 2008). This is likely not the case due to daytime consumption of highly labile compounds formed by photosynthesis that would make daytime respiration higher (Fenchel and Glud 2000; Glud et al. 2009). These uncertainties are not unique to the aquatic eddy covariance technique but are associated with all commonly used approaches for measuring the benthic oxygen fluxes.

Statistical analyses

The role of temperature in the seagrass die-off in 2015 was evaluated by comparing summer (June–August) water temperature records for the years surrounding the die-off event (2012–2017), and determining the proportion of time water temperatures exceeded the proposed 28°C eelgrass optimum temperature threshold (Staehr and Borum 2011) during the peak growing period (June) of each year. High-resolution water temperature data were obtained from NOAA’s National Data Buoy Center (NDBC) for the nearby Wachapreague, VA (Station WAHV2). The 6-min sea surface temperature data were averaged to produce hourly values. The temperature record for summer 2018 was incomplete and therefore excluded from this analysis.

The effects of seagrass loss and recovery on ecosystem metabolism were determined using analyses of variance (ANOVAs) between summer averages of R, GPP, and NEM prior to the die-off event (2014), during the die-off event (2015), and during the recovery period (2016, 2017).

An annual oxygen budget was constructed for the meadow by binning all 115 daily metabolism values by month of year. This resulted in a model-year for seagrass oxygen metabolism that integrates all the data collected over the past 11 years. Months that had never been sampled (September and December) were interpolated using adjacent months. Annual R, GPP, and NEM were calculated from this model and converted to rates of carbon metabolism assuming a photosynthetic quotient (moles O₂:moles CO₂) equal to 1 (Kirk 1983; Duarte et al. 2010). The

2015 die-off event and the meadow development period in 2007 were each excluded from the analysis to determine their effects on the final annual budget. These exclusions had little to no effect on annual NEM, and we therefore included all of our data in this analysis. Our results were compared to the metabolic rates reported in Duarte et al. (2010) by calculating averages for the temperate and *Z. marina* meadows reported in their supplemental dataset (S1 dataset).

Results

Aquatic eddy covariance data

An example of a 65-hour eddy covariance deployment in South Bay in June 2014 is shown in Fig. 2. The water level, velocity, and microelectrode oxygen measurements along with the MiniDOT oxygen measurements for calibration are shown in Figs. 2a, 2b. The water level signal occasionally flattened out (Fig. 2a) due to the water level falling below the pressure sensor, located 21.7 cm above the Vector's sensor head (Fig. 1c). The vertical velocity signal shows expected higher turbulence levels at higher current speeds (Fig. 2a). In addition, part of this pattern may result from an increase in absolute noise at higher current speeds or the occasional presence of small surface waves. The hourly oxygen fluxes derived from these measurements are shown in Fig. 2c. Hourly fluxes were well-correlated to PAR as is evident from negative fluxes during the nighttime, representing an oxygen uptake due to respiration, and positive fluxes during the day, representing net oxygen release from the seagrass benthos up into the water column as photosynthesis was exceeding respiration. The tight relationship between PAR and hourly oxygen fluxes becomes more evident during the 3rd day of this deployment, around hour 62 (Fig. 2c), where a decrease in light levels during the day coincided with a decrease in oxygen flux. The stimulating effect of flow on nighttime respiration also appears clearly in Fig. 2, which shows higher nighttime oxygen fluxes coinciding with higher current speed. The maximum daytime flux in this deployment was $823 \text{ mmol O}_2 \text{ m}^{-2} \text{ d}^{-1}$, which is close to the maximum hourly oxygen flux ever measured in South Bay ($909 \text{ mmol O}_2 \text{ m}^{-2} \text{ d}^{-1}$ in July 2016). The maximum hourly nighttime flux in this deployment ($-462 \text{ mmol O}_2 \text{ m}^{-2} \text{ d}^{-1}$) was also one of the highest nighttime fluxes ever recorded at this site.

The hourly oxygen fluxes obtained from a simultaneous deployment of two eddy covariance systems in April 2015 are shown in Fig. 3. The hourly fluxes between the two systems agreed well, and resulted in similar daily rates of R, GPP, and NEM for the 24-hr period shown (R

$= -91$, $GPP = 117$, and $NEM = 26$ $\text{mmol O}_2 \text{ m}^{-2} \text{ d}^{-1}$ for System 1 and $R = -96$, $GPP = 118$, and $NEM = 22$ $\text{mmol O}_2 \text{ m}^{-2} \text{ d}^{-1}$ for System 2). All successful parallel deployments resulted in comparable metabolic rates between the two systems ($R^2 = 0.8$ and 0.9 for R and GPP , respectively, $n = 20$).

Long-term record of ecosystem metabolism

Our long-term record of seagrass metabolism shows that over the last 11 years South Bay has been, on average, in metabolic balance. Fig. 4a shows all 115 daily rates of R and GPP plotted relative to a 1:1 line, which represents metabolic balance ($NEM = 0$; $GPP:R = 1$). The points fall close to this line and indicate a balanced metabolic state over all deployments, in spite of some day-to-day variability between autotrophy and heterotrophy. This variability also shows up on a monthly timescale, as shown in our full record of average monthly R , GPP , NEM , and seagrass

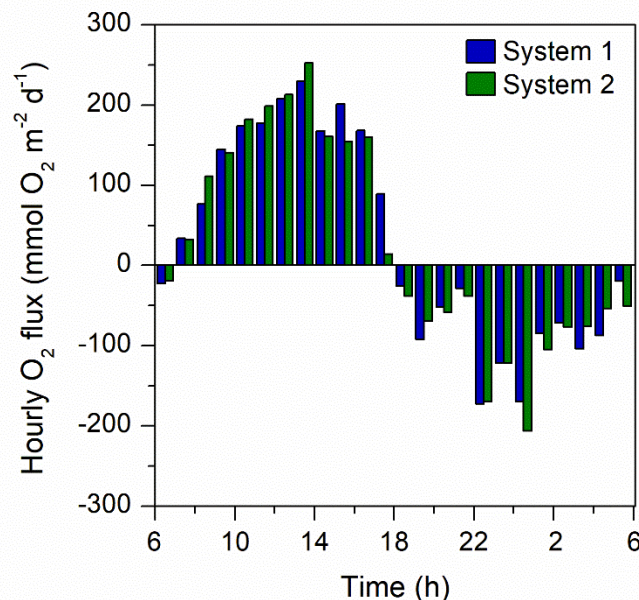


Fig. 3: Comparison of simultaneous eddy covariance deployments over 24 hours in April 2015. The two systems were deployed 10 m apart with no overlapping footprints. The hourly O_2 fluxes derived from each system agreed well, which confirms the reproducibility of our measurements and shows that the aquatic eddy covariance technique integrates well over the patchiness of the seagrass meadow.

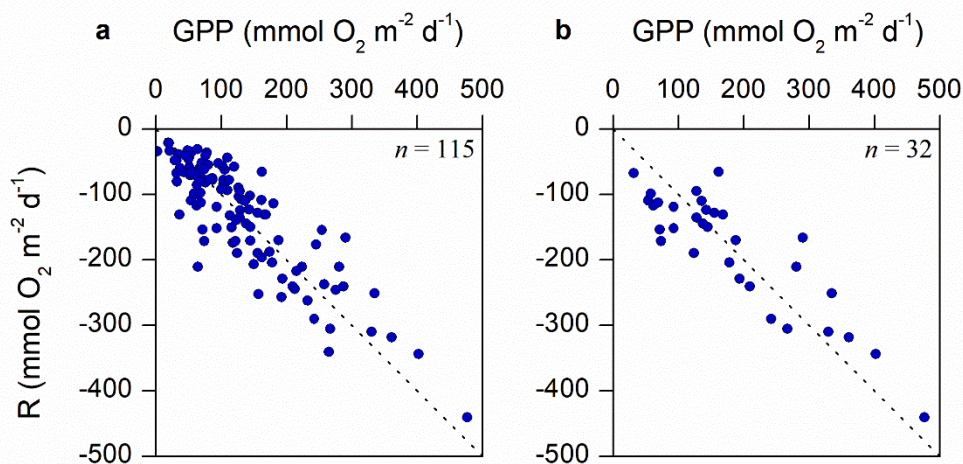


Fig. 4: a) All 115 daily respiration (R) versus gross primary production (GPP) rates relative to a 1:1 line (dotted line); b) daily R vs. GPP for June 2012, and 2014–2018.

density (Fig. 5). In fact, the variability of R and GPP throughout the 11-year record was equally large on a daily, monthly, and seasonal timescale, based on Levene's test for equality of variances ($p > 0.05$, $n = 115, 29, 20$, respectively) (Levene 1960). This is also evident in Fig. 4b, where R and GPP vary as much in the month of June interannually as they do monthly or seasonally (Figs. 4a, 5). The coefficients of variation (CV), which are a measure of relative variability, were also calculated for R and GPP for each timescale (Table 2), and further indicate that there was a similar magnitude of variability across all time scales (average CV = 67, 59, and 63 for daily, monthly, and seasonal timescales, respectively). Additionally, R and GPP varied almost equally for each timescale (Table 2).

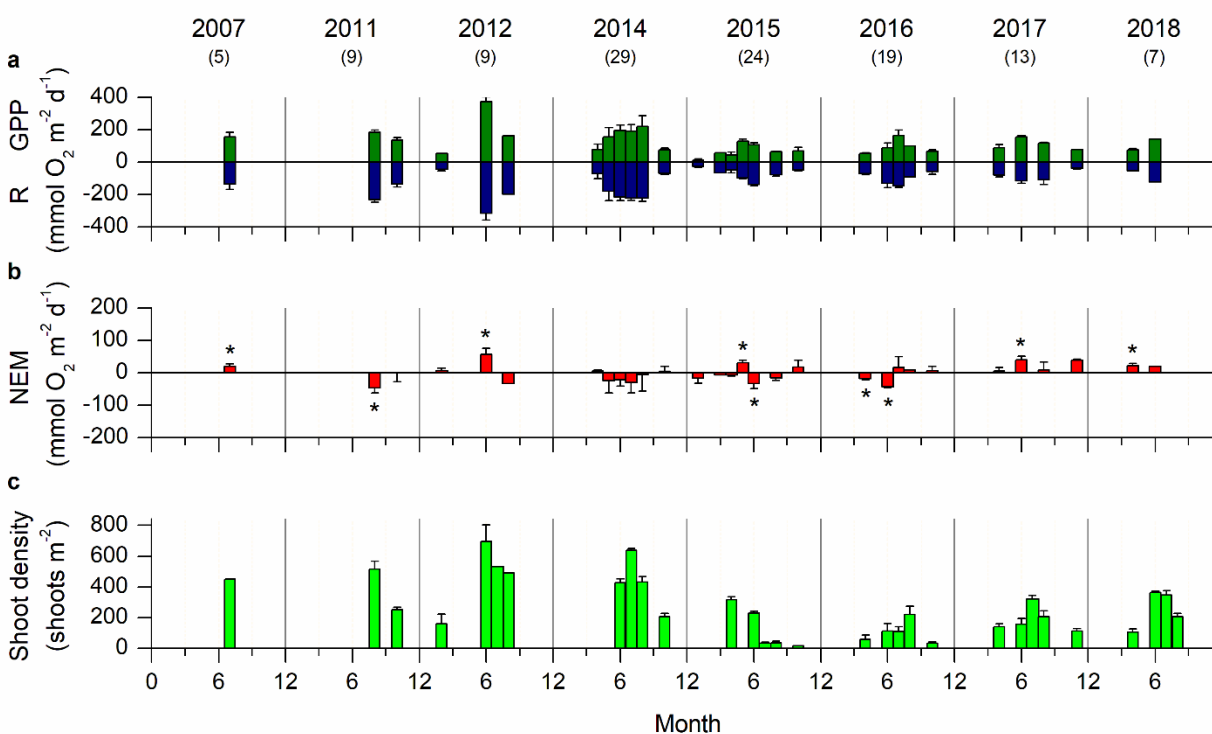


Fig. 5: Long-term dataset of monthly eelgrass a) gross primary production (GPP) and respiration (R), b) net ecosystem metabolism (NEM), and c) eelgrass shoot density. Monthly averages were obtained for July 2007 (Hume et al. 2011), August, October 2011, and February, June, August 2012 (Rheuban et al. 2014b), and April, May, June, July, August, October 2014; January, March, April, May, June, August, October 2015; April, June, July, August, October 2016; April, June, August, November 2017; and April and June 2018 (this study). Asterisks mark months where NEM was significantly different from 0 ($p < 0.05$, $n = 3-9$). Error bars: SE based on the number of daily metabolic rates averaged per month (see Table 1 N daily rates column) and the average of 10 replicate 0.25 m² quadrat seagrass counts. The number of 24-hour deployments contributing to the monthly averages for each year are shown in parentheses.

On a monthly timescale, average R and GPP generally mirrored each other, resulting in average NEM values that were not significantly different from 0 ($p > 0.05$, $n = 3-9$) throughout

most of the record, with the exception of July 2007, June 2012, May 2015, June 2017, and April 2018 when the meadow was net autotrophic ($p < 0.05$) and August 2011, June 2015, and April, June 2016 when the meadow was net heterotrophic ($p < 0.05$). The highest monthly average GPP values were found for summer 2012 (June average GPP = $372 \text{ mmol O}_2 \text{ m}^{-2} \text{ d}^{-1}$) and summer 2014 (June average GPP = $196 \text{ mmol O}_2 \text{ m}^{-2} \text{ d}^{-1}$ and August average GPP = $218 \text{ mmol O}_2 \text{ m}^{-2} \text{ d}^{-1}$). Seagrass shoot densities were also highest during these two summers, reaching a maximum of $696 \text{ shoots m}^{-2}$ in June 2014.

Table 2: Coefficients of variation (%) for the magnitudes of respiration (R) and gross primary production (GPP) on a daily, monthly, and seasonal timescale.

	Daily	Monthly	Seasonally
R	65	59	64
GPP	69	59	62

Die-off event

Field observations during summer 2015 showed a decline in seagrass shoot density by over 90% (Figs. 6, 7c). This die-off event is attributed to water temperatures during the peak growing period in June 2015 that exceeded the suggested temperature threshold of 28°C for *Z. marina* (Staeher and Borum 2011) (Fig. 7). Summer water temperatures in 2012–2017 often exceeded this threshold for extended periods of time during the late summer (July

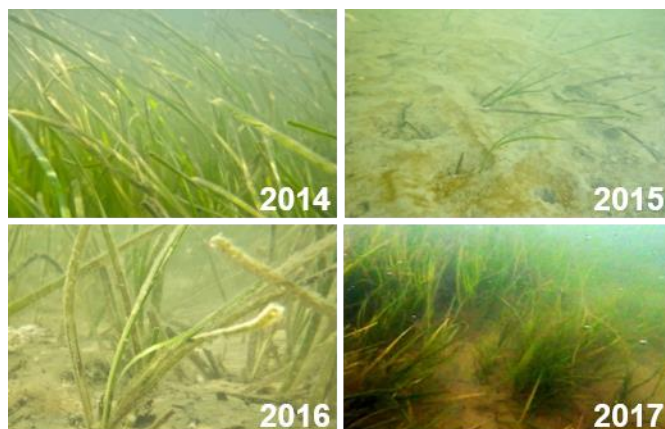


Fig. 6: Photos from our study site in South Bay in July 2014, 2015, 2016, 2017, showing a dramatic decline in seagrass cover after the die-off event in 2015, and a partial recovery in 2016 and 2017.

and August) (Fig. 7a). However, such warm events rarely occurred during the month of June, with the exception of June 2015 when the die-off occurred (Figs. 7a, 7b). Water temperatures at this time exceeded 28°C 36% of the time. There was a 15-day warming event where temperatures exceeded the threshold for most of the day (12 to 24 hours, mean = 20 hours), resulting in 13

consecutive days with mean daily temperature averages at or above 28°C. In comparison, June water temperatures during the years surrounding the die-off event only reached or exceeded 28°C 11% of the time on average, with discontinuous warming events lasting from one to five days, during which water temperatures only exceeded the threshold for an average of 10 hours per day. The seagrass shoot densities measured in July for these years further highlight the link between an exceptionally warm June in 2015 and the observed loss of seagrass (Figs. 7b, 7c).

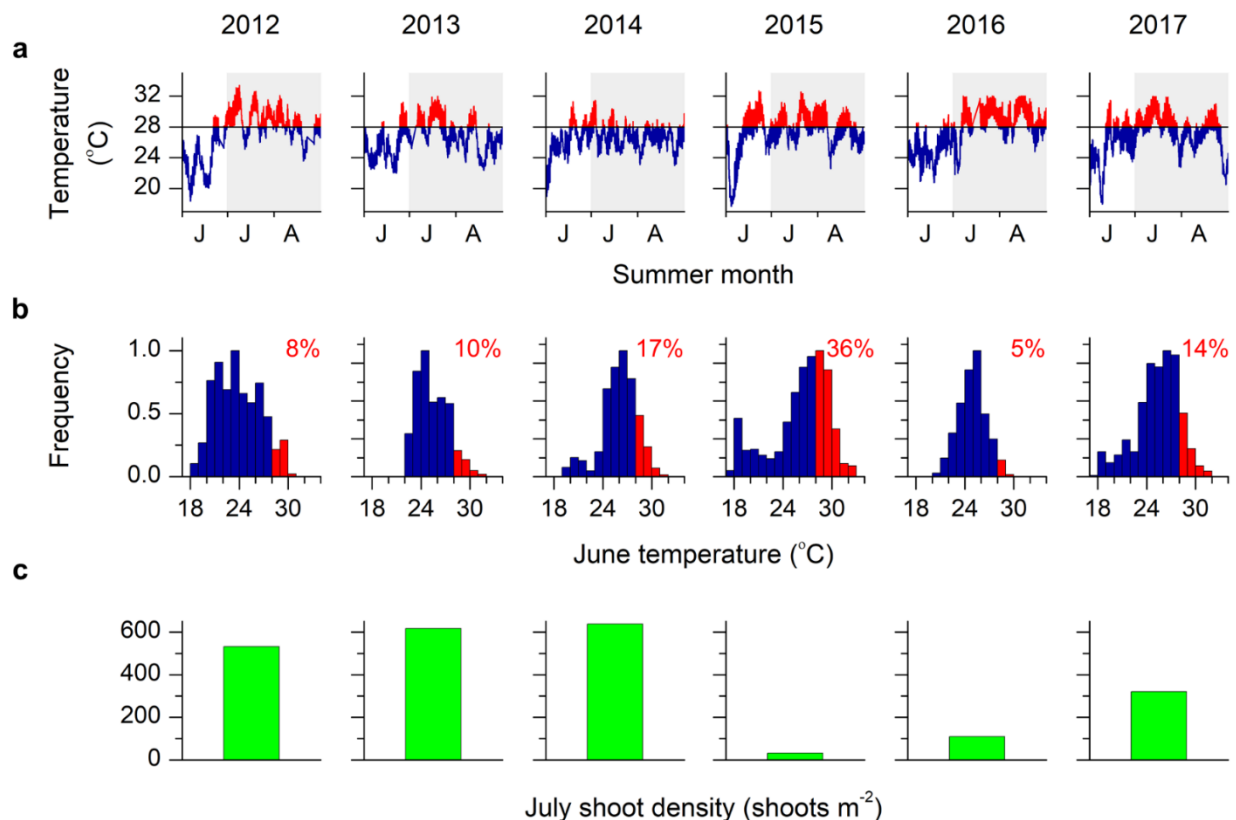


Fig. 7: High water temperatures in June as a possible explanation for the dieback event during summer 2015, with a) hourly water temperatures from the National Buoy Data Center (Wachapreague station) between June 1st and August 31st 2012–2017. Blue: water temperatures below the 28°C thermal tolerance threshold for eelgrass. Red: water temperature exceeding this threshold. Shaded: July and August. b) Frequency of temperature observations between 17°C and 34°C (at 1°C intervals) for June of each year: red and blue bins represent observations above and below 28°C, respectively. Reported values represent the proportion of time temperatures exceeded this threshold during June of each year. c) Resulting seagrass shoot densities in July of each year. The water temperature record for summer 2018 was incomplete and therefore omitted from this analysis.

The trophic status of South Bay shifted from metabolic balance to net heterotrophy during the die-off in 2015, and then to net autotrophy during the subsequent recovery period in 2016–2018 (Fig. 8). The decline in seagrass density in 2015 was accompanied by a significant decline in the magnitudes of R and GPP (Fig. 8). Mean summer R decreased by 48% from -219 ± 12 mmol

$\text{O}_2 \text{ m}^{-2} \text{ d}^{-1}$ (mean \pm SE) in 2014 to -115 ± 11 $\text{mmol O}_2 \text{ m}^{-2} \text{ d}^{-1}$ in 2015 ($p < 0.001$; $n = 16$ and 10, respectively). Mean GPP declined by 55% from 197 ± 22 $\text{mmol O}_2 \text{ m}^{-2} \text{ d}^{-1}$ in 2014 to 89 ± 11 $\text{mmol O}_2 \text{ m}^{-2} \text{ d}^{-1}$ in 2015 ($p < 0.001$; $n = 16$ and 10, respectively). This resulted in a slight decrease in NEM in 2015 and a shift in trophic status from balanced during summer 2014 (mean NEM = -22 ± 10 , $p = 0.15$, $n = 16$) to net heterotrophy during summer 2015 (mean NEM = -26 ± 15 , $p = 0.025$, $n = 10$). The years following the die-off showed a slow, partial recovery, as shown in the seagrass density and metabolism records in Figs. 5 and 8. Mean summer R did not change significantly after its initial decrease in 2015. GPP, however, increased during 2016 and 2017, back to levels comparable to the mean GPP during summer 2014 ($p = 0.13$). The net autotrophy during summer 2017 (mean NEM = 32 ± 11 $\text{mmol O}_2 \text{ m}^{-2} \text{ d}^{-1}$, $p = 0.02$, $n = 8$) corresponded to an 83% increase in seagrass shoot density following the die-off event. Seagrass shoot density in summer 2018 further represented a 69% increase from summer 2017 and a >200% increase from summer 2015. However, mean shoot density in summer 2018 was still only ~60% of that prior to the die-off event.

Annual oxygen balance in South Bay

The annual oxygen balance created from the entire 11-year record shows an average representative year of seagrass metabolism in South Bay (Fig. 9). Seagrass metabolism (R and GPP) were mostly in balance throughout the year, although some months were net autotrophic (e.g. November, NEM = 39 $\text{mmol O}_2 \text{ m}^{-2} \text{ d}^{-1}$) or heterotrophic (e.g. August, NEM = -21 $\text{mmol O}_2 \text{ m}^{-2} \text{ d}^{-1}$). The lowest rates of R and GPP occurred in the winter (January mean R = -28 and mean GPP = 11) and the highest occurred in the summer (mean June R = -185 $\text{mmol O}_2 \text{ m}^{-2} \text{ d}^{-1}$ and

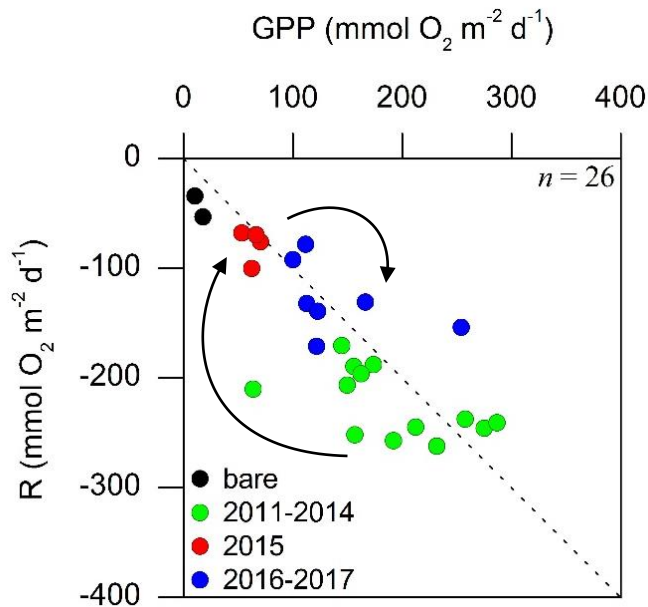


Fig. 8: Time course of seagrass ecosystem metabolism over the seagrass loss and partial recovery period in South Bay, plotted as daily respiration (R) versus gross primary production (GPP) for July and August 2011-2014 (green), 2015 (die-off event, red), and 2016–2017 (recovery, blue), in comparison to R and GPP at a bare site (Rheuban et al. 2014a). Arrows illustrate the time course of the die-off event.

mean GPP = $182 \text{ mmol O}_2 \text{ m}^{-2} \text{ d}^{-1}$). This follows seasonal patterns of seagrass shoot density in South Bay. A strong linear relationship ($p < 0.001$) was found between seagrass metabolism and seagrass shoot density over the 11-year period (Fig. 10), where seagrass shoot density explained 75% and 69% of the variability in monthly R and GPP, respectively.

The average annual R, GPP, and NEM for the 11-year period were 95.0, -94.0 , and $1.0 \text{ mmol O}_2 \text{ m}^{-2} \text{ d}^{-1}$, which corresponds to 0.36 moles of O_2 produced (and therefore 0.36 moles of CO_2 sequestered) by 1 m^2 of seagrass meadow per year. This NEM value is negligible and indicates South Bay is in a balanced metabolic state over the course of a year.

Discussion

This study synthesizes the most extensive dataset to date on seagrass metabolism, covering 115 full days derived from high-quality in situ oxygen fluxes measured by aquatic eddy covariance. The good agreement between hourly oxygen fluxes and metabolic rates obtained during parallel deployments with two systems demonstrates the reproducibility of our aquatic eddy covariance measurements and shows that this technique integrates well over the spatial heterogeneity at the site.

Over the 11-year time span, our measurements captured a wide range of environmental conditions and showed the highly variable nature of seagrass metabolism from daily to interannual

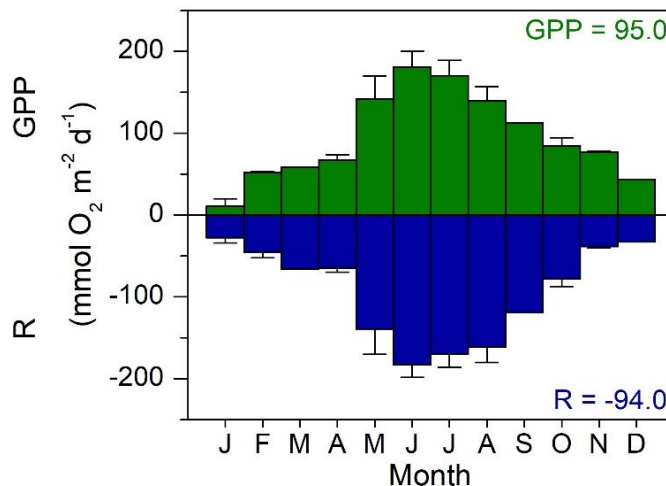


Fig. 9: Annual oxygen budget in South Bay, constructed by integrating over 11 years of seasonal measurements of gross primary production (GPP, green) and respiration (R, blue). Annual average GPP was $95.0 \text{ mmol O}_2 \text{ m}^{-2} \text{ d}^{-1}$ and annual average R was $-94.0 \text{ mmol O}_2 \text{ m}^{-2} \text{ d}^{-1}$, resulting in a net ecosystem metabolism (NEM) of $1.0 \text{ mmol O}_2 \text{ m}^{-2} \text{ d}^{-1}$.

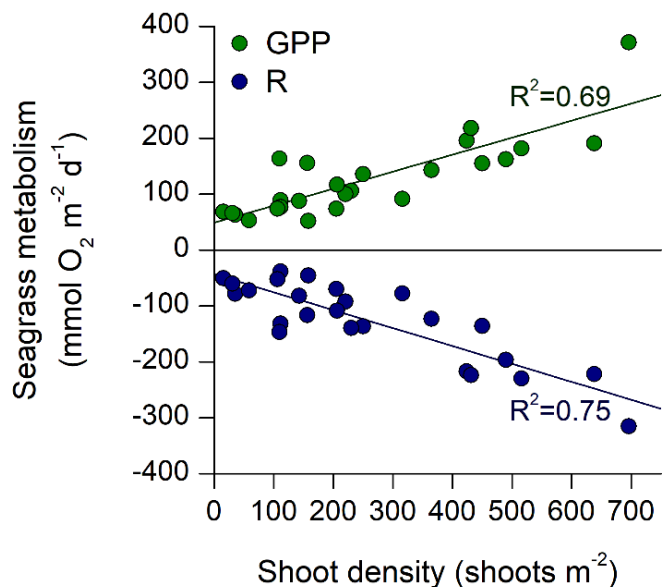


Fig. 10: Density as a driver of monthly seagrass gross primary production (GPP, green) and respiration (R, blue). Lines are lines of fit ($p < 0.001$). $N = 29$ monthly averages.

timescales. It allowed us to accurately quantify annual seagrass ecosystem metabolism from in situ measurements and determine the trophic status of the meadow over longer time scales than have been previously reported. The meadow was metabolically balanced over the 11-year period but varied between metabolic balance, autotrophy, and heterotrophy on an interannual scale. Our long-term measurements captured the resilience and recovery of the seagrass meadow from a marine heat wave that caused widespread seagrass loss. This caused a shift in trophic status to net heterotrophy during the summer of the die-off, and later to net autotrophy during the partial recovery in the following years. These results provide insights into the potential responses of other temperate systems where warming oceans may lead to increased seagrass heat stress events.

Annual net ecosystem metabolism

Our annual oxygen budget for the 11 years of this study indicates that seagrass metabolism in the South Bay meadow is lower than that recorded in other *Z. marina* meadows (Fig. 9, Table 3). Although it can be difficult to compare metabolic rates from different studies due to methodological differences, on a global scale most seagrass meadows tend to be net autotrophic (global average NEM = 27 mmol O₂ m⁻² d⁻¹; Duarte et al. 2010). This corresponds to a carbon uptake of 9.9 moles or 119 g per m² annually (Table 3), which is considerably higher than our estimated annual carbon sequestration rate for South Bay (4.4 g C m⁻² y⁻¹). Furthermore, our average R and GPP values are about half the global averages reported for seagrass meadows by Duarte et al. (2010) (Table 3), but still fall within the range of values reported.

Several natural factors may contribute to our lower average metabolic rates. First, South Bay is an oligotrophic environment, where nutrient limitation may result in lower metabolic rates.

Table 3: Minimum, maximum, and mean gross primary production (GPP), respiration (R), and net ecosystem metabolism (NEM) rates (in mmol O₂ m⁻² d⁻¹) from this study compared to rates reported by Duarte et al. (2010) for seagrass global, temperate, and *Zostera marina* sites. Average, minimum, and maximum metabolic rates are also reported for our site prior to the die-off event (before June 2015) and after the die-off event (June 2015 – June 2018).

Sites	References	GPP			R			NEM	
		mean	max	min	mean	max	min	mean	max
Global	Duarte et al. 2010	225	1300	0.4	188	1050	0.6	27	532
Temperate		166	795	5.9	130	606	12	34	532
<i>Zostera marina</i>		179	452	15	176	366	31	8.4	185
South Bay	this study	95	476	1.8	94	440	21	1.0	125
all data		135	476	29	137	440	20	-1.7	125
before die-off		92	254	1.8	84	229	31	8.4	100

Second, our metabolic rates integrate over a die-off and partial recovery event. Seagrass shoot density between summer 2015 and 2018 ranged from ~5 to 60% of its original value (Figs. 5c, 7c). Consequently, the range and mean of R and GPP also decreased after the die-off event by a factor of 1.6 to 1.9 relative to 2014 (Figs. 5, 8; Table 3). Metabolic rates averaged over the period prior to the die-off event match well those reported for the temperate sites and *Z. marina* meadows in Duarte et al. (2010) (Table 3).

When comparing these metabolic rates, it is important to note the difference in sampling techniques and the slight bias towards the spring and summer months in Duarte et al. (2010), which together accounted for 61% of the rates reported for temperate seagrass meadows in that study. While summer months have also been preferentially sampled in our study, our annual budget (Fig. 9) weighs each month equally and therefore takes into account monthly and seasonal variations in R and GPP throughout the year. For reference, a simple averaging of our 115 daily values of R and GPP would have yielded rates that were on average 35% larger than those obtained from our weighted annual budget.

In addition to sampling timing and frequency, the temporal and spatial scales of measurement are expected to yield different metabolic rates. For example, while some studies estimate seagrass metabolism from 24-hr benthic chamber incubations (e.g. Gazeau et al. 2005; Barrón and Duarte 2009; Apostolaki et al. 2010), others carry out short incubations (~1–4 hours) over midday or peak sunlight hours (e.g. Stutes et al. 2007; Anton et al. 2009). Primary production is strongly driven by light over hourly to diel timescales (e.g. Rheuban et al. 2014b; Berg et al. 2019), and as illustrated in Fig. 2c, such sampling strategies may therefore lead to overestimates of production. Measurements made at small spatial scales—either by measuring individual leaf or shoot productivity, or over a small surface area (often $< 0.25 \text{ m}^2$) on the benthos—may result in inaccurate estimates when scaled up to represent whole-ecosystem metabolism due to heterogeneous community composition or processes such as self-shading that affect metabolism over larger spatial scales (Pedersen et al. 2013). Most techniques for measuring seagrass metabolism are also intrusive and alter natural flow, light, and temperature conditions, which are known drivers of seagrass metabolism (e.g. Koch et al. 2006; Lee et al. 2007; Rheuban et al. 2014b). In order to obtain more accurate and comparable metabolic rates, it is therefore preferable to conduct measurements frequently and under natural, undisturbed environmental conditions.

The extensive amount of data we collected using the aquatic eddy covariance technique—115 days over the past decade—shows the highly variable nature of seagrass metabolism. This variability would not be captured by many approaches that have been used in the past. The variability also indicates that infrequent measurements made to represent an entire month, season, or year, could lead to inaccurate conclusions about trophic status. We found equal variability across these timescales, and trophic status fluctuating between autotrophy, metabolic balance, and heterotrophy (Figs. 4, 5). For example, seagrass metabolism in June 2014 varied between -83 (heterotrophic) and 84 (autotrophic) $\text{mmol O}_2 \text{ m}^{-2} \text{ d}^{-1}$, but the average NEM over all nine 24-hr records during this time reflected metabolic balance ($-22 \text{ mmol O}_2 \text{ m}^{-2} \text{ d}^{-1}$, not significantly different from zero). We show in Fig. 4 that the variability in paired R and GPP across all years during the month of June was almost as high as the variability expected across all seasons. Over the decade, our averaged annual metabolic rates include periods of high and low seagrass density, capturing variability that would not be reflected in a one-year study. For context, this within-site variability is as high as the variability observed between all temperate sites over a broad geographic range reported in Duarte et al. (2010) (Table 3). These examples illustrate that to accurately estimate annual NEM, it is crucial to integrate measurements that are made frequently enough over the targeted timescale to capture the natural variability.

Seasonal variations in seagrass ecosystem metabolism

Our results showed a strong linear relationship between seagrass ecosystem metabolism and seagrass shoot density (Fig. 10). This suggests that seagrass is the main driver of benthic ecosystem metabolism in South Bay. Throughout the 11-year record, seagrass density accounted for $\sim 70\%$ of the variability between seasons in R and GPP. Seasonal differences in temperature and light additionally affect production and respiration rates and are also reflected in seasonal biomass (e.g. Verhagenl and Nienhuis 1983; Orth and Moore 1986; Moore et al. 1997). Our long-term studies at this site show that biomass per shoot is consistent over time throughout the bay, so that density is a good proxy for seagrass biomass (McGlathery et al. 2012). High seagrass shoot density leads to higher GPP through increased primary producer biomass. It is also correlated with higher ecosystem respiration through increased plant and microbial respiration, the latter being fueled by oxygen and labile organic matter released from seagrass leaves, roots, and rhizomes (Wetzel and Penhale 1979; Frederiksen and Glud 2006). Dense seagrass canopies also contribute

indirectly to increased ecosystem respiration by promoting organic matter deposition in seagrass sediment (Gacia et al. 2002; Hendriks et al. 2008; Fourqurean et al. 2012).

This tight relationship explains why R and GPP over the course of a year (Fig. 9) follow the temporal patterns in seagrass biomass described for *Z. marina* populations in the region by Orth and Moore (1986) and measured in the present study. The highest rates of R and GPP occur in June and July, which corresponds to peak standing crop biomass and density. The following decrease in seagrass metabolism reflects the loss of leaves during the late-summer die-back, caused by high water temperatures. The low standing stock then persists until spring, with highest growth rates occurring during the late spring and early summer. This explains the rapid increase in R and GPP observed between April and June (Fig. 9).

We would expect to observe a period of net autotrophy during the growing season, yet when we averaged all NEM values between April and June, the system was in metabolic balance ($\text{NEM} = 0.08 \text{ mmol O}_2 \text{ m}^{-2} \text{ d}^{-1}$, $p = 0.10$, $n = 60$). This observation has two possible explanations. First, the tight correlation observed between R and GPP (Fig. 4a) shows that when GPP increases, ecosystem R increases as well, indicating fast internal cycling of carbon. Second, we propose that the daily rate of CO_2 uptake (measured by eddy covariance as O_2 release) needed to accumulate biomass between minimum and peak biomass is negligible. Specifically, we calculated a rough estimate for the amount of carbon that needs to be fixed per day to account for the seagrass biomass increase from January (minimum biomass) to June (maximum biomass). Biomass samples were collected in January and June 2015 according to the methods used by McGlathery et al. (2012). The biomass accumulation over these 5 months (51 g DW m^{-2}) correspond to a carbon accumulation of 0.1 g C m^{-2} per day, assuming carbon makes up 35% of seagrass biomass (McGlathery 2017). This carbon accumulation only requires a net uptake of $9.4 \text{ mmol CO}_2 \text{ m}^{-2} \text{ d}^{-1}$, which is negligible relative to our average R and GPP (Fig. 9), and explains why NEM values remain close to 0 during the seagrass growth period.

Carbon sink capacity

Quantifying the carbon retention capacity of seagrass meadows based on NEM includes carbon uptake through photosynthesis and carbon release through respiration. While these are balanced in South Bay over the 11-year period (average $\text{NEM} = 1.0 \text{ mmol O}_2 \text{ m}^{-2} \text{ d}^{-1}$), carbon accumulation and burial in the sediments also contribute to long-term carbon retention (e.g. Greiner et al. 2013; Duarte 2017; Oreska et al. 2017). Most of the sediment carbon at our study

R and GPP values and further indicates a fast internal cycling of carbon within the system (Fig. 11).

Seagrass disturbance and resilience

This study has shown how the significant loss of primary producer biomass in summer 2015 led to a large (~50%) decrease in both R and GPP (Fig. 8), and ultimately a shift in trophic status from balanced to net heterotrophic. This shift was likely caused by two processes: the loss of aboveground biomass, resulting in a decrease in photosynthesis and respiration carried out by the seagrass; and stimulation of microbial respiration by both increased organic matter inputs from the dead tissue and resuspension of sediment organic matter. Partial recovery from the die-off event also led to a shift in trophic status, this time towards net autotrophy ($NEM > 0$ in summer 2017), reflecting the increased production of seagrass biomass relative to community respiration (Figs. 5, 6, 8).

Disturbance events, like the one we have observed, have been shown to negatively affect sediment carbon storage (e.g. Thorhaug et al. 2017; Arias-Ortiz et al. 2018; Trevathan-tackett et al. 2018). The loss of seagrass biomass leads to reduced carbon accumulation in the sediment due to lower rates of primary production and the loss of canopy-flow interactions that promote sedimentation of particulate organic carbon. The loss of these interactions may further lead to increased sediment erosion, which exposes previously buried organic matter to oxic conditions and enhances its remineralization (Marbá et al. 2015). This effect has been observed in South Bay, where much of the carbon accumulated over the 14 years after its restoration was rapidly lost in patches where seagrass disappeared in 2015 (McGlathery et al. 2017). Studies have shown that such losses were followed by an increase in CO_2 emissions from seagrass meadows due to organic matter remineralization (Pendleton et al. 2012; Arias-Ortiz et al. 2018). Seagrass die-off events therefore induce loss of carbon accumulated over long time scales, with the added potential to create a positive climate feedback loop. This is particularly problematic given the increased frequency of coastal marine heatwaves in the past century (Oliver et al. 2018) causing seagrass die-off events around the world (e.g. Marbá and Duarte 2010; Arias-Ortiz et al. 2018) and especially threatening seagrass meadows like South Bay that are located at the edge of their thermal tolerance limits (Waycott et al. 2009). The dramatic seagrass decline in South Bay in response to prolonged heating during the growing season in summer 2015 highlights the vulnerability of such meadows to future climate scenarios.

Literature cited

- Anton, A., J. Cebrian, C. M. Duarte, K. L. H. Jr, and J. Goff. 2009. Low impact of hurricane Katrina on seagrass community structure and functioning in the northern Gulf of Mexico. *Bull. Mar. Sci.* 85: 45–59.
- Apostolaki, E. T., M. Holmer, N. Marbá, and I. Karakassis. 2010. Metabolic imbalance in coastal vegetated (*Posidonia oceanica*) and unvegetated benthic ecosystems. *Ecosystems* 13: 459–471. doi:10.1007/s10021-010-9330-9
- Arias-Ortiz, A., O. Serrano, P. Masqué, and others. 2018. A marine heatwave drives massive losses from the world’s largest seagrass carbon stocks. *Nat. Clim. Chang.* doi:10.1038/s41558-018-0096-y
- Barrón, C., and C. M. Duarte. 2009. Dissolved organic matter release in a *Posidonia oceanica* meadow. *Mar. Ecol. Prog. Ser.* 374: 75–84. doi:10.3354/meps07715
- Barrón, C., C. M. Duarte, M. Frankignoulle, and A. V. Borges. 2006. Organic carbon metabolism and carbonate dynamics in a Mediterranean seagrass (*Posidonia oceanica*) meadow. *Estuaries and Coasts* 29: 417–426.
- Beck, M. W., K. L. Heck, K. W. Able, and others. 2001. The Identification, Conservation, and Management of Estuarine and Marine Nurseries for Fish and Invertebrates. *Bioscience* 51: 633. doi:10.1641/0006-3568(2001)051[0633:TICAMO]2.0.CO;2
- Berg, P., M. L. Delgard, P. Polsenaere, K. J. McGlathery, S. C. Doney, and A. C. Berger. 2019. Dynamics of benthic metabolism, O₂, and pCO₂ in a temperate seagrass meadow. *Limnol. Oceanogr.* Ino.11236. doi:10.1002/Ino.11236
- Berg, P., R. N. Glud, A. C. Hume, H. Stahl, K. Oguri, V. Meyer, and H. Kitazato. 2009. Eddy correlation measurements of oxygen uptake in deep ocean sediments. *Limnol. Oceanogr.* 7: 576–584. doi:10.4319/lom.2009.7.576
- Berg, P., and M. Huettel. 2008. Integrated benthic exchange dynamics. *Oceanography* 21: 164–167.
- Berg, P., C. E. Reimers, J. H. Rosman, M. Huettel, M. L. Delgard, M. A. Reidenbach, and H. T. Özkan-Haller. 2015. Technical note: Time lag correction of aquatic eddy covariance data measured in the presence of waves. *Biogeosciences* 12: 6721–6735. doi:10.5194/bg-12-6721-2015
- Berg, P., H. Røy, F. Janssen, V. Meyer, B. B. Jørgensen, M. Huettel, and D. De Beer. 2003. Oxygen uptake by aquatic sediments measured with a novel non-invasive eddy-correlation technique. *Mar. Ecol. Prog. Ser.* 261: 75–83. doi:10.3354/meps261075
- Berg, P., H. Røy, and P. L. Wiberg. 2007. Eddy correlation flux measurements: The sediment surface area that contributes to the flux. *Limnol. Oceanogr.* 52: 1672–1684. doi:10.4319/lo.2007.52.4.1672
- Champenois, W., and A. V. Borges. 2012. Seasonal and interannual variations of community metabolism rates of a *Posidonia oceanica* seagrass meadow. *Limnol. Oceanogr.* 57: 347–361. doi:10.4319/lo.2012.57.1.0347
- Costanza, R., R. Arge, R. De Groot, and others. 1997. The value of the world’s ecosystem services and natural capital. *Nature* 387: 253–260. doi:10.1038/387253a0
- Duarte, C. M. 2017. Reviews and syntheses: Hidden forests, the role of vegetated coastal habitats

- in the ocean carbon budget. *Biogeosciences* 14: 301–310. doi:10.5194/bg-14-301-2017
- Duarte, C. M., H. A. Kennedy, N. Marbá, and I. Hendriks. 2013. Assessing the capacity of seagrass meadows for carbon burial: Current limitations and future strategies. *Ocean Coast. Manag.* 83: 32–38. doi:10.1016/j.ocecoaman.2011.09.001
- Duarte, C. M., I. J. Losada, I. E. Hendriks, I. Mazarrasa, and N. Marbá. 2016. Erratum: The role of coastal plant communities for climate change mitigation and adaptation (*Nature Climate Change* (2013) 3 (961-968)). *Nat. Clim. Chang.* 6: 802. doi:10.1038/nclimate3062
- Duarte, C. M., N. Marbá, E. Gacia, J. W. Fourqurean, J. Beggins, C. Barrón, and E. T. Apostolaki. 2010. Seagrass community metabolism: Assessing the carbon sink capacity of seagrass meadows. *Global Biogeochem. Cycles* 24: 1–8. doi:10.1029/2010GB003793
- Duarte, C. M., and Y. T. Prairie. 2005. Prevalence of Heterotrophy and Atmospheric CO₂ Emissions from Aquatic Ecosystems. 862–870. doi:10.1007/s10021-005-0177-4
- Durako, M. J. 1994. Seagrass die-off in Florida Bay (USA) - Changes in shoot demographic characteristics and population dynamics in *Thalassia testudinum*. *Mar. Ecol. Prog. Ser.* 110: 59–66. doi:10.3354/meps110059
- Ehlers, A., B. Worm, and T. B. H. Reusch. 2008. Importance of genetic diversity in eelgrass *Zostera marina* for its resilience to global warming. *Mar. Ecol. Prog. Ser.* 355: 1–7. doi:10.3354/meps07369
- Fenchel, T., and R. N. Glud. 2000. Benthic primary production and O₂-CO₂ dynamics in a shallow-water sediment : Spatial and temporal heterogeneity. *Ophelia* 53: 159–171. doi:10.1080/00785236.2000.10409446
- Fourqurean, J. W., C. M. Duarte, H. A. Kennedy, and others. 2012. Seagrass ecosystems as a globally significant carbon stock. *Nat. Geosci.* 5: 505–509. doi:10.1038/ngeo1477
- Fourqurean, J. W., and J. C. Zieman. 1991. Photosynthesis, respiration and whole plant carbon budget of the seagrass *Thalassia testudinum*. *Mar. Ecol. Prog. Ser.* 69: 161–170. doi:10.2307/44634775
- Fraser, M. W., G. A. Kendrick, J. Statton, R. K. Hovey, A. Zavala-Perez, and D. I. Walker. 2014. Extreme climate events lower resilience of foundation seagrass at edge of biogeographical range. *J. Ecol.* 102: 1528–1536. doi:10.1111/1365-2745.12300
- Frederiksen, M., D. Krause-jensen, M. Holmer, and J. Sund. 2004. Long-term changes in area distribution of eelgrass (*Zostera marina*) in Danish coastal waters. 78: 167–181. doi:10.1016/j.aquabot.2003.10.002
- Frederiksen, M. S., and R. N. Glud. 2006. Oxygen dynamics in the rhizosphere of *Zostera marina*: A two-dimensional planar optode study. *Limnol. Oceanogr.* 51: 1072–1083. doi:10.4319/lo.2006.51.2.1072
- Gacia, E., and C. M. Duarte. 2001. Sediment Retention by a Mediterranean *Posidonia oceanica* Meadow: The Balance between Deposition and Resuspension. *Estuar. Coast. Shelf Sci.* 52: 505–514. doi:10.1006/ecss.2000.0753
- Gacia, E., C. M. Duarte, and J. J. Middelburg. 2002. Carbon and nutrient deposition in a Mediterranean seagrass (*Posidonia oceanica*) meadow. *Limnol. Oceanogr.* 47: 23–32. doi:10.4319/lo.2002.47.1.0023
- Gazeau, F., C. M. Duarte, J.-P. Gattuso, and others. 2005. Whole-system metabolism and CO₂

- fluxes in a Mediterranean Bay dominated by seagrass beds (Palma Bay, NW Mediterranean). *Biogeosciences Discuss.* 1: 755–802. doi:10.5194/bgd-1-755-2004
- Gazeau, F., C. M. Duarte, J. Gattuso, and others. 2004. Whole-system metabolism and CO₂ fluxes in a Mediterranean Bay dominated by seagrass beds (Palma Bay, NW Mediterranean). *Biogeosciences Discuss.* 1: 755–802. doi:10.5194/bgd-1-755-2004
- Glud, R. N. 2008. Oxygen dynamics of marine sediments. *Mar. Biol. Res.* 4: 243–289. doi:10.1080/17451000801888726
- Glud, R. N., J. Woelfel, and U. Karsten. 2009. Benthic microalgal production in the Arctic : applied methods and status of the current database. *52*: 559–571. doi:10.1515/BOT.2009.074
- Greiner, J. T., K. J. McGlathery, J. Gunnell, and B. A. McKee. 2013. Seagrass Restoration Enhances “Blue Carbon” Sequestration in Coastal Waters. *PLoS One* 8: 1–8. doi:10.1371/journal.pone.0072469
- Greiner, J. T., G. M. Wilkinson, K. J. McGlathery, and K. A. Emery. 2016. Sources of sediment carbon sequestered in restored seagrass meadows. *Mar. Ecol. Prog. Ser.* 551: 95–105. doi:10.3354/meps11722
- Hansen, J. C. R., and M. A. Reidenbach. 2012. Wave and tidally driven flows in eelgrass beds and their effect on sediment suspension. *Mar. Ecol. Prog. Ser.* 448: 271–287. doi:10.3354/meps09225
- Hendriks, I. E., T. Sintes, T. J. Bouma, and C. M. Duarte. 2008. Experimental assessment and modeling evaluation of the effects of the seagrass *Posidonia oceanica* on flow and particle trapping. *Mar. Ecol. Prog. Ser.* 356: 163–173. doi:10.3354/meps07316
- Herzka, S. Z., and K. H. Dunton. 1997. Seasonal photosynthetic patterns of the seagrass *Thalassia testudinum* in the western Gulf of Mexico. *152*: 103–117.
- Hume, A. C., P. Berg, and K. J. McGlathery. 2011. Dissolved oxygen fluxes and ecosystem metabolism in an eelgrass (*Zostera marina*) meadow measured with the eddy correlation technique. *Limnol. Oceanogr.* 56: 86–96. doi:10.4319/lo.2011.56.1.0086
- Kendrick, G. A., M. J. Aylward, B. J. Hegge, M. L. Cambridge, K. Hillman, A. Wyllie, and D. A. Lord. 2002. Changes in seagrass coverage in Cockburn Sound , Western Australia between 1967 and 1999. *73*: 75–87.
- Kirk, J. T. O. 1983. Light and Photosynthesis in Aquatic Ecosystems. *J. Mar. Biol. Assoc. United Kingdom* 67: 863. doi:10.1017/S0025315400057143
- Koch, E., J. Ackerman, J. Verduin, and M. Keulen. 2006. Fluid dynamics in seagrass ecology - from molecules to ecosystems. *Seagrasses Biol. Ecol. Conserv.* 193–225. doi:10.1007/1-4020-2983-7
- Lamb, J. B., J. A. J. M. van de Water, D. G. Bourne, and others. 2017. Seagrass ecosystems reduce exposure to bacterial pathogens of humans, fishes, and invertebrates. *Science (80-.).* 355: 731–733. doi:10.1126/science.aal1956
- Lawson, S. E., P. L. Wiberg, K. J. McGlathery, and D. C. Fugate. 2007. Wind-driven sediment suspension controls light availability in a shallow coastal lagoon. *Estuaries and Coasts* 30: 102–112. doi:10.1007/BF02782971
- Lee, K.-S., S. R. Park, and Y. K. Kim. 2007. Effects of irradiance, temperature, and nutrients on

- growth dynamics of seagrasses: A review. *J. Exp. Mar. Bio. Ecol.* 350: 144–175.
doi:10.1016/j.jembe.2007.06.016
- Lee, X., W. J. Massman, and B. E. Law. 2004. *Handbook of micrometeorology : a guide for surface flux measurement and analysis*, Kluwer Academic Publishers.
- Levene, H. 1960. Robust tests for equality of variances. *Contrib. to Probab. Stat. Essays Honor Harold Hotell.* 279–292.
- Long, M. H., P. Berg, and J. L. Falter. 2015a. Seagrass metabolism across a productivity gradient using the eddy covariance, Eulerian control volume, and biomass addition techniques. *J. Geophys. Res. Ocean.* 120: 3624–3639. doi:10.1002/2014JC010352
- Long, M. H., P. Berg, K. J. McGlathery, and J. C. Zieman. 2015b. Sub-tropical seagrass ecosystem metabolism measured by eddy covariance. *Mar. Ecol. Prog. Ser.* 529: 75–90. doi:10.3354/meps11314
- Long, M. H., K. Sutherland, S. D. Wankel, D. J. Burdige, and R. C. Zimmerman. 2019. Ebullition of oxygen from seagrasses under supersaturated conditions. 1–11. doi:10.1002/lno.11299
- Lorrai, C., D. F. McGinnis, P. Berg, A. Brand, and A. Wüest. 2010. Application of oxygen eddy correlation in aquatic systems. *J. Atmos. Ocean. Technol.* 27: 1533–1546. doi:10.1175/2010JTECHO723.1
- Macreadie, P. I., P. H. York, and C. D. H. Sherman. 2014. Resilience of *Zostera muelleri* seagrass to small-scale disturbances: The relative importance of asexual versus sexual recovery. *Ecol. Evol.* 4: 450–461. doi:10.1002/ece3.933
- Marbá, N., A. Arias-Ortiz, P. Masqué, G. A. Kendrick, I. Mazarrasa, G. R. Bastyan, J. Garcia-Orellana, and C. M. Duarte. 2015. Impact of seagrass loss and subsequent revegetation on carbon sequestration and stocks. *J. Ecol.* 103: 296–302. doi:10.1111/1365-2745.12370
- Marbá, N., and C. M. Duarte. 2010. Mediterranean warming triggers seagrass (*Posidonia oceanica*) shoot mortality. *Glob. Chang. Biol.* 16: 2366–2375. doi:10.1111/j.1365-2486.2009.02130.x
- Martin, S., J. Clavier, J. M. Guarini, and others. 2005. Comparison of *Zostera marina* and maerl community metabolism. *Aquat. Bot.* 83: 161–174. doi:10.1016/j.aquabot.2005.06.002
- McGinnis, D. F., S. Cherednichenko, S. Sommer, P. Berg, L. Rovelli, R. Schwarz, R. N. Glud, and P. Linke. 2011. Simple, robust eddy correlation amplifier for aquatic dissolved oxygen and hydrogen sulfide flux measurements. *Limnol. Oceanogr. Methods* 9: 340–347. doi:10.4319/lom.2011.9.340
- McGlathery, K. J., L. K. Reynolds, L. W. Cole, R. J. Orth, S. R. Marion, and A. Schwarzschild. 2012. Recovery trajectories during state change from bare sediment to eelgrass dominance. *Mar. Ecol. Prog. Ser.* 448: 209–221. doi:10.3354/meps09574
- McGlathery, K. J., K. Sundbäck, and I. C. Anderson. 2007. Eutrophication in shallow coastal bays and lagoons: The role of plants in the coastal filter. *Mar. Ecol. Prog. Ser.* 348: 1–18. doi:10.3354/meps07132
- Moore, K. A., R. L. Wetzel, and R. J. Orth. 1997. Seasonal pulses of turbidity and their relations to eelgrass (*Zostera marina* L.) survival in an estuary. 215: 115–134.
- Nagelkerken, I., G. van der Velde, M. W. Gorissen, G. J. Meijer, T. Van't Hof, and C. den

- Hartog. 2000. Importance of Mangroves, Seagrass Beds and the Shallow Coral Reef as a Nursery for Important Coral Reef Fishes, Using a Visual Census Technique. *Estuar. Coast. Shelf Sci.* 51: 31–44. doi:10.1006/ecss.2000.0617
- Olivé, I., J. Silva, M. M. Costa, and R. Santos. 2016. Estimating Seagrass Community Metabolism Using Benthic Chambers: The Effect of Incubation Time. *Estuaries and Coasts* 39: 138–144. doi:10.1007/s12237-015-9973-z
- Oliver, E. C. J., M. G. Donat, M. T. Burrows, and others. 2018. Longer and more frequent marine heatwaves over the past century. *Nat. Commun.* 1–12. doi:10.1038/s41467-018-03732-9
- Oreska, M. P. J., K. J. McGlathery, J. H. Porter, H. Asmus, R. M. Asmus, and A. Vaquer. 2017. Seagrass blue carbon spatial patterns at the meadow-scale J. Cebrian [ed.]. *PLoS One* 12: e0176630. doi:10.1371/journal.pone.0176630
- Oreska, M. P. J., G. M. Wilkinson, K. J. McGlathery, M. Bost, and B. A. McKee. 2018. Non-seagrass carbon contributions to seagrass sediment blue carbon. *Limnol. Oceanogr.* 63: S3–S18. doi:10.1002/lno.10718
- Orth, R. J., T. I. M. J. B. Carruthers, W. C. Dennison, and others. 2006a. A Global Crisis for Seagrass Ecosystems. *Bioscience* 56: 987–996. doi:10.1641/0006-3568(2006)56
- Orth, R. J., M. L. Luckenbach, S. R. Marion, K. A. Moore, and D. J. Wilcox. 2006b. Seagrass recovery in the Delmarva Coastal Bays, USA. *Aquat. Bot.* 84: 26–36. doi:10.1016/j.aquabot.2005.07.007
- Orth, R. J., and K. J. McGlathery. 2012. Eelgrass recovery in the coastal bays of the Virginia Coast Reserve, USA. *Mar. Ecol. Prog. Ser.* 448: 173–176. doi:10.3354/meps09596
- Orth, R. J., K. J. McGlathery, and L. W. Cole. 2012. Eelgrass recovery induces state changes in a coastal bay system. *Mar Ecol Prog Ser* 448: 173–176. doi:10.3354/meps09522
- Orth, R. J., and K. A. Moore. 1986. Seasonal and Year-to Year Variations in the Growth of *Zostera marina* L.(Eelgrass) in the Lower Chesapeake Bay. *Aquat. Botany* 24: 335–341. doi:10.1017/CBO9781107415324.004
- Pedersen, O., T. D. Colmer, and K. Sand-jensen. 2013. Underwater photosynthesis of submerged plants – recent advances and methods. 4: 1–19. doi:10.3389/fpls.2013.00140
- Pendleton, L., D. C. Donato, B. C. Murray, and others. 2012. Estimating Global “Blue Carbon” Emissions from Conversion and Degradation of Vegetated Coastal Ecosystems. *PLoS One* 7. doi:10.1371/journal.pone.0043542
- Rasmussen, E. 1977. The wasting disease of eelgrass (*Zostera marina*) and its effects on environmental factors and fauna. *Seagrass Ecosyst.*
- Rheuban, J. E., and P. Berg. 2013. The effects of spatial and temporal variability at the sediment surface on aquatic eddy correlation flux measurements. *Limnol. Oceanogr. Methods* 11: 351–359. doi:10.4319/lom.2013.11.351
- Rheuban, J. E., P. Berg, and K. J. McGlathery. 2014a. Multiple timescale processes drive ecosystem metabolism in eelgrass (*Zostera marina*) meadows. *Mar. Ecol. Prog. Ser.* 507: 1–13. doi:10.3354/meps10843
- Rheuban, J. E., P. Berg, and K. J. McGlathery. 2014b. Ecosystem metabolism along a colonization gradient of eelgrass (*Zostera marina*) measured by eddy correlation. *Limnol.*

- Oceanogr. 59: 1376–1387. doi:10.4319/lo.2014.59.4.1376
- Robbins, B. D. 1997. Quantifying temporal change in seagrass areal coverage : the use of GIS and low resolution aerial photography. 58: 259–267.
- Romero, J., M. Perez, M. A. Mateo, and E. Sala. 1994. The belowground organs of the Mediterranean seagrass *Posidonia oceanica* as a biogeochemical sink.
- Safak, I., P. L. Wiberg, D. L. Richardson, and M. O. Kurum. 2015. Controls on residence time and exchange in a system of shallow coastal bays. *Cont. Shelf Res.* 97: 7–20. doi:10.1016/j.csr.2015.01.009
- Staehr, P. A., and J. Borum. 2011. Seasonal acclimation in metabolism reduces light requirements of eelgrass (*Zostera marina*). *J. Exp. Mar. Bio. Ecol.* 407: 139–146. doi:10.1016/j.jembe.2011.05.031
- Stutes, J., J. Cebrián, A. L. Stutes, A. Hunter, and A. A. Corcoran. 2007. Benthic metabolism across a gradient of anthropogenic impact in three shallow coastal lagoons in NW Florida. *Mar. Ecol. Prog. Ser.* 348: 55–70. doi:10.3354/meps07036
- Terrados, J., and C. M. Duarte. 2000. Experimental evidence of reduced particle resuspension within a seagrass (*Posidonia oceanica* L.) meadow. *J. Exp. Mar. Bio. Ecol.* 243: 45–53. doi:10.1016/S0022-0981(99)00110-0
- Thorhaug, A., H. M. Poulos, J. López-Portillo, T. C. W. Ku, and G. P. Berlyn. 2017. Seagrass blue carbon dynamics in the Gulf of Mexico: Stocks, losses from anthropogenic disturbance, and gains through seagrass restoration. *Sci. Total Environ.* 605–606: 626–636. doi:10.1016/j.scitotenv.2017.06.189
- Trevathan-tackett, S. M., C. Wessel, J. Cebrián, P. J. Ralph, P. Masqué, and P. I. Macreadie. 2018. Effects of small- - induced seagrass loss on blue carbon storage : Implications for management of degraded seagrass ecosystems. 1351–1359. doi:10.1111/1365-2664.13081
- Verhagenl, J. H. G., and P. H. Nienhuis. 1983. A Simulation Model of Production , Seasonal Changes in Biomass and Distribution of Eelgrass (*Zostera marina*) in Lake Grevelingen. 10: 187–195.
- Waycott, M., C. M. Duarte, T. J. B. Carruthers, and others. 2009. Accelerating loss of seagrasses across the globe threatens coastal ecosystems. *Proc. Natl. Acad. Sci.* 106: 12377–12381. doi:10.1073/pnas.0905620106
- Wetzel, R. G., and P. A. Penhale. 1979. Transport of carbon and excretion of dissolved organic carbon by leaves and roots/rhizomes in seagrasses and their epiphytes. *Aquat. Bot.* 6: 149–158. doi:10.1016/0304-3770(79)90058-5

CHAPTER 2: TEMPERATURE THRESHOLD FOR SEAGRASS (*ZOSTERA MARINA*) METABOLISM DERIVED FROM IN SITU AQUATIC EDDY COVARIANCE MEASUREMENTS

Amelie C. Berger, Peter Berg

This chapter will soon be submitted for publication in Limnology and Oceanography letters.

Abstract

Seagrass meadows are increasingly threatened by warming oceans. It is therefore essential to enhance our understanding of the stress response of seagrass to increasing temperatures and extreme heating events. This study relies on an extensive database of hourly aquatic eddy covariance data on seagrass (*Zostera marina*) metabolism measured in a 20 km² restored meadow at the Virginia Coast Reserve (VCR) (USA) to determine, for the first time, the temperature stress threshold (T_{th}) of *Z. marina* under naturally varying in situ conditions. We used a non-linear model to identify 28.6°C as the threshold above which substantial negative effects on net photosynthesis are observed. On average, daytime oxygen fluxes decreased by 50% on afternoons when T_{th} was exceeded, which shifted daily net ecosystem metabolism from metabolic balance to net heterotrophy and therefore a loss in carbon. This study highlights the vulnerability of eelgrass to future warming projections in the Mid-Atlantic region and globally.

Introduction

Seagrass meadows provide valuable ecosystem service to coastal areas (e.g. Costanza et al. 1997; Beck et al. 2001; Koch et al. 2009) and play an important role as significant carbon sinks in the global carbon cycle, due to high rates of primary production and carbon burial in their sediments (Duarte et al. 2010; Fourqurean et al. 2012; Oreska et al. 2017). However, seagrass ecosystems worldwide have been declining as a result of increasing global temperatures and local extreme events during which water temperatures exceed the thermal tolerance limits of the species (e.g. Moore and Jarvis 2008; Marbá and Duarte 2010; Arias-Ortiz et al. 2018; Berger et al. 2020). Such die-off events not only cause the loss of seagrass ecosystem services, but may also trigger substantial CO₂ emissions from seagrass meadows through the remineralization of previously buried organic matter (Pendleton et al. 2012; Arias-Ortiz et al. 2018). To better anticipate changes

in seagrass ecosystems under future warming scenarios, it is critical to enhance our understanding of seagrass response to thermal stress.

Temperature effects on seagrass growth are complex and not fully clarified. It is well-known that increasing temperatures stimulate seagrass photosynthesis until reaching an optimum temperature threshold (T_{th}) (e.g. Marsh et al. 1986; Lee et al. 2007). Beyond this threshold, increasing temperatures cause thermal damage to the photosynthetic apparatus (Wahid et al. 2007; York et al. 2013), and the photosynthetic efficiency of the plant declines (e.g. Marsh et al. 1986; Abe et al. 2008; Niu et al. 2012). Respiration, however, increases more rapidly than photosynthesis with increasing temperature and continues to do so well-past T_{th} . This metabolic imbalance leads to a carbon deficit within the plants, which results in impaired growth and loss of seagrass biomass (Moore et al. 2006; Lee et al. 2007; Collier et al. 2011; Ewers 2013). It is no surprise, therefore, that determining T_{th} for seagrass species has been the focus of many studies aiming to better understand the impacts of thermal stress on seagrasses (e.g. Nejrup and Pedersen 2008; Collier et al. 2011; Pedersen et al. 2016; Egea et al. 2019; Rasmusson et al. 2020).

Eelgrass (*Zostera marina*) is a widespread temperate seagrass species that is particularly at risk of local extinction at the southern edge of its distribution off the Mid-Atlantic coast (Koch and Orth 2003; Wilson and Lotze 2019), due to the expected increase in the frequency, duration, and intensity of extreme heating events throughout the 21st century (Frölicher et al. 2018; Oliver et al. 2019). The temperature threshold for *Z. marina* has been estimated between 25–30°C (Lee et al. 2007). Some studies relate T_{th} to changes in seagrass biomass or cover, taking advantage of large spatial scales and long timeseries (Lefcheck et al. 2017; Paul Richardson et al. 2018; Shields et al. 2019). However, the temporal resolution of seagrass cover or biomass data is often coarse (monthly to biennially), and the estimated T_{th} may not accurately reflect the temperature at which seagrasses become physiologically stressed. Other studies aiming to determine this critical threshold do so by incubating leaf fragments (e.g. Marsh et al. 1986; Rasmusson et al. 2020) or whole shoots (Nejrup and Pedersen 2008) at discrete temperature intervals (often 2–5°C) and under controlled light conditions. Leaf fragment incubations last for a few hours, while whole-shoot incubations last several weeks. Photosynthetic rates and growth parameters such as new leaf production and leaf elongation are usually measured at the end of the experiment. These studies provide valuable insights into the thermal limits of seagrasses, but are difficult to apply at the ecosystem-scale given that they were performed under controlled conditions and often excluded

non-photosynthetic organs (roots and rhizomes), which play an important role in whole-plant carbon balance and therefore seagrass response to temperature stress.

To more realistically constrain T_{th} for eelgrass ecosystems, it is critical to measure in situ eelgrass metabolism under naturally varying environmental conditions. Our goal in this study was to determine T_{th} in a vulnerable eelgrass meadow at the southern edge of the species' distribution. To do this, we relied on a substantial database of in situ eelgrass ecosystem metabolism measured by aquatic eddy covariance (AEC) at the Virginia Coast Reserve (VCR) (Hume et al. 2011; Rheuban et al. 2014a; b; Berger et al. 2020; this study). This technique is a relative new approach for measuring instantaneous changes in seagrass metabolism as a result of naturally fluctuating temperatures, as it is non-invasive (Lorrai et al. 2010) and measures benthic oxygen fluxes at a high temporal resolution (Rheuban and Berg 2013) over a 10–100 m² footprint (Berg et al. 2007), thus capturing whole-ecosystem processes. Preliminary data analyses of binned cool days (temperatures < 25°C) and hot days (afternoon temperatures > 28°C) revealed a strong negative effect of temperature threshold exceedance on our measured oxygen fluxes (Fig. 1). This motivated further investigation into the precise threshold at which this negative effect occurs. We used a modeling approach on these high-quality data to determine, for the first time, the precise temperature stress threshold for eelgrass based on in situ measurements.

Methods

Study site

The VCR Long-Term Ecological Research (VCR-LTER) site, located along the Atlantic side

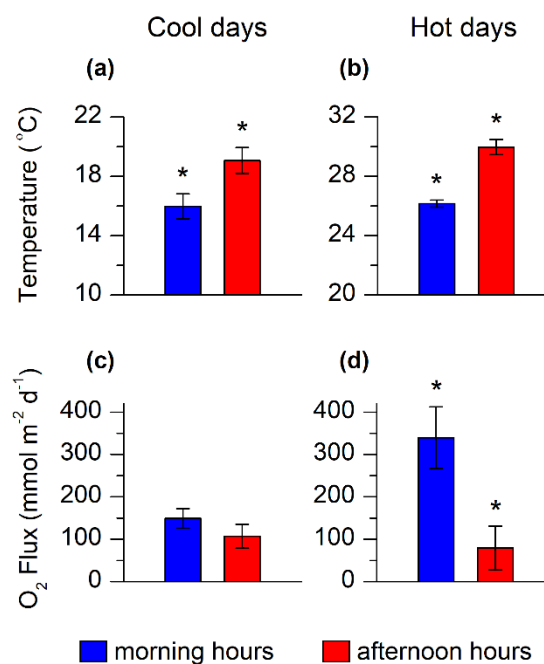


Fig. 1: High temperatures significantly affect seagrass metabolism. Mean temperature (**a**, **b**) and oxygen flux (**c**, **d**) during 3 hours in the morning (blue) and 3 hours in the afternoon (red) were compared for a subset of 6 days where water temperatures were relatively cool (14–22°C) (**a**, **c**) and 7 days where water temperatures exceeded the proposed 28°C threshold (Moore and Jarvis, 2008) in the afternoon (**b**, **d**). These bins were produced to have similar PAR levels in the morning and afternoon, to ensure any observed differences in oxygen fluxes would not result from varying light conditions. Error bars are \pm SE ($n = 18$ and 21 for cool days and hot days, respectively). Asterisks designate statistically significant differences between morning and afternoon hours ($p < 0.05$).

of the Delmarva Peninsula, is home to the largest successful eelgrass restoration project in the world (Orth and McGlathery 2012). This study took place in South Bay, which contains the largest of four previously restored eelgrass meadows at this site ($\sim 20 \text{ km}^2$ as of 2018, Orth et al. *in review*). Our measurements were conducted in the original restoration area of the meadow, a 7 km^2 region located just west of a barrier island and connected to the Atlantic Ocean by two inlets north and south of the meadow. This creates a low-energy hydrodynamic environment where light conditions are favorable to seagrass growth (Lawson et al. 2007). South Bay is shallow (mean water depth = 1.2 m) and experiences semi-diurnal tides with a tidal range of 1 m. The eelgrass meadows of the VCR-LTER are growing close to the southern geographical limit for *Z. marina* (Moore et al. 2006).

In June 2015, the VCR-LTER region experienced a marine heatwave, which led to a dramatic eelgrass die-off event in South Bay (Aoki et al. 2021, Berger et al. 2020). Long-term seagrass monitoring efforts at the six original restoration plots at the center of South Bay captured this $\sim 90\%$ decline in eelgrass shoot density and its slow recovery in the following years (Aoki et al. 2021, Berger et al. 2020).

Eelgrass ecosystem metabolism was measured via AEC at two sites in South Bay: one in northern part of the meadow (“northern site,” $37^\circ 16' 34.2'' \text{N}$, $75^\circ 48' 44.4'' \text{W}$); and one in the center of the meadow (“center site,” $37^\circ 15' 43.6'' \text{N}$, $75^\circ 48' 54.6'' \text{W}$). The center site is one of the original restoration plots and has been part of a long-term study (2007–2018) on eelgrass metabolism measured by AEC (Berger et al. 2020). In summer 2019, the northern site was added to our study design and we measured eelgrass metabolism alternately at both sites throughout the summer. Current speeds during the summer months at the center site range from 0.2 to 14.5 cm s^{-1} (mean: 3.1 cm s^{-1}), and those at the northern site range from 0.4 to 16.2 cm s^{-1} (mean: 5.1 cm s^{-1}).

Seagrass metabolism measurements by aquatic eddy covariance

Seagrass ecosystem metabolism was measured using the AEC technique (Berg et al. 2003), applied here as described in detail in Berger et al. (2020). Briefly, this technique uses high-resolution (16–64 Hz) measurements of dissolved oxygen and current velocity (x, y, z) to derive in situ benthic oxygen fluxes over $10\text{--}100 \text{ m}^2$, thus capturing ecosystem-scale processes under naturally varying light, flow, and temperature conditions. The oxygen and velocity sensors are mounted on a thin, stainless steel frame designed to minimize disturbances to natural flow (Berg and Huettel 2008).

In this study, we used a mix of previously-collected and novel benthic flux data (Hume et al. 2011; Rheuban et al. 2014a; b; Berger et al. 2020), focusing on the spring and summer months between 2014 and 2018 ($n = 60$ days). During summer 2019, we measured benthic fluxes for 3–7 consecutive days (usually 1 to 4 deployments, each 24–48 hours in duration), alternating between the center and northern site (Fig. 1), totaling 45 days of data over the summer. For this new sampling period, we used a RINKO-EC micro planar optode (JFE Advantech, Japan) to measure dissolved oxygen, as opposed to the Clark-Type microelectrodes (Unisense) used through 2018. The RINKO-EC sensor was considerably less fragile, thus ensuring a larger deployment success rate. Due to its larger tip size (8 mm), and to not interfere with concurrent velocity measurements, the sensor was placed 1.5 cm away from the edge of the velocity sensor’s measuring volume, which was set at 30 cm above the seafloor. To account for the time lag between velocity and oxygen concentration measurements resulting from this distance, we applied a time-shift correction that maximized the covariance between w' and C' over a 0–2 s period. Because of its tip size, the RINKO-EC sensor can potentially interfere the velocity measurements (Huettel et al. 2020). We therefore deployed two AEC systems side-by-side, facing in opposite direction to measure benthic oxygen fluxes during flood tide and ebb tide, respectively. This ensured maximum measurement accuracy throughout the tidal cycle. The systems were deployed 10 m apart so their footprints would not overlap. When processing the data collected by each system, we excluded data collected while the main current direction came from behind the sensor. During slack tide, we treated data on a case by case basis, often averaging the fluxes from both systems.

All AEC deployments coincided with measurements of photosynthetically active radiation (PAR), and water temperature. We used 2π Odyssey PAR loggers to measure PAR at 5 min intervals, and PME miniDOT[®] optodes to measure dissolved oxygen concentration and temperature at 1 min intervals. Both sensors were deployed at the top of the canopy, 30 cm above the sediment surface.

Identifying the temperature stress threshold

To determine the eelgrass thermal stress threshold T_{th} , we derived the relationship between oxygen fluxes and PAR and temperature from our measured in situ hourly data (Fig. 2). In short, this model describes a P-I relationship under non-stressful temperatures (Fig. 2a), and an attenuated P-I relationship under stressful temperatures (Fig. 2a, b). The model identifies the temperature T_{th} at which net photosynthesis deviates from that which would be expected solely

from a P-I relationship (Fig. 2c, e). The underlying P-I relationship also accounts for variations in respiration throughout the diel cycle—decreasing linearly at a rate of $4.9 \text{ mmol O}_2 \text{ m}^{-2} \text{ hr}^{-1}$ during the night and increasing by the same rate throughout the day (Juska and Berg, *in prep*). The decrease in net photosynthesis detected by our model can therefore be attributed uniquely to the effects of temperature threshold exceedance.

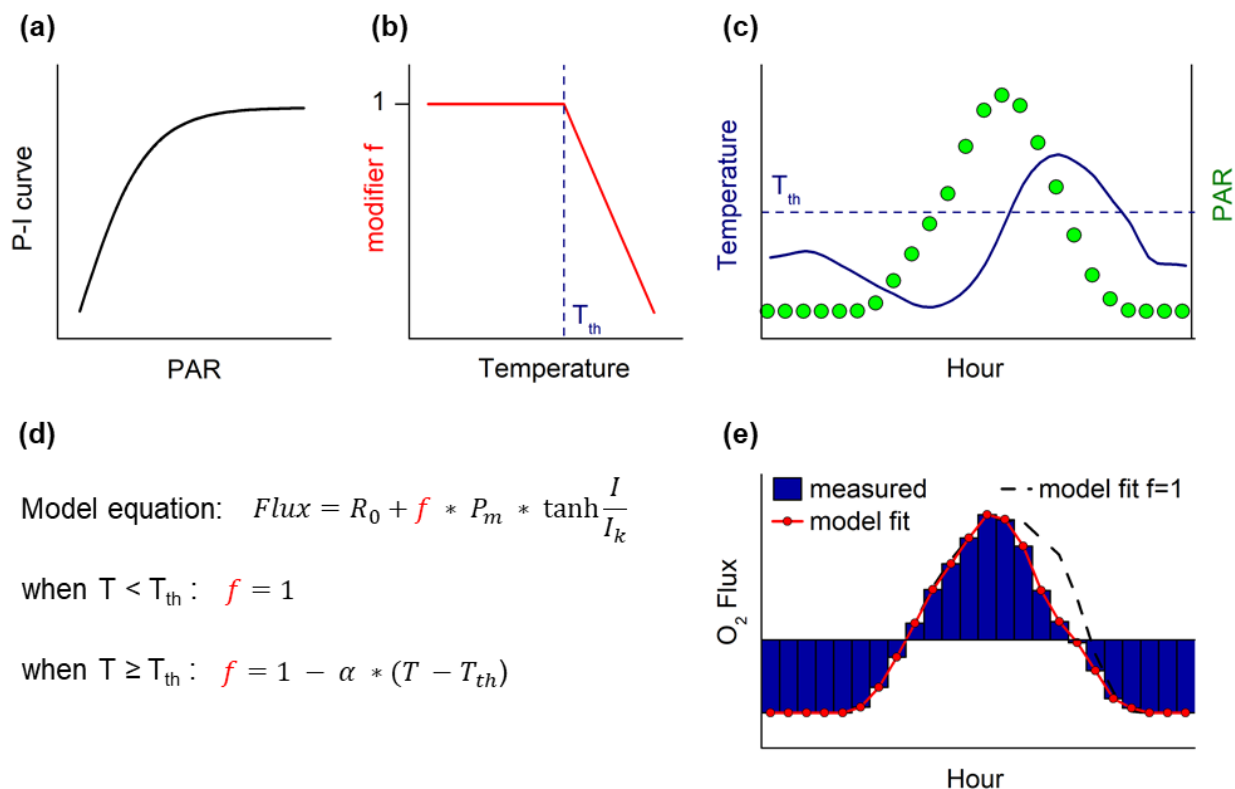


Fig. 2: Conceptual representation of the model used to determine the temperature threshold (T_{th}) above which seagrass metabolism is negatively affected. The model equation (d) is essentially that of a P-I curve (a) modified by a factor f (b), which is equal to 1 when temperature $< T_{th}$ and < 1 when temperature $\geq T_{th}$. The fitting parameters were R_0 (average dark respiration), which decreased linearly at a rate of $4.9 \text{ mmol O}_2 \text{ m}^{-2} \text{ hr}^{-1}$ during nighttime hours, and increased by the same rate during the day; P_m (maximum net photosynthetic rate); I (available light, i.e. PAR); I_k (light saturation); T_{th} (temperature threshold); and α (constant). (c) and (e) show an ideal set of hourly temperature (blue line), PAR (green dots), and oxygen fluxes (blue bars). Red line: oxygen fluxes predicted by our model. Dashed line: oxygen fluxes predicted by a simple P-I curve when $f = 1$.

This program was run on five subsets of our hourly data where the range of temperatures was sufficiently large (on average from $25\text{--}31^\circ\text{C}$) to capture the effects of increasing temperatures on seagrass metabolism. Each of these subsets contained 36–89 hours of data and were binned by hour of day to represent a full diel cycle. The program was also run on all subsets combined ($n = 356$ hours). Typically, 16.8×10^8 iterations were used to produce an accurate fit to the measured data.

Results

Effects of thermal stress on seagrass metabolism

To determine the exact temperature threshold at which seagrass net photosynthesis decreases, we fit our model (Fig. 2) to oxygen flux data (binned by hour of day, $n = 356$ hours) selected from periods of high water temperatures (ranging from 26–30°C) in June 2015, 2019, and July 2019 (Fig. 3). Figure 3 illustrates our model fit compared to that of a simple P-I fit on oxygen flux data pulled from April 2015, 2017, and 2018, and similarly binned by hour of day ($n = 429$ hours, temperatures ranging from 15–18°C). Positive oxygen fluxes represent a release of oxygen (due to photosynthesis), and negative oxygen fluxes represent oxygen uptake (respiration). While the P-I relationship accurately ($R^2 = 0.99$) predicted oxygen fluxes during cool days, it would have

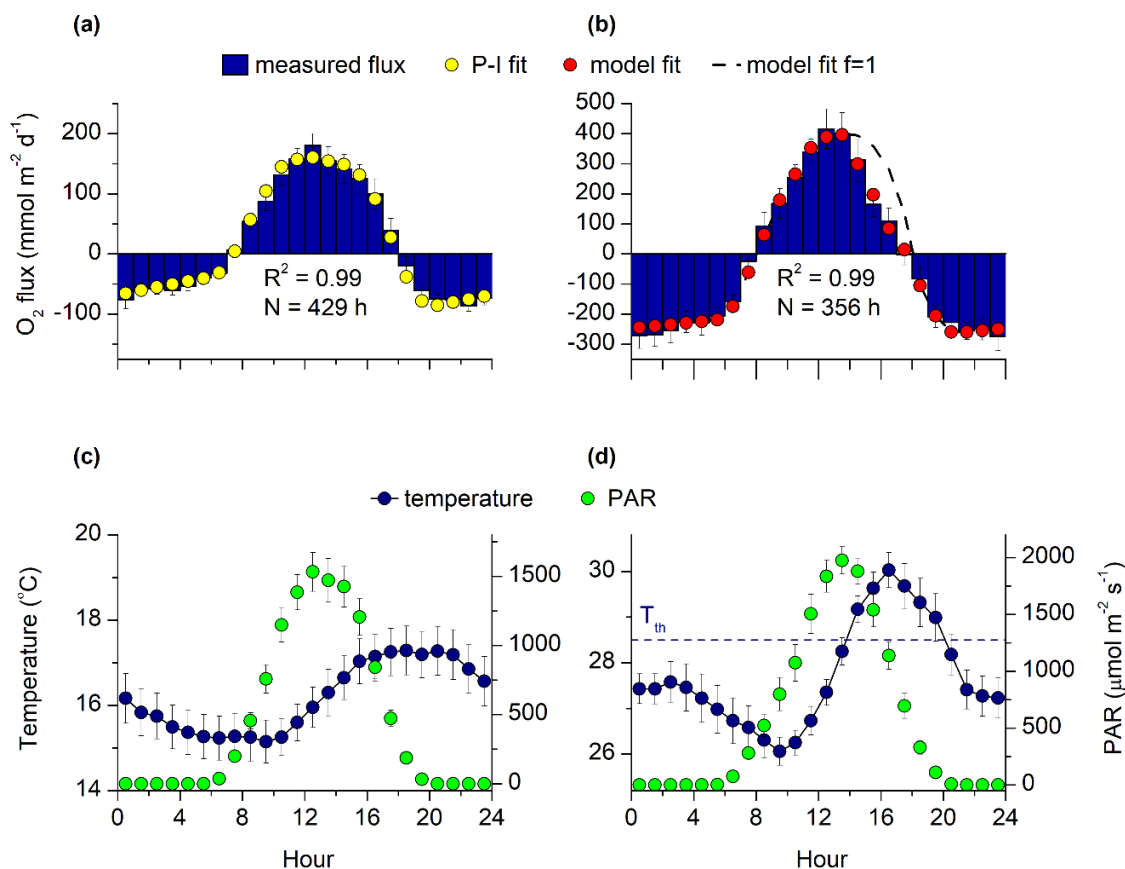


Fig. 3: Oxygen flux (blue bars), temperature (blue dots), and PAR (green dots) measured in April 2015, 2017, and 2018 (**a, c**) and June 2015, 2019 and July 2019 (**b, d**), binned by hour of day ($n = 429$ and 356 hours binned, respectively). Temperatures in April ranged from 15.1°C to 17.3°C, and summer temperatures ranged from 26.1°C to 30.0°C. Yellow dots: oxygen fluxes predicted by a P-I relationship (**a**). Red dots: oxygen fluxes predicted by our model (**b**). Dashed line in (**b**): predicted oxygen fluxes by our model if the effects of temperature were not accounted for (f set equal to 1). Error bars are \pm SE.

overestimated afternoon fluxes during hot days, as shown in Figure 3b (dashed line) where the modifier f was set to 1. When our model took into account the existence of a temperature threshold, the decrease in net photosynthesis as a result of thermal stress was well predicted ($R^2 = 0.99$, Fig. 3b). The oxygen flux predicted by our model after T_{th} was exceeded was 26% lower than what a simple P-I relationship would have predicted. The largest difference in oxygen flux prediction occurred at hour 16.5 (Fig. 3b), where the predicted oxygen flux under thermal stress was 70% lower than that predicted without accounting for T_{th} . On average, our model correctly predicted afternoon fluxes ~50% lower than what a simple P-I relationship would have predicted. This difference accounts for a cumulative 577 mmol O₂ m⁻² d⁻¹.

Our model was then fit to the individual warm periods ($n = 36$ –89 hours of data each, binned by hour of day) during summers 2015 and 2019 and the model outputs (T_{th} , α , R_0 , P_m , and I_k) and fit (R^2) are shown in Table 1. Our model fit each dataset extremely well ($R^2 = 0.9$ –1), and produced temperature threshold estimates between 27.8–29.5°C, averaging 28.6°C.

Table 1: Model results from 6 runs on aquatic eddy covariance data from June 2015, 2019 and July 2019 at the northern and center sites. T_{th} = temperature threshold (°C), α = parameter where $f = 1 - \alpha * (T - T_{th})$, R_0 = average nighttime respiration (mmol O₂ m⁻² d⁻¹), P_m = maximum photosynthetic rate (mmol O₂ m⁻² d⁻¹), and I_k = light saturation constant (μ mol m⁻² s⁻¹). N is given in hours, and R^2 is the coefficient of determination.

Warm period	Site	T_{th}	α	R_0	P_m	I_k	R^2	N
All data	both	28.6	0.2	-242	684	1161	0.99	356
June 2015	center	29.1	0.7	-127	338	1002	0.97	84
June 2019	center	28.1	0.05	-159	442	961	0.96	36
July 2019	northern	27.9	0.2	-336	825	1130	0.95	80
July 2019	center	28.8	0.3	-235	841	1718	0.92	89
late July 2019	northern	29.3	0.2	-294	1738	2334	0.92	67
Average		28.6						

Discussion

A key aspect in understanding seagrass response to thermal stress is knowing the temperature threshold above which negative effects on seagrass production are observed. Many studies have addressed this question (e.g. Marsh et al. 1986; Hammer et al. 2018; Rasmusson et al. 2020). However, they relied on ex situ approaches. Here we combined a non-linear model with

our extensive database of hourly oxygen fluxes measured in situ by AEC under naturally varying field conditions to identify a 28.6°C thermal tolerance threshold *Z. marina* at the ecosystem scale.

Temperature threshold

Our temperature threshold estimate of 28.6°C agrees well that of some other studies conducted on *Z. marina* at its thermal distribution boundary (Moore and Jarvis 2008; Carr et al. 2012; Shields et al. 2018). Carr et al. (2012) found a threshold of 28.5°C using a vegetation growth model for eelgrass at the VCR, while Moore and Jarvis (2008) and Shields et al. (2018) related seagrass declines in the Chesapeake Bay to temperatures above 28°C. Other studies identified a similar range for T_{th} between 25 and 30°C (e.g. Marsh et al. 1986; Hammer et al. 2018; Rasmusson et al. 2020). However, their approaches involved ex-situ incubations at discrete and coarse temperature intervals (often from 25 or 27°C to 30°C, and thus skipping 28°C) and were therefore unable to identify a precise temperature threshold (e.g. Hammer et al. 2018 estimated T_{th} fell between 26°C and 30°C).

Globally, however, T_{th} estimates for *Z. marina* vary between 16–35°C, and average ~20°C (Lee et al. 2007). This variation is largely attributed to latitude. For example, eelgrass populations growing in Massachusetts (USA), Denmark, and Korea have shown decreased photosynthesis and growth at temperatures exceeding 20°C (Marsh et al. 1986; Lee et al. 2005; Nejrup and Pedersen 2008). In China, negative temperature effects were observed above 16–20°C (Niu et al. 2012). These geographical differences in thermal stress tolerance suggest there are eelgrass “eco-types,” i.e. different populations that are genetically adapted to the environmental conditions where they are growing (Nejrup and Pedersen 2008). Eelgrass populations acclimated to lower temperatures, however, would likely be much more vulnerable to global warming and temperatures reaching 28.6°C compared to populations at the low-latitude edge of the specie’s geographical distribution.

The large range in temperature threshold estimates may also result from different methodological approaches. Lab incubations are conducted under controlled environmental conditions (namely PAR, e.g. Abe et al. 2008) and for different lengths of time – from 15–30 min (Marsh et al. 1986) to 6 weeks (Nejrup and Pedersen 2008). Some may also only incubate leaf fragments (e.g. Marsh et al. 1986; Dennison 1987; Rasmusson et al. 2020) instead of whole shoots. Consequent metabolism measurements may therefore be overestimated as they exclude the respiration rates of seagrass roots and rhizomes, which are important to the carbon balance of the plant (Pregnall et al. 1984). While whole-shoot incubations include below-ground biomass (e.g.

Nejrup and Pedersen 2008), it may still be difficult to extrapolate results to represent ecosystem scale processes where intact shoots rooted in the sediment are growing under naturally fluctuating environmental conditions. We therefore have confidence in our $T_{th} = 28.6^{\circ}\text{C}$ estimate as it results from high quality, ecosystem scale, in situ seagrass metabolism data that were successfully matched by our model predictions (Fig. 3, Table 1). Our use of continuous environmental data also enabled us to produce a more precise estimate for the thermal tolerance threshold of eelgrass.

Effects of thermal stress on seagrass metabolism

Our results showed a strong, negative effect of temperature threshold exceedance on seagrass metabolism (Fig. 3). We found a reduction in net photosynthesis of up to 70%, coinciding with peak temperature during the 24-hour cycle (Fig. 3b, d). On average, net photosynthesis was reduced by 50% compared to photosynthetic rates under the same light levels but non-stressful temperature conditions (Fig. 3b). Nejrup and Pedersen (2008) found a comparable decrease in eelgrass photosynthetic rates above 25–30°C. This decline in net oxygen flux reflects both the inhibition of photosynthesis at high temperatures and increased respiration, which may result in a metabolic shift towards heterotrophy. In fact, the gross primary production calculated from our 24-hour cycle (comprised of 356 hours of oxygen fluxes on hot days, Fig. 3b) was 11% lower ($\text{GPP} = 213 \text{ mmol O}_2 \text{ m}^{-2} \text{ d}^{-1}$) compared to that calculated from fluxes predicted by a simple P-I relationship ($\text{GPP} = 238 \text{ mmol O}_2 \text{ m}^{-2} \text{ d}^{-1}$, dashed line in Fig. 3b). This difference was enough to result in a negative carbon balance (net ecosystem metabolism = $-30.6 \text{ mmol O}_2 \text{ m}^{-2} \text{ d}^{-1}$), whereas under non-stressful temperatures the meadow would have been in metabolic balance (net ecosystem metabolism = $-3.6 \text{ mmol O}_2 \text{ m}^{-2} \text{ d}^{-1}$).

Carbon balance plays a critical role in the response of eelgrass to stress. Under high temperature conditions, seagrass carbon acquisition is reduced, and the plant allocates more energy to maintenance or repair processes to withstand heat stress, rather than allocating resources to growth, reproduction, and storage (Sokolova 2013; Moreno-Marín et al. 2018). This not only affects seagrass survival and resilience through reduce growth and increased mortality (Marsh et al. 1986; Moreno-Marín et al. 2018), but through decreased reproductive performance as well (Johnson et al. 2020; Qin et al. 2020). In addition to increased seagrass die-off events, the increase in frequency and severity of extreme events (Oliver et al. 2019) may erode the ability of eelgrass to maintain their habitats and genetic diversity and therefore their resilience and adaptability to climate change (Ehlers et al. 2008).

Future projections for Z. marina

Eelgrass at the VCR is growing at the southern thermal boundary of the species' geographic range (Moore and Jarvis 2008). This study supports the idea that this ecosystem is increasingly vulnerable to temperature stress, as negative effects can be seen beyond 28.6°C, a temperature threshold often exceeded in the summertime. This suggests eelgrass population at higher latitudes will be more vulnerable to warming and extreme temperature events. Future warming scenarios project an average shift of the southern eelgrass range by 1.4–6.5°N by 2100, which would result in complete eelgrass loss in the VCR and Chesapeake Bay region (Wilson and Lotze 2019). While this may lead to a community shift to more heat tolerant seagrass species (Moreno-Marín et al. 2018; Shields et al. 2019), the consequences on the ecosystem service of eelgrass meadows, particularly carbon storage, may be extreme. The ongoing increase in ocean temperatures and the frequency of severe heating events calls for appropriate metrics to describe relationships between these events and impacts on marine ecosystems.

Literature cited

- Abe, M., A. Kurashima, and M. Maegawa. 2008. High water-temperature tolerance in photosynthetic activity of *Zostera marina* seedlings from Ise Bay, Mie Prefecture, central Japan. *Fish. Sci.* **74**: 1017–1023. doi:10.1111/j.1444-2906.2008.01619.x
- Arias-Ortiz, A., O. Serrano, P. Masqué, and others. 2018. A marine heatwave drives massive losses from the world's largest seagrass carbon stocks. *Nat. Clim. Chang.* doi:10.1038/s41558-018-0096-y
- Beck, M. W., K. L. Heck, K. W. Able, and others. 2001. The Identification, Conservation, and Management of Estuarine and Marine Nurseries for Fish and Invertebrates. *Bioscience* **51**: 633. doi:10.1641/0006-3568(2001)051[0633:TICAMO]2.0.CO;2
- Berg, P., and M. Huettel. 2008. Integrated benthic exchange dynamics. *Oceanography* **21**: 164–167.
- Berg, P., H. Røy, F. Janssen, V. Meyer, B. B. Jørgensen, M. Huettel, and D. De Beer. 2003. Oxygen uptake by aquatic sediments measured with a novel non-invasive eddy-correlation technique. *Mar. Ecol. Prog. Ser.* **261**: 75–83. doi:10.3354/meps261075
- Berg, P., H. Røy, and P. L. Wiberg. 2007. Eddy correlation flux measurements: The sediment surface area that contributes to the flux. *Limnol. Oceanogr.* **52**: 1672–1684. doi:10.4319/lno.2007.52.4.1672
- Berger, A. C., P. Berg, K. J. McGlathery, and M. L. Delgard. 2020. Long-term trends and resilience of seagrass metabolism: A decadal aquatic eddy covariance study. *Limnol. Oceanogr.* 1–16. doi:10.1002/lno.11397
- Carr, J. A., P. D'Odorico, K. J. McGlathery, and P. L. Wiberg. 2012. Modeling the effects of climate change on eelgrass stability and resilience: Future scenarios and leading indicators of

- collapse. *Mar. Ecol. Prog. Ser.* **448**: 289–301. doi:10.3354/meps09556
- Collier, C. J., S. Uthicke, and M. Waycott. 2011. Thermal tolerance of two seagrass species at contrasting light levels: Implications for future distribution in the Great Barrier Reef. *Limnol. Oceanogr.* **56**: 2200–2210. doi:10.4319/lo.2011.56.6.2200
- Costanza, R., R. Arge, R. De Groot, and others. 1997. The value of the world's ecosystem services and natural capital. *Nature* **387**: 253–260. doi:10.1038/387253a0
- Dennison, W. C. 1987. Effects of light on seagrass photosynthesis, growth and depth distribution. *Aquat. Bot.* **27**: 15–26. doi:10.1016/0304-3770(87)90083-0
- Duarte, C. M., N. Marbá, E. Gacia, J. W. Fourqurean, J. Beggins, C. Barrón, and E. T. Apostolaki. 2010. Seagrass community metabolism: Assessing the carbon sink capacity of seagrass meadows. *Global Biogeochem. Cycles* **24**: 1–8. doi:10.1029/2010GB003793
- Egea, L. G., R. Jiménez–Ramos, I. Hernández, and F. G. Brun. 2019. Effect of In Situ short–term temperature increase on carbon metabolism and dissolved organic carbon (DOC) fluxes in a community dominated by the seagrass *Cymodocea nodosa*. *PLoS One* **14**: 1–20. doi:10.1371/journal.pone.0210386
- Ehlers, A., B. Worm, and T. B. H. Reusch. 2008. Importance of genetic diversity in eelgrass *Zostera marina* for its resilience to global warming. *Mar. Ecol. Prog. Ser.* **355**: 1–7. doi:10.3354/meps07369
- Ewers, C. J. 2013. Assessing physiological thresholds for eelgrass (*Zostera marina* L.) survival in the face of climate change. *Biol. Sci.* doi:https://doi.org/10.15368/theses.2013.126
- Fourqurean, J. W., C. M. Duarte, H. A. Kennedy, and others. 2012. Seagrass ecosystems as a globally significant carbon stock. *Nat. Geosci.* **5**: 505–509. doi:10.1038/ngeo1477
- Frölicher, T. L., E. M. Fischer, and N. Gruber. 2018. Marine heatwaves under global warming. *Nature* **560**: 360–364. doi:10.1038/s41586-018-0383-9
- Hammer, K. J., J. Borum, H. Hasler-sheetal, E. C. Shields, K. Sand-jensen, and K. A. Moore. 2018. High temperatures cause reduced growth, plant death and metabolic changes in eelgrass *Zostera marina*. *Mar. Ecol. Prog. Ser.* **604**: 121–132.
- Hume, A. C., P. Berg, and K. J. McGlathery. 2011. Dissolved oxygen fluxes and ecosystem metabolism in an eelgrass (*Zostera marina*) meadow measured with the eddy correlation technique. *Limnol. Oceanogr.* **56**: 86–96. doi:10.4319/lo.2011.56.1.0086
- Johnson, A. J., E. C. Shields, G. A. Kendrick, and R. J. Orth. 2020. Recovery Dynamics of the Seagrass *Zostera marina* Following Mass Mortalities from Two Extreme Climatic Events. *Estuaries and Coasts*. doi:10.1007/s12237-020-00816-y
- Koch, E. W., E. B. Barbier, B. R. Silliman, and others. 2009. Non-linearity in ecosystem services: Temporal and spatial variability in coastal protection. *Front. Ecol. Environ.* **7**: 29–37. doi:10.1890/080126
- Koch, E. W., and R. J. Orth. 2003. The Mid-Atlantic coast of the United States. *World atlas of seagrasses* 216.
- Lawson, S. E., P. L. Wiberg, K. J. McGlathery, and D. C. Fugate. 2007. Wind-driven sediment suspension controls light availability in a shallow coastal lagoon. *Estuaries and Coasts* **30**: 102–112. doi:10.1007/BF02782971
- Lee, K.-S., S. R. Park, and Y. K. Kim. 2007. Effects of irradiance, temperature, and nutrients on

- growth dynamics of seagrasses: A review. *J. Exp. Mar. Bio. Ecol.* **350**: 144–175. doi:10.1016/j.jembe.2007.06.016
- Lee, K. S., S. R. Park, and J. B. Kim. 2005. Production dynamics of the eelgrass, *Zostera marina* in two bay systems on the south coast of the Korean peninsula. *Mar. Biol.* **147**: 1091–1108. doi:10.1007/s00227-005-0011-8
- Lefcheck, J. S., D. J. Wilcox, R. R. Murphy, S. R. Marion, and R. J. Orth. 2017. Multiple stressors threaten the imperiled coastal foundation species eelgrass (*Zostera marina*) in Chesapeake Bay, USA. *Glob. Chang. Biol.* **23**: 3474–3483. doi:10.1111/gcb.13623
- Lorrai, C., D. F. McGinnis, P. Berg, A. Brand, and A. Wüest. 2010. Application of oxygen eddy correlation in aquatic systems. *J. Atmos. Ocean. Technol.* **27**: 1533–1546. doi:10.1175/2010JTECHO723.1
- Marbá, N., and C. M. Duarte. 2010. Mediterranean warming triggers seagrass (*Posidonia oceanica*) shoot mortality. *Glob. Chang. Biol.* **16**: 2366–2375. doi:10.1111/j.1365-2486.2009.02130.x
- Marsh, J. a, W. C. Dennison, R. S. Alberte, and S. Alberte. 1986. Effects of temperature on photosynthesis and respiration in eelgrass (*Zostera marina* L.). *J. Exp. Mar. Bio. Ecol.* **101**: 257–267. doi:10.1016/0022-0981(86)90267-4
- Moore, K. A., and J. C. Jarvis. 2008. Eelgrass Diebacks in the Lower Chesapeake Bay : Implications for Long-term Persistence. *J. Coast. Res.* **55**: 135–147. doi:10.2112/SI55-014.acteristics
- Moore, K. A., F. T. Short, R. J. Orth, and C. M. Duarte. 2006. *Zostera : Biology , Ecology , and Management*.
- Moreno-Marín, F., F. G. Brun, and M. F. Pedersen. 2018. Additive response to multiple environmental stressors in the seagrass *Zostera marina* L. *Limnol. Oceanogr.* **63**: 1528–1544. doi:10.1002/lno.10789
- Nejrup, L. B., and M. F. Pedersen. 2008. Effects of salinity and water temperature on the ecological performance of *Zostera marina*. *Aquat. Bot.* **88**: 239–246. doi:10.1016/j.aquabot.2007.10.006
- Niu, S., P. Zhang, J. Liu, D. Guo, and X. Zhang. 2012. The effect of temperature on the survival, growth, photosynthesis, and respiration of young seedlings of eelgrass *Zostera marina* L. *Aquaculture* **350–353**: 98–108. doi:10.1016/j.aquaculture.2012.04.010
- Oliver, E. C. J., M. T. Burrows, M. G. Donat, and others. 2019. Projected Marine Heatwaves in the 21st Century and the Potential for Ecological Impact. *Front. Mar. Sci.* **6**: 1–12. doi:10.3389/fmars.2019.00734
- Oreska, M. P. J., K. J. McGlathery, J. H. Porter, H. Asmus, R. M. Asmus, and A. Vaquer. 2017. Seagrass blue carbon spatial patterns at the meadow-scale J. Cebrian [ed.]. *PLoS One* **12**: e0176630. doi:10.1371/journal.pone.0176630
- Orth, R. J., M. L. Luckenbach, S. R. Marion, K. A. Moore, and D. J. Wilcox. 2006. Seagrass recovery in the Delmarva Coastal Bays, USA. *Aquat. Bot.* **84**: 26–36. doi:10.1016/j.aquabot.2005.07.007
- Orth, R. J., and K. J. McGlathery. 2012. Eelgrass recovery in the coastal bays of the Virginia Coast Reserve, USA. *Mar. Ecol. Prog. Ser.* **448**: 173–176. doi:10.3354/meps09596
- Paul Richardson, J., J. S. Lefcheck, and R. J. Orth. 2018. Warming temperatures alter the relative abundance and distribution of two co-occurring foundational seagrasses in chesapeake bay,

- USA. Mar. Ecol. Prog. Ser. **599**: 65–74. doi:10.3354/meps12620
- Pedersen, O., T. D. Colmer, J. Borum, A. Zavala-Perez, and G. A. Kendrick. 2016. Heat stress of two tropical seagrass species during low tides - impact on underwater net photosynthesis, dark respiration and diel in situ internal aeration. *New Phytol.* **210**: 1207–1218. doi:10.1111/nph.13900
- Pendleton, L., D. C. Donato, B. C. Murray, and others. 2012. Estimating Global “Blue Carbon” Emissions from Conversion and Degradation of Vegetated Coastal Ecosystems. *PLoS One* **7**. doi:10.1371/journal.pone.0043542
- Pregnall, A. M., R. D. Smith, T. A. Kursar, and R. S. Alberte. 1984. Metabolic adaptation of *Zostera marina* (eelgrass) to diurnal periods of root anoxia. *Mar. Biol.* **83**: 141–147. doi:10.1007/BF00394721
- Qin, L. Z., S. H. Kim, H. J. Song, and others. 2020. Long-term variability in the flowering phenology and intensity of the temperate seagrass *Zostera marina* in response to regional sea warming. *Ecol. Indic.* **119**: 106821. doi:10.1016/j.ecolind.2020.106821
- Rasmusson, L. M., P. Buapet, R. George, M. Gullström, P. C. B. Gunnarsson, and M. Björk. 2020. Effects of temperature and hypoxia on respiration, photorespiration, and photosynthesis of seagrass leaves from contrasting temperature regimes. *ICES J. Mar. Sci.* doi:10.1093/icesjms/fsaa093
- Rheuban, J. E., and P. Berg. 2013. The effects of spatial and temporal variability at the sediment surface on aquatic eddy correlation flux measurements. *Limnol. Oceanogr. Methods* **11**: 351–359. doi:10.4319/lom.2013.11.351
- Rheuban, J. E., P. Berg, and K. J. McGlathery. 2014a. Multiple timescale processes drive ecosystem metabolism in eelgrass (*Zostera marina*) meadows. *Mar. Ecol. Prog. Ser.* **507**: 1–13. doi:10.3354/meps10843
- Rheuban, J. E., P. Berg, and K. J. McGlathery. 2014b. Ecosystem metabolism along a colonization gradient of eelgrass (*Zostera marina*) measured by eddy correlation. *Limnol. Oceanogr.* **59**: 1376–1387. doi:10.4319/lo.2014.59.4.1376
- Shields, E. C., K. A. Moore, and D. B. Parrish. 2018. Adaptations by *Zostera marina* Dominated Seagrass Meadows in Response to Water Quality and Climate Forcing. doi:10.3390/d10040125
- Shields, E. C., D. Parrish, and K. A. Moore. 2019. Short-Term Temperature Stress Results in Seagrass Community Shift in a Temperate Estuary. *Estuaries and Coasts* **42**: 755–764. doi:10.1007/s12237-019-00517-1
- Sokolova, I. M. 2013. Energy-limited tolerance to stress as a conceptual framework to integrate the effects of multiple stressors. *Integr. Comp. Biol.* **53**: 597–608. doi:10.1093/icb/ict028
- Wahid, A., S. Gelani, M. Ashraf, and M. R. Foolad. 2007. Heat tolerance in plants: An overview. *Environ. Exp. Bot.* **61**: 199–223. doi:10.1016/j.envexpbot.2007.05.011
- Wilson, K., and H. K. Lotze. 2019. Projected range shift of eelgrass *Zostera marina* in the Northwest Atlantic with climate change. *Mar. Ecol. Prog. Ser.* **620**: 47–62. doi:10.3354/meps12973
- York, P. H., R. K. Gruber, R. Hill, P. J. Ralph, D. J. Booth, and P. I. Macreadie. 2013. Physiological and Morphological Responses of the Temperate Seagrass *Zostera muelleri* to Multiple

Stressors : Investigating the Interactive Effects of Light and Temperature. **8**: 1–12.
doi:10.1371/journal.pone.0076377

CHAPTER 3: OCEAN WARMING EFFECTS ON SEAGRASS (*ZOSTERA MARINA*) AND ITS RESILIENCE TO MARINE HEATWAVES

Amelie C. Berger, Peter Berg, Karen McGlathery, Lillian Aoki, Kylor Kerns

This chapter will soon be submitted for publication in Global Change Biology.

Abstract

Seagrass meadows are among many marine ecosystems increasingly threatened by warming oceans. Following a marine heatwave in June 2015, the eelgrass (*Zostera marina*) meadows of Virginia Coast Reserve (VCR) (USA) experienced a die-off event. Eelgrass recovery in the following years was slow and spatially heterogeneous. This study investigates the effects of thermal stress on seagrass loss and recovery. Using hourly summer water temperature measurements from 2016–2020, we developed a novel approach to quantifying the stress of ocean warming and marine heatwaves on seagrass. This approach included two metrics: the cumulative heat stress (as heating degree-hours, HDHs) and thermal stress relief (as cooling degree-hours, CDHs), both relative to the 28.6°C eelgrass thermal tolerance threshold previously determined in situ. These metrics were compared to spatiotemporal patterns in summertime seagrass shoot density and length. Results revealed that the healthiest parts of the meadow benefited from greater thermal stress relief (2–3x) from tidal cooling (inputs of cooler ocean water) during periods of heat stress, leading to ~65% higher shoot densities compared to the center of the meadow, which experienced higher heat stress (1.8x) with less relief. HDHs and CDHs were also useful for assessing the intensity of heating events between 2017–2020, as well as the heating event that caused the eelgrass die-off at the VCR in June 2015. We found that heat stress cumulating ~100–200°C-hours can trigger such an event. The added effects of sulfide toxicity after the initial heat stress response likely exacerbated the stress experienced in the meadow. Sulfur isotope analyses of seagrass leaves and sediment suggest higher sulfide intrusion in 2015, as shown in the lighter sulfur isotope signatures of seagrass samples from that year ($\delta^{34}\text{S} = 8.4\text{‰}$). This study outlines a novel approach to quantifying heat stress in seagrass ecosystems. By using a thermal tolerance threshold rather than a climatological one, our metrics incorporate ecosystem vulnerability and may be more relevant to future studies on the effects of warming oceans on marine ecosystems.

Introduction

Global climate change represents a major threat to coastal ecosystems worldwide. The increased occurrence of extreme heating events such as marine heatwaves—periods of at least five consecutive days when water temperatures exceed a local climatological threshold (90th percentile of long-term temperature data, Hobday et al. 2016)—in the past few decades has led to dramatic changes in the biodiversity, distributional range, and physiological function of foundation species or habitats (e.g. Wernberg et al. 2016b; Smale et al. 2019). These changes can have devastating impacts on marine ecosystems, such as mass coral bleaching (e.g. Skirving et al. 2019; Duarte et al. 2020) and widespread declines in kelp forests (e.g. Wernberg et al. 2016a; Thomsen et al. 2019) and seagrass meadows (e.g. Thomson et al. 2015; Arias-Ortiz et al. 2018; Berger et al. 2020). This is of significant concern globally as coastal ecosystems support commercially important fisheries and local economies (e.g. Costanza et al. 1997; Nagelkerken et al. 2000; Rees et al. 2010), provide coastal protection (Koch et al. 2009), and play an important role in biogeochemical cycling and maintaining water quality (e.g. Mateo et al. 2003; Armitage and Fourqurean 2016; Aoki et al. 2020a). Seagrass meadows in particular are valued as significant carbon sinks in the global carbon cycle (Fourqurean et al. 2012; Oreska et al. 2017; Macreadie et al. 2019). Extreme warming events in seagrass meadows lead to widespread loss of ecosystem services and primary producer biomass, and may trigger the release of substantial amounts of CO₂ due to the remineralization of previously buried organic matter (Pendleton et al. 2012; Arias-Ortiz et al. 2018; Smale et al. 2019; Aoki et al. 2021). To better predict seagrass ecosystem trajectories and minimize adverse feedbacks on the climate system in light of the continued ocean warming and increased marine heatwave occurrences predicted through the 21st century (Frölicher et al. 2018; Oliver et al. 2019), it is critical to enhance our understanding of thermal stress impacts on seagrass meadows.

Seagrass die-off events can occur when water temperatures exceed the thermal tolerance limits of the species (e.g. Moore and Jarvis 2008; Marbá and Duarte 2010; Arias-Ortiz et al. 2018; Berger et al. 2020). Beyond a certain optimum temperature threshold (T_{th}), increasing temperatures damage the photosynthetic apparatus of the plants (Wahid et al. 2007; York et al. 2013). This leads to a decrease in photosynthesis and, because respiration is concurrently stimulated, ultimately a carbon deficit within the seagrass that causes reduced growth and the loss of biomass (Moore et al. 2006; Lee et al. 2007; Collier et al. 2011; Ewers 2013). The temperature threshold for eelgrass (*Z. marina*) was recently determined to be 28.6°C, based on in situ measurements of eelgrass

ecosystem metabolism and temperature under naturally varying conditions (Berger et al. *in prep*). Eelgrass has a wide geographic distribution, but has experienced high temperature-related die-offs in the Mid-Atlantic region (Moore and Jarvis 2008; Berger et al. 2020), the southern edge of its range (Moore et al. 2006). Eelgrass in this region is therefore particularly vulnerable to future warming. The most recent die-off event occurred as a result of a marine heatwave at the Virginia Coast Reserve (VCR) in June 2015 (Aoki et al. 2020b; Berger et al. 2020). The significant loss of eelgrass biomass that summer was followed by several years of slow and spatially heterogeneous recovery within the meadows, suggesting more complex and spatially-varying heat stress dynamics.

While it has been established that the eelgrass die-off resulted from an increased frequency of temperatures above T_{th} in June 2015 compared to other years (Berger et al. 2020), little is known about how the duration and intensity of thermal stress affect seagrass loss and recovery, and how they might vary spatially within the meadow. In the coral literature, the intensity and duration of heat exposure are captured in the use of degree heating weeks as a thermal stress metric to predict coral bleaching and mortality (Liu et al. 2014; Hughes et al. 2017). This metric is a measure of the heating above a local threshold (maximum monthly sea surface temperature, or SST, based on long-term records), where the temperature anomalies above this threshold are cumulatively summed. To date, however, very little research has focused on thermal stress metrics for seagrass environments, which would be helpful in predicting large-scale seagrass losses and finding suitable habitats for restoration (Strydom et al. 2020).

Seagrass mortality as a result of high water temperatures may be exacerbated by another stressor: sulfide intrusion (e.g. Greve et al. 2003a; Borum et al. 2005). Sulfide is produced by sulfate reducing bacteria in anoxic sediments and, if it diffuses into aboveground seagrass tissues, can suppress photosynthesis and growth, ultimately leading to seagrass mortality (e.g. Pedersen et al. 2004; Borum et al. 2005; Calleja et al. 2007). This may occur during periods of high oxygen demand from the plants, the sediments, and the water column – such as periods of anoxia or warming (e.g. Holmer and Nielsen 1997; Greve et al. 2003; Frederiksen and Glud 2006). This sulfide intrusion into seagrass tissues is reflected in their sulfur isotopic signatures ($\delta^{34}\text{S}$) (e.g. Frederiksen et al. 2006), which indicates whether the sulfur source is from sulfate ($\delta^{34}\text{S} \approx 21\text{‰}$) (Rees et al. 1978; Frederiksen et al. 2006) or toxic sulfide gas ($\delta^{34}\text{S} \approx -15\text{--}25\text{‰}$) (Canfield 2001; Böttcher et al. 2004).

Our goal in this study was two-fold. To better understand the response of seagrass ecosystems to thermal stress, we created a thermal stress metric that accounted for the intensity and duration of heating above the previously determined eelgrass temperature stress threshold (28.6°C, Berger et al. *in prep*), thus following a similar methodology to that outlined in coral reef studies. This metric was applied to four years of continuous summer water temperature measurements to understand how temperature stress affected seagrass loss and recovery patterns at our study site following the high-temperature-related die-off event in 2015 (Berger et al. 2020, Aoki et al. 2021). We further investigated potential synergistic effects between heat stress and other stressors, by considering the role of sediment temperature and sulfide intrusion on seagrass resilience.

Methods

Study site

The Virginia Coast Reserve Long-Term Ecological Research (VCR-LTER) site hosts the largest successful eelgrass restoration project globally (Orth and McGlathery 2012; Orth et al. 2020). This project started in 2001 with the broadcast-seeding of 0.2–0.4 ha plots in four shallow subtidal coastal bays on the Atlantic side of the Delmarva peninsula (Orth et al. 2006). South Bay contains the largest of these restored eelgrass meadows (~20 km² as of 2018, Orth et al. 2020). This study focused on the area of South Bay where the originally-seeded plots coalesced into a 7 km² continuous eelgrass meadow by 2012 (Orth and McGlathery 2012). This meadow is situated between a barrier island to its east and a channel to its west, and connected to the Atlantic Ocean by two inlets north and south of the meadow (Fig. 1). The eelgrass growing in South Bay are doing so under favorable light and low-energy hydrodynamic conditions (Lawson et al. 2007; Oreska et al. 2021) and away from direct anthropogenic stressors. The South Bay meadow is therefore an ideal system for studying the isolated effects of warming on seagrass meadows.

In June 2015, the coastal bays at the VCR experienced a marine heatwave, which led to a ~90% decline in eelgrass biomass in South Bay (Berger et al. 2020; Aoki et al. 2021). Long-term seagrass monitoring efforts captured this die-off and the slow subsequent recovery at the six of the original restoration plots in the center of the meadow. However, aerial imagery and expanded seagrass monitoring after the die-off revealed heterogenous patterns in seagrass cover, with much lower shoot densities in the center compared to the outer portions of the meadow (Aoki et al. 2021;

this study). This implied there was a difference in exposure to thermal stress within the meadow, and prompted our efforts to better understand the relationship between temperature and seagrass loss and recovery at the landscape-scale.

To do this, we set up a network of 15 sites two years after the 2015 die-off event along an east-west and north-south transect spanning the general length and width of the meadow (Fig. 1). These sites were used to monitor summer water temperatures, and a subset of sites ($n = 7$) were selected for eelgrass shoot density counts every 10–14 days during summer 2019 (Fig. 1). Results from a pilot study suggested there was a relatively strong temperature gradient between sites closest to the inlets and the center of the meadow; and a weaker, more occasional gradient between sites closest to the western channel and the center sites. This study therefore focused on the north-south transect (numbered sites, Fig. 1). To explore the end members of the temperature gradient, we compared temperature and seagrass growth at two sites: one in the less dense, patchier center of the meadow (“center site,” $37^{\circ}15'43.6''\text{N}$, $75^{\circ}48'54.6''\text{W}$), and one more dense and in the northern part of the meadow (“northern site,” $37^{\circ}16'34.2''\text{N}$ $75^{\circ}48'44.4''\text{W}$) (respectively, sites 0 and 4 in Fig. 1).

Water temperature measurements

Water temperature within the seagrass canopy (20 cm above the sediment surface) was measured at 15 sites every summer from 2017–2020. HOBO Pendant[®] temperature loggers recorded water temperature every 10 min at each site. The 10-min data were then averaged to

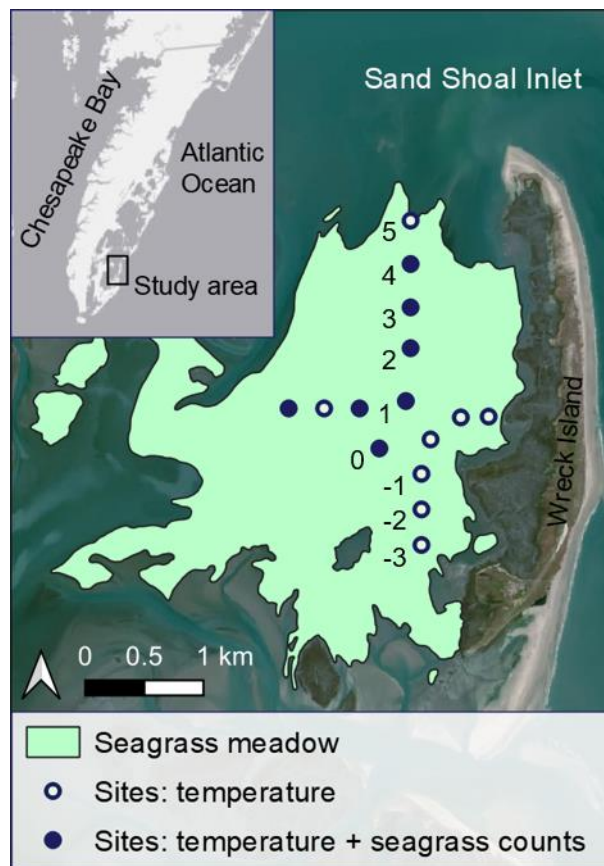


Fig. 1: Location of study sites in the South Bay eelgrass meadow at the Virginia Coast Reserve Long-Term Ecological Research (VCR-LTER) site. Summer water temperatures were measured from 2017 to 2020 at all 15 sites. Seagrass shoot densities were counted every ~2 weeks during summer 2019 at 7 of the 15 sites (filled-in circles). Numbers represent site position along a North-South transect in the meadow.

produce an hourly water temperature record. Table 1 lists measurement dates and the resulting number of hours in our record for each year, including shorter pilot study in 2016. In August 2018, sediment temperature was also measured by burying temperature loggers 2.5 cm and 5 cm into the sediment for ~10 days.

Table 1: Sampling periods for temperature measurements conducted in 2016–2020. Following a pilot study in 2016 (*) we expanded our temperature network to 15 sites. Sampling periods were meant to capture summer temperatures in June–August of each year. We also report here the total number of hours on record.

Year	# sites	Deployment dates	Total # hours	Average # hours per site
2016*	7	Jun 20 – Aug 20	7983	1141
2017	15	May 26 – Oct 19	47259	3151
2018	15	May 31 – Sept 10	33920	2261
2019	15	May 14 – Oct 28	58148	3877
2020	15	Jun 1 – Aug 23	29785	1986

Seagrass metrics

During summer 2019 and at seven of the 15 temperature sites, seagrass shoot density was counted within a 25 m radius of the temperature logger. This subset of sites was chosen to capture variations in seagrass metrics along the stronger North-Center gradient, and between the center of the meadow and the eastern channel. Seagrass shoots were counted within 10 0.25 m² quadrats thrown haphazardly around each site. After counting, we estimated maximum shoot length by measuring the length of the 3 longest shoots within each quadrat. These data were collected every 7–14 days at all seven sites from early July to mid-August. Shoot densities and lengths were measured from mid-May to early July at our northern and center site (sites 4 and 0, respectively, Fig. 1), to capture variations in early-summer seagrass expansion between the two end-member sites on our temperature gradient. No seagrass data were collected at the northernmost site (site 5, Fig. 1) as this represented the edge of the meadow.

Seagrass resilience and thermal stress metric

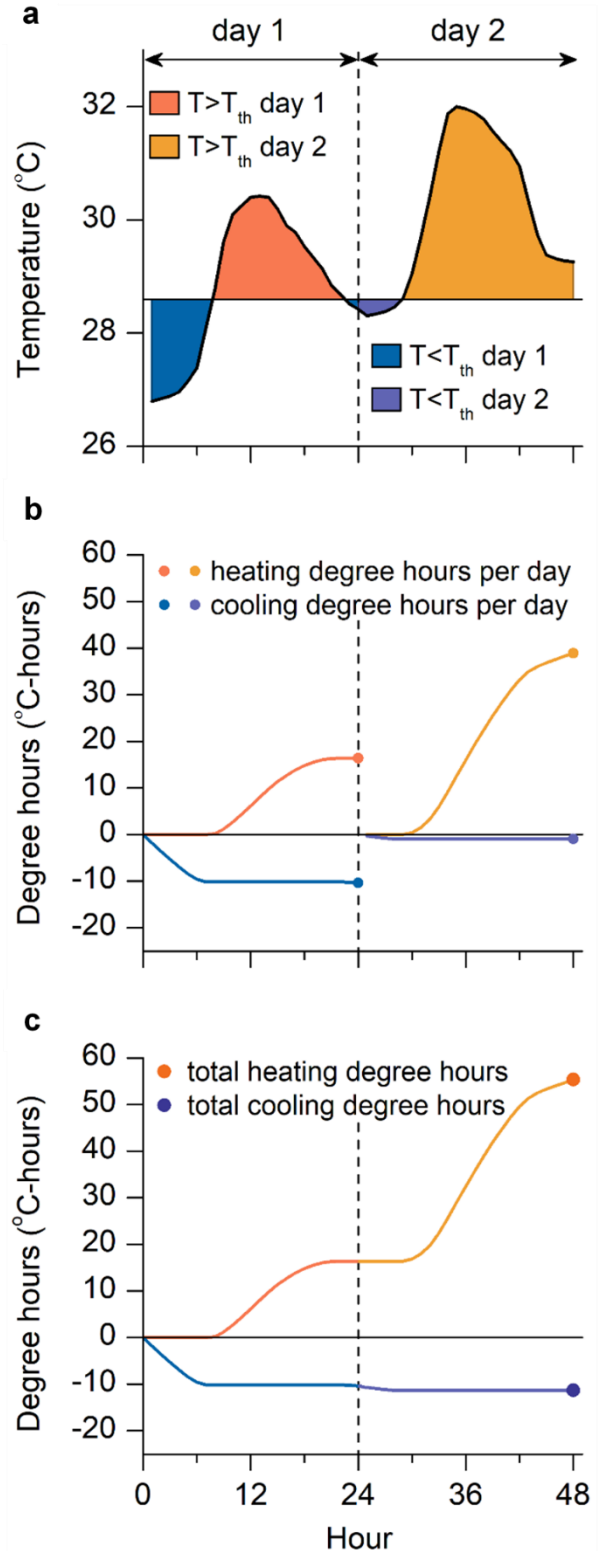
Spatial and temporal patterns of temperature stress in South Bay were evaluated based on the duration and magnitude of warming above the eelgrass thermal tolerance threshold ($T_{th} = 28.6^{\circ}\text{C}$, Berger et al. *in prep*) at each site and during each summer. In the coral literature, degree

heating weeks are calculated by cumulating temperature anomalies of mean weekly water temperatures that are above the average maximum SST for the month. Building on this concept, we cumulated the hourly water temperature anomalies above 28.6°C for each 24-hour period of our temperature record (Fig. 2b). The resulting variable, daily heating degree-hours (daily HDHs) was calculated as:

$$HDH = \sum_{i=1}^n (T_i - T_{th}) \quad (1)$$

where T_{th} is the temperature threshold and T_i is the temperature at hour i (when $T_i > T_{th}$). Daily HDHs were calculated for $i = 1$ to $n = 24$ (Table 2). Higher values of daily HDHs reflect more extreme water temperature during the 24-hour period (e.g. Fig. 2a, 2b). This metric was therefore used to identify the most prominent warming events each summer as successive days with significant warming (high HDH values). Once these events were identified, we calculated the total HDHs as in equation (1) but for the entire duration of the heating event (e.g. Fig. 2c, Table 2). Because total HDH values are contingent on the duration of the heating event, we compared the severity of heating events

Fig. 2: Visual representation of the heat stress metrics used in this study. Based on an hourly temperature record (a), we identify the temperature anomalies above (warm colors) and below (cool colors) the seagrass thermal stress threshold (T_{th}) of 28.6°C. For each 24-hour period, these temperature anomalies are cumulatively summed (b), resulting in daily heating and cooling degree-hours (daily HDHs and CDHs, respectively). Heating and cooling degree-hours are also cumulated over an entire heating event (c), illustrated here by two hot days, resulting in one value for heat stress (total HDHs) and one for heat stress relief (total CDHs).



between years by dividing total HDHs by the number of days. To avoid confusion with the daily HDHs defined above, we will refer here to mean HDHs per day (Table 2). We also took into account spatiotemporal variations in the amount and duration of cooling (when temperature $< T_{th}$) during heating events. We calculated total cooling degree-hours (CDH, Table 2, Fig. 2) using equation (1) for $T_i < T_{th}$, and cooling CDHs per day (CDH/n days).

Table 2: Acronyms and definitions of the metrics used to quantify heat stress in this study.

Variable name	Definition
HDHs	Heating Degree-Hours (°C-hrs): HDHs represent the amount of heating above a temperature threshold (T_{th}), calculated as the cumulative sum of hourly water temperature anomalies above (T_{th}). High HDH values reflect more extreme heating in terms of duration and/or magnitude of high water temperatures.
daily HDHs	HDHs cumulated over each 24-hour period.
total HDHs	HDHs cumulated over an entire heating event.
mean HDHs per day	To allow for better comparison of heating events between years, mean HDHs per day are calculated as total HDHs/n days during the heating event. They represent the average heat stress of a typical day during the event.
CDHs	Cooling Degree-Hours (°C-hrs): CDHs represent the amount of cooling, or thermal stress relief, when temperatures drop below T_{th} , calculated as the cumulative sum of hourly water temperature anomalies below (T_{th}). Higher absolute CDH values reflect longer and/or more extreme relief from thermal stress.
total CDHs	CDHs cumulated over an entire heating event.
mean CDHs per day	Similar to mean DHDs per day, mean CDHs per day represent the average thermal stress relief during a typical day during the event. Calculated as total CDHs/n days.

To better understand the link between thermal stress and seagrass resilience, these thermal stress metrics were related to spatiotemporal patterns in seagrass shoot density and length during summer 2019. We assessed the relationship between thermal stress and peak shoot densities, maximum shoot length, and seagrass growth by using changes in shoot density during the natural meadow expansion and die-back periods as proxy. We also aimed to estimate the amount of heat stress necessary to cause a seagrass die-off event similar to the one we observed in 2015. Seagrass shoot density counts from 2015 revealed a ~25% decrease in shoot density between April 27th and June 27th (shoot density = 316 shoots m^{-2} and 230 shoots m^{-2} , respectively) (Berg et al. 2019) — a

period during which we would normally expect a significant increase (Orth and Moore 1986; Berger et al. 2020). The observed decrease in shoot density suggests the 2015 die-off (which resulted in a 90% decrease in shoot density) had started between these sampling dates. The heat stress (total HDHs) over this period was therefore significant enough to trigger seagrass mortality. Because we had no in situ water temperature measurements in 2015, we used available data from the National Oceanic and Atmospheric Administration’s (NOAA) National Data Buoy Center for the nearby Wachapreague, VA (Sta. WAHV2). We first evaluated whether these records could serve as proxy for water temperatures at our study site (center site) by comparing the amount of heat stress (total HDHs) calculated from both the buoy and in situ temperature records for the time periods when both datasets overlapped. We were then able to use the Wachapreague record to calculate heat stress from April 27th to June 27th, 2015 and estimate the minimum total HDH value we know could trigger a seagrass die-off event, in comparison to the total HDHs from other years (2012–2014 and 2016–2020) where no decrease in shoot density was observed.

Sulfide presence in the sediment and seagrass tissue

To detect sulfide intrusion in seagrass tissues, we analyzed the sulfur isotopic signature of seagrass leaf samples collected from biomass cores taken at the center site in June and/or July 2012–2019 (n = 3 cores per collection date, n = 33 cores total). In some cases, adjacent sediment samples were also collected and were therefore included in this analysis (n = 15 samples). Seagrass biomass was rinsed, sorted, dried (at 60°C), and ground in preparation for the sulfur isotope analyses. Sediment samples were also dried and ground. All samples were analyzed at the MBL Stable Isotope Laboratory in Woods Hole, MA.

To assess whether there was sulfide intrusion during the die-off year (2015), we compared the $\delta^{34}\text{S}$ of seagrass leaves and sediment ($\delta^{34}\text{S}_{\text{seagrass}}$ and $\delta^{34}\text{S}_{\text{sediment}}$, respectively) between collection dates. Where we had both $\delta^{34}\text{S}_{\text{seagrass}}$ and $\delta^{34}\text{S}_{\text{sediment}}$ for a given sampling date, we calculated the proportion of total sulfur in the plant coming from sulfide (Frederiksen et al. 2006) as:

$$F_{\text{sulfide}} = \frac{\delta^{34}\text{S}_{\text{seagrass}} - \delta^{34}\text{S}_{\text{sulfate}}}{\delta^{34}\text{S}_{\text{sediment}} - \delta^{34}\text{S}_{\text{sulfate}}} \quad (2)$$

where $\delta^{34}\text{S}_{\text{sulfate}}$ is the sulfur isotopic signature of seawater. While this was not measured, $\delta^{34}\text{S}_{\text{sulfate}}$ values are fairly constant worldwide (Rees et al. 1978). We therefore used $\delta^{34}\text{S}_{\text{sulfate}} =$

21‰ to approximate F_{sulfide} and evaluate relative changes in the contribution of sulfide to leaf sulfur in our record.

Results

Spatiotemporal variations in temperature stress and seagrass growth

For each of our summer water temperature datasets (2017–2020) and for the center and northern sites, we compared the temperature timeseries, daily HDHs, and total HDHs and CDHs over the most prominent heating events as determined by the daily HDHs (Fig 3b, Table 3). Figure 3a shows the timeseries from June 1st to August 31st 2019 for both sites. Mean hourly summer temperature at the center site was significantly higher than that of the northern site by 0.7°C ($27.2 \pm 0.05^{\circ}\text{C}$ and $26.5 \pm 0.05^{\circ}\text{C}$, respectively, $n = 2208$ hours) (two-sample t-test, $p < 0.01$). While the general variations over the summer agreed fairly well between the two sites, there are some time periods during which temperatures at the northern site drop well below those at the center site. For example, between July 18th and July 22nd, temperatures at the northern site drop to $\sim 25.5^{\circ}\text{C}$, while temperatures at the center site remain above the 28.6°C thermal stress threshold, only dropping to $\sim 30^{\circ}\text{C}$. Temperatures at the center site varied on a diel basis, whereas those at the northern site reflected a tidal cycle (Fig. 3a, 7).

We used daily HDH values to identify periods of temperature stress in the seagrass meadow (e.g. end of June through most of July 2019, Fig. 3b) for each year (Table 3). The highest daily HDH values (i.e. the days of highest thermal stress) occurred at the center site on July 15th and July 20th 2019, with 75°C -hours and 72°C -hours respectively (Fig. 3b, Table 3). Thermal stress at the northern site was $\sim 60\%$ lower on those days, with only 30°C -hours, peaking a few days later at 40°C -hours. Heating events in 2017–2020 lasted ~ 3 – 4 weeks, but varied in intensity as can be seen in the daily HDH and mean HDH and CDH per day values in Table 3. The most intense warming periods occurred in 2019 and 2020. Each event lasted ~ 4 weeks and had similarly high levels of heating (mean HDH per day = 30.5°C -hours and 15.5°C -hours at the center and northern sites, respectively) and low levels of cooling (mean CDH per day = -6°C -hours and -15.5°C -hours at the center and northern sites, respectively). Heating events in other years were less intense as they cumulated less heat (mean HDH per day values on average 56% lower) and more cooling (mean CDH per day values on average 60% higher) (Table 3).

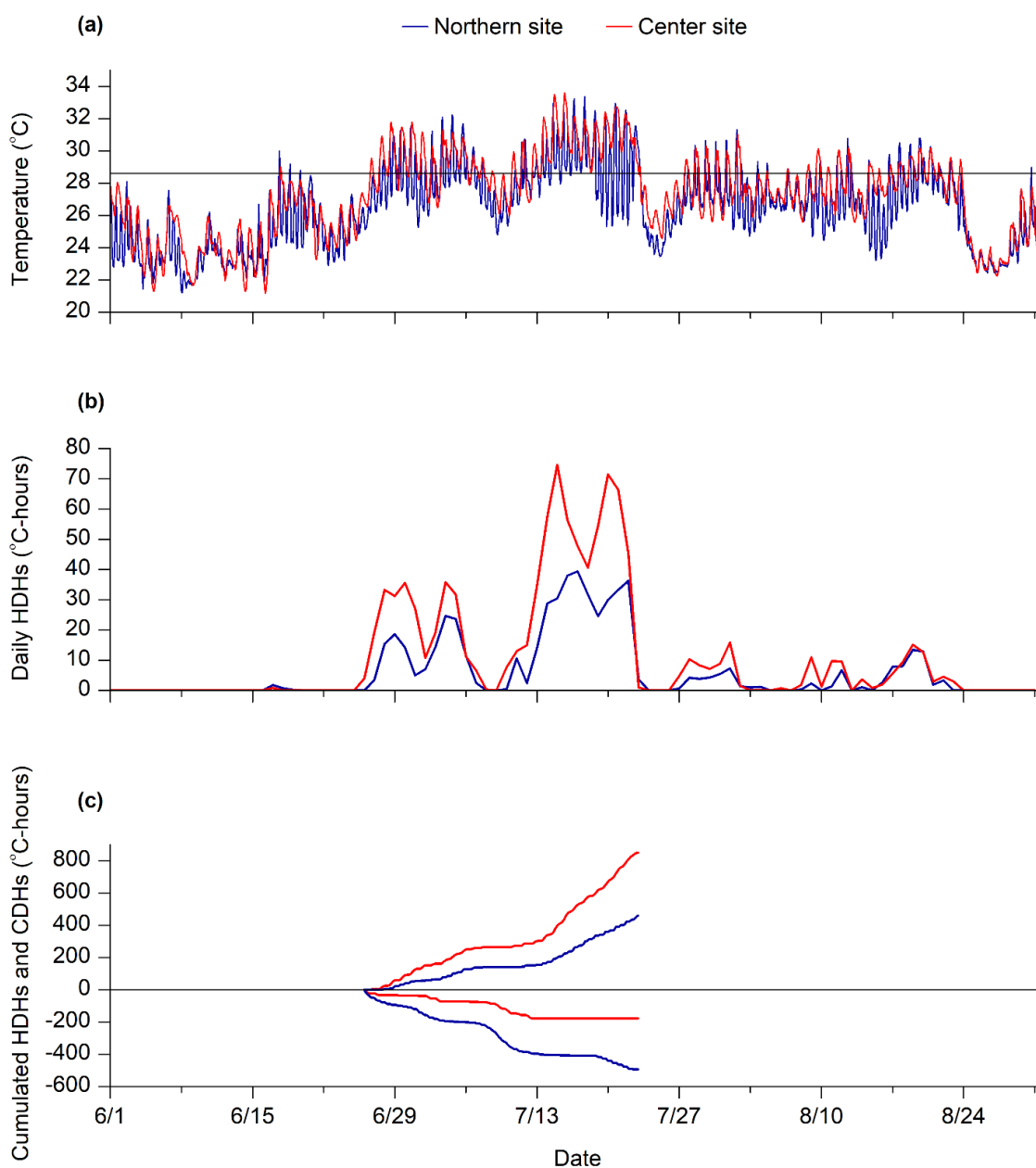


Fig. 3: Differences in thermal stress between the center and northern site in the meadow. **(a)** Hourly temperature timeseries from June 1st to Aug 31st 2019 at the center site (red) and northern site (blue), relative to the 28.6°C temperature threshold (black line). **(b)** Daily heating degree-hours (HDHs) relative to 28.6°C at the center (red) and northern site (blue), and **(c)** cumulative heating and cooling degree-hours (HDHs and CDHs, respectively) relative to 28.6°C at the center (red) and northern (blue) site during the warmest period of the summer.

Over the main hot period in 2019, thermal stress at the center site was 1.8 times higher than at the northern site (total HDH values of 850°C-hours and 460°C-hours, respectively) (Fig3c). The amount of cooling also strongly differed between the sites. The northern site cumulated 2.8 times

more CDHs compared to the center site ($-494^{\circ}\text{C}\cdot\text{hours}$ and $-179^{\circ}\text{C}\cdot\text{hours}$, respectively). Including all years on record (2017–2020), the center site experienced 1.4 to 2.1 (on average 1.8) times more heat stress than the northern site and received on average half (and as low as a third) the amount of thermal relief from temperatures below 28.6°C (Table 3).

Table 3: Comparison of prominent warming events during summers 2017–2020 with: event dates, duration (days), mean and maximum temperature ($^{\circ}\text{C}$), maximum daily heating degree-hours (HDH, $^{\circ}\text{C}\cdot\text{hours}$), mean HDHs per day ($^{\circ}\text{C}\cdot\text{hours}$), mean cooling degree-hours (CDHs) per day ($^{\circ}\text{C}\cdot\text{hours}$), for the northern and center site.

Year	2017		2018		2019		2020	
Warmest period	7/2 – 7/23		6/19 – 7/7 and 8/5 – 8/31		6/26 – 7/22		6/28 – 7/30	
Duration (d)	22		19, 27		27		29	
Site	center	northern	center	northern	center	northern	center	northern
Mean temperature ($^{\circ}\text{C}$)	29.0	27.6	29.0, 28.4	28.4, 27.9	29.6	28.5	29.4	28.7
Max temperature ($^{\circ}\text{C}$)	32.5	32.6	32.6, 32.7	32.7, 31.8	33.6	33.4	33.4	33.5
Max daily DHH ($^{\circ}\text{C}\cdot\text{hr}$)	35	21	63, 38	45, 21	75	39	47	39
mean DHH per day ($^{\circ}\text{C}\cdot\text{hr}$)	19	9	25, 11	16, 8	31	17	30	14
mean DCH per day ($^{\circ}\text{C}\cdot\text{hr}$)	-10	-34	-15, -15	-19, -25	-7	-18	-5	-13

Figure 4 shows the amount of heating (mean HDH per day) and cooling (mean CDH per day) over all warm periods (2017–2020) at all sites along the north-south transect in the South Bay meadow. Maximum heating occurred at site 1, one of the central sites (mean HDH per day = $19^{\circ}\text{C}\cdot\text{hours}$) and decreased by 63% at the northern edge of the meadow (site 5). This decrease in heating

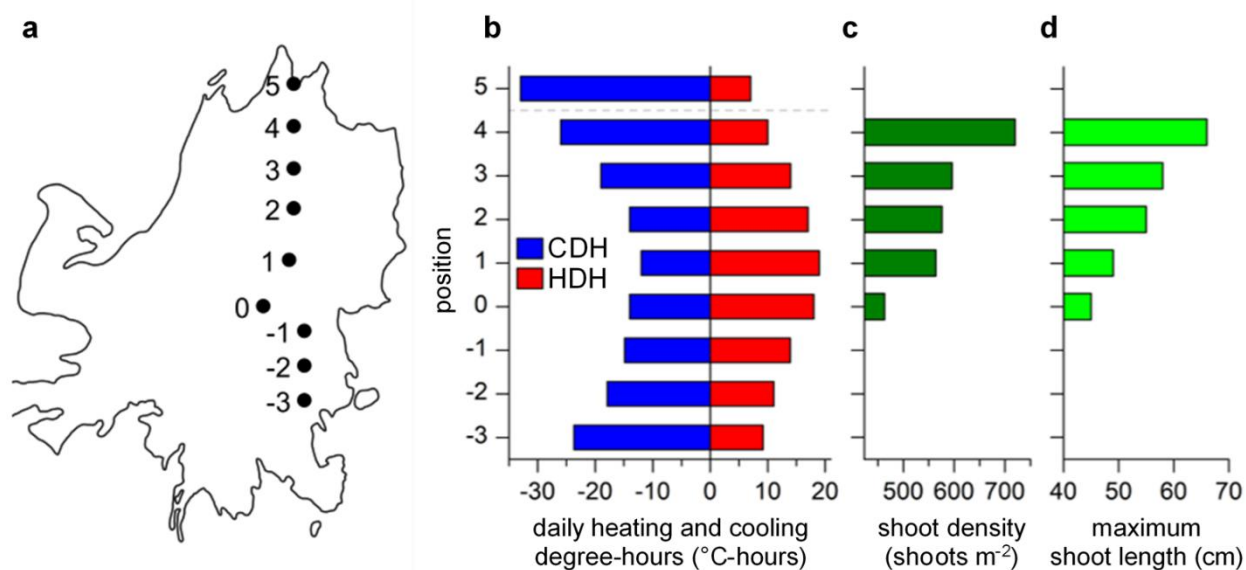


Fig. 4: Patterns of heating, cooling (b), seagrass shoot density (dark green, c), and maximum shoot length (light green, d) along a north-south transect in the meadow (a). Heating and cooling at each site were calculated as mean daily heating degree-hours (HDHs) (red) and cooling degree-hours (CDHs) (blue). Dashed grey line: meadow boundary.

was concurrent with a 64% increase in cooling between those sites. There is a similar trend in temperatures from the center of the meadow towards the southern inlet. Differences in heating and cooling was much less pronounced along the east-west transect. However, heating decreased and cooling increased slightly closer to the western channel compared to the center of the meadow. Seagrass metrics used as proxies for seagrass growth along the northern transect in 2019 followed the observed heating and cooling trends. Seagrass shoot density and length generally increased from the center northward as the amount of heating decreased and the amount of cooling increased (433 to 503 shoots m^{-2} and 45 to 66 cm, respectively).

Figure 5 shows how the difference in heat stress between the northern site (site 4, Fig. 4) and center site (site 0, Fig. 4) affected seagrass density patterns from early July to mid-August 2019. Over the last 10 days of the growing season, shoot densities increased substantially more at the northern site (43% vs. 7%). Subsequent decline rates, however, were comparable (47% vs. 37%).

Thermal stress and die-off events

To quantify the thermal stress during the June 2015 event, we first assessed the comparability of the Wachapreague buoy records to those from our center site. The total HDHs calculated during summer hot events (2016–2020) were essentially identical between the two sites (Fig. 6a, $R^2 = 1$ and regression slope = 0.99, $p < 0.01$). Slightly greater variation was found for calculations between April 27th and June 27th 2018–2020 (Fig. 6b), with differences of 10–36 °C-hours cumulated over the ~2-month period.

Warming between April 27 and June 27, 2015 was more prominent compared to that during the same period in other years (Fig. 6b). The heating event lasted for an uninterrupted 2-week period, reaching maximum peak daily HDH of 33°C-hours and totaling 220°C-hours. In comparison, average total HDHs over this time period in the other years was 33°C-hours. The year

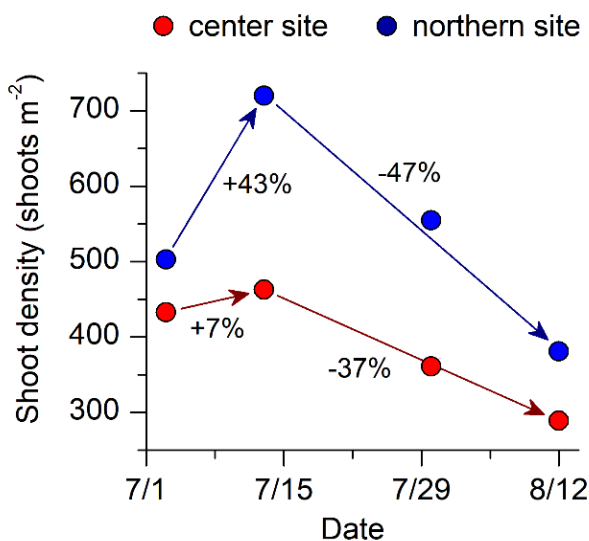


Fig. 5: Shoot densities at the center site (red) and northern site (blue) from July 3rd to August 12th 2019. Numbers represent rates of increase and decline (in %) over the last week of the growing season and progression into late summer, respectively. SE error bars masked by symbols.

with the second highest amount of thermal stress was 2018, which peaked at a daily HDH value of 27°C-hours and totaled at 82°C-hours (Fig. 6b).

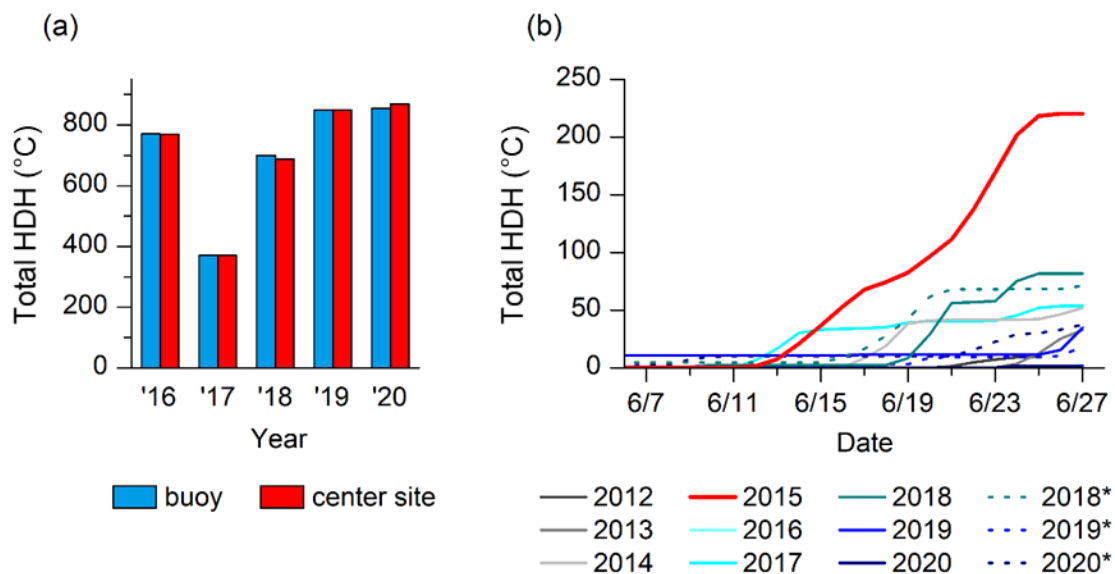


Fig. 6: (a) Comparison of heat stress (total heating degree-hours, HDHs) between temperature records from the center site and the National Data Buoy Center (NDBC) station WAHV2 during summer hot events in 2016–2020. **(b)** shows unusually high heat stress (cumulative HDHs) in June 2015 compared to other years (2012–2016, buoy records, and 2017–2020, in situ records). Asterisks (*) show cumulative HDHs calculated from matching buoy records.

Sediment temperatures

High temperatures occur not only in the water column, but the sediment as well. Figure 7 shows the temperature timeseries at the northern and center site from August 6–8 2018 in the water column, and 2.5 and 5 cm deep in the sediment. Temperature fluctuations at both sites were attenuated with increasing depth in the sediment, with peak temperatures during low tide on average 1.3°C warmer in the water column than 2.5 cm deep in the sediment, and on average 1.9°C warmer than 5 cm deep in the sediment. These differences were significant in the statistical sense (2 sample t-test, $p < 0.05$, $n = 13$ and 7 for the northern and center site, respectively). Temperature differences between the water column and sediment during high tide, however, were smaller. On average, the water column was 0.4°C cooler than the sediment (non-significant, 2 sample t-test, $p > 0.1$, $n = 12$ and 6 for the northern and center site, respectively).

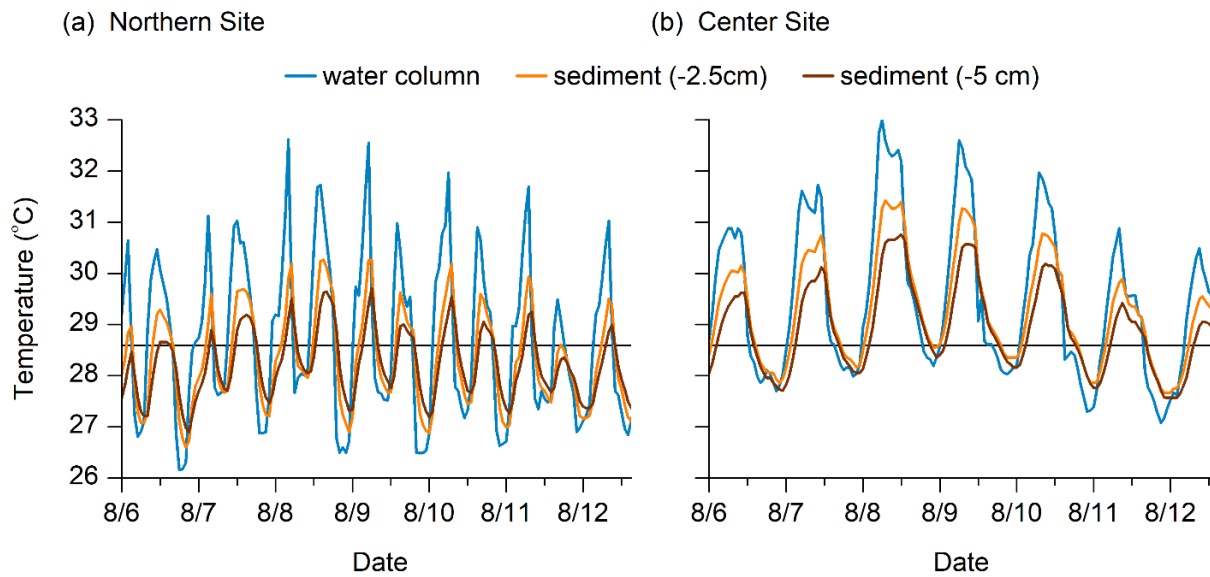


Fig. 7: Temperature attenuation in the sediment compared to the water column at the northern site **(a)** and center site **(b)**. Hourly temperatures from 8/6 to 8/8 2017 in the water column (blue) and in the root zone, 2.5 cm (orange) and 5 cm (brown) into the sediment.

Sulfide

The sulfur isotopic signatures ($\delta^{34}\text{S}$) of leaf samples from June and/or July 2012–2019 are shown in Figure 8. The $\delta^{34}\text{S}$ of samples taken outside of 2015 averaged 13.9‰. From June to July 2015, however, the $\delta^{34}\text{S}$ of seagrass tissues dropped from 13.5 ± 0.7 ‰ to 8.4 ± 0.5 ‰ ($n = 11$ samples). The F_{sulfide} values calculated from seagrass and sediment $\delta^{34}\text{S}$ values showed a higher contribution of sulfide to plant sulfur in July 2015 compared to previous or subsequent years (34% vs 16–25%, respectively).

Discussion

Duration and intensity of thermal stress above the thermal threshold were key to understanding eelgrass response to temperature stress. Sites near the ocean inlet experienced greater cooling during

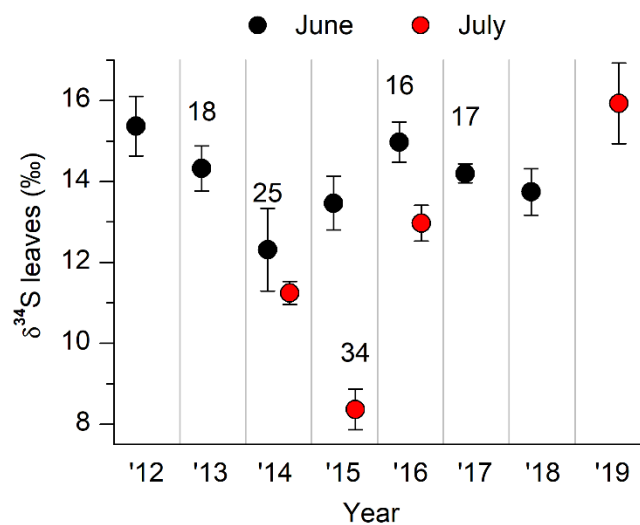


Fig. 8: Timeseries of the $\delta^{34}\text{S}$ of seagrass leaves collected in June (black) and/or July (red) of each year from 2012–2019. Numbers represent the proportion of sulfur in the seagrass tissue coming from sediment sulfide (F_{sulfide} , expressed as a percentage). Error bars are \pm SE.

incoming tides and had higher shoot density and canopy height. The beginning of heat stress during the early growing season and the added effects of sulfide toxicity also played an important role in seagrass mortality in 2015. These results show that thermal stress at the scale of hours and days can strongly impact eelgrass expansion and late-summer die-back, with implications for eelgrass recovery from marine heat waves in a warming ocean.

Thermal stress metrics

The ongoing increase in ocean temperatures and the frequency of severe heating events calls for appropriate metrics to describe relationships between these events and impacts on marine ecosystems. It is most common for these metrics to be based on climatological thresholds. For example, the definition for marine heatwaves is based on the 90th percentile of mean SSTs (Hobday et al. 2016), and the calculation of degree heating weeks to predict coral bleaching is based on the maximum monthly SST (Liu et al. 2014). Both of these rely on long-term records of SSTs, and have the merit to identify periods of unusually high temperatures. However, in one study this has been deemed insufficient to explain spatial variations of seagrass loss (Strydom et al. 2020). We argue that to identify a harmful event in the context of negative ecological impacts, it would be more relevant to base thermal stress calculations on the inherent vulnerability of an ecosystem to temperature stress. We used the thermal tolerance threshold for eelgrass (28.6°C), determined from in situ measurements of seagrass ecosystem metabolism in our study system. The thresholds for defining marine heatwaves at the VCR in June and July are on average 27.6°C and 29.4°C, respectively (Aoki et al. 2021). During the month of June, it would therefore be possible to identify a marine heatwave while no thermal stress is experienced in the meadows. In July, however, marine heatwaves identified in this way would certainly have negative effects on seagrass ecosystems, though negative effects could also be seen in heating events that fall below the 29.4°C threshold. Additionally, the calculations that produce degree heating weeks and are used to identify marine heatwaves rely on mean daily and weekly temperatures, which might underestimate some heating. In this study, we used a finer temporal scale (degree-hours). We found our metrics to be useful in comparing the intensity of heat stress between years (Table 3) and sites (Fig. 4). Particularly, comparing daily HDHs enabled us to identify the most stressful periods in the temperature record, which might have been averaged over had we only used average weekly temperatures (Fig. 3). The use of mean HDHs per day was helpful in comparing the cumulated heat stress over different heating events. For example, both 2018 and 2019 had a 27-day warm

period, however the one in 2018 was about half as intense as the one in 2019, with peak HDH values at the center site of 38°C-hours and 75°C-hours, respectively, and mean HDHs per day of 31°C-hours and 11°C-hours, respectively (Table 3). Our metrics also included the effects of cooling when quantifying thermal stress. The addition of CDHs provides more information about heat stress by enabling us to differentiate sites that may have the same cumulative HDHs, but different temperature profiles. For example, one site could exhibit more extreme temperature fluctuations with extreme warming but also cooling relative to the temperature threshold (a tidally-influenced site, for example). This site would therefore experience short pulses of high temperatures followed by cooler periods of thermal stress relief. In contrast, another site could have the same total HDH value, but not experience any relief from thermal stress. Instead, temperatures might be less extreme relative to T_{th} , but the thermal stress experienced by the ecosystem would be persistent. While intermittent cooling has not been widely considered in studies quantifying heat stress effects on marine ecosystems, Storlazzi et al. (2020) have highlighted the benefits of tidal cooling in buffering the effects on ocean warming on coral reefs. We therefore strongly suggest considering both heat stress and relief from heat stress in future studies on heat disturbances on marine ecosystems.

Thermal stress effects on seagrass growth

We observed higher shoot densities and shoot lengths (by 67% and 63%, respectively) at sites that experienced much less heating and more cooling (mean HDH per day to CDH per day ratio of 0.4) compared to sites at the center of the meadow (mean of 1.4 for the 3 most stressed sites, Fig. 4). While there was some variability in shoot length and density between the more stressed sites at the center of the meadow (Fig. 4), these results indicate a general trend of more thriving seagrass at sites that benefit from proximity to the ocean inlet (Fig. 1), and therefore benefitting from tidal cooling during hot days. The contrast in exposure to thermal stress between the center and northern part of the meadow is also evident in the contrasting expansion rates at the end of the growing season (7% and 43% increase in shoot density respectively, Fig. 5). This difference between the two sites (36%) is much larger than the difference in rates of decline into the late summer (10%). This suggests that thermal stress may play a more important role in seagrass expansion during the growing season, as opposed to the late summer during natural eelgrass senescence. This is further supported by the observed decline in seagrass shoot density

between April 27 and June 27, 2015 (Berg et al. 2019), a period during which heat stress was considerable (Fig. 6b).

The role of sulfide toxicity

While high water temperatures are largely recognized as the main driver of eelgrass die-off events (e.g. Berger et al. 2020), our results suggest sulfide toxicity may have also contributed to the eelgrass mortality we observed in 2015 (Fig. 8). Multiple studies have already linked seagrass mortality to the combined effects of high water temperatures and sulfide intrusion (Greve et al. 2003; Borum et al. 2005; Holmer et al. 2005). Elevated temperatures cause an increase in oxygen demand from seagrass tissues, which, combined with potentially low oxygen availability (e.g. during ecosystem respiration at night and/or at low tide in dense canopies) may lead tissues to become anoxic and thus susceptible to sulfide intrusion (Greve et al. 2003). Our results suggest a higher proportion of sulfide intake in 2015 compared to other years ($F_{\text{sulfide}} = 25\%$ and 34% in 2014 and 2015, respectively, Fig. 8). Furthermore, in our case study, we suggest there may have been an increase in sulfide production in the sediment during the early stages of the die-off. The ratio of live to dead seagrass biomass (above and belowground) in June 2015 was 0.74, compared to a ratio consistently > 1 (on average 1.4, $n = 7$) during the early summer in other years (samples from 2014, 2016, 2017). This indicates a greater proportion of dead seagrass biomass just after the die-off event started. Our study also shows that, while dampened, temperature fluctuations in the sediment follow those of the water column and may also reach relatively high temperatures ($> 28.6^{\circ}\text{C}$, Fig. 7). With the resulting increased respiration rates in the sediment and the newly added organic matter, it is possible that the initial warming led higher sulfide concentrations in the sediment. Combined with the weakened resistance to sulfide intrusion of thermally-stressed seagrass, we believe that sulfide toxicity exacerbated the seagrass decline.

The combined effects of two stressors likely had a stronger negative effect on eelgrass survival compared to exposure to thermal stress only (Moreno-Marín et al. 2018). This feedback should be taken into consideration when assessing future impacts of marine heating on seagrass ecosystems.

High temperature-induced die-off events

Because the amount of thermal stress calculated during summer heating events at our center site and at the Wachapreague station were so similar, we were confident in using the Wachapreague buoy record from 2015 to accurately estimate the amount of thermal stress that initiated the die-off event (Fig. 6). Not only did the 2015 heating event last much longer (~2 weeks), and reach a higher daily HDH than in other years, it cumulated a total of 220°C-hours, more than 2.5 times the amount cumulated in the second hottest June (2018, Fig. 6b). The amount of heat stress during the growing season that may trigger an eelgrass die-off event therefore lies between ~100–200°C-hours. While this estimate is broad, it may provide a baseline for determining the suitability of potential restoration sites, and for predicting future changes in seagrass cover. The actual amount of heat stress capable of causing widespread seagrass mortality may decrease over the years, however, as the increase in frequency and severity of extreme events (Oliver et al. 2019) may erode the ability of eelgrass to maintain their habitats and genetic diversity and therefore their resilience and adaptability to climate change (Ehlers et al. 2008).

Literature cited

Aoki, L. R., K. J. McGlathery, and M. P. J. Oreska. 2020a. Seagrass restoration reestablishes the coastal nitrogen filter through enhanced burial. *Limnol. Oceanogr.* **65**: 1–12. doi:10.1002/lno.11241

Aoki, L. R., K. J. McGlathery, P. L. Wiberg, and A. Al-Haj. 2020b. Depth Affects Seagrass Restoration Success and Resilience to Marine Heat Wave Disturbance. *Estuaries and Coasts* **43**: 316–328. doi:10.1007/s12237-019-00685-0

Aoki, L. R., K. J. McGlathery, P. L. Wiberg, M. P. J. Oreska, A. C. Berger, P. Berg, and R. J. Orth. 2021. Seagrass Recovery Following Marine Heat Wave Influences Sediment Carbon Stocks. *Front. Mar. Sci.* **7**. doi:10.3389/fmars.2020.576784

Arias-Ortiz, A., O. Serrano, P. Masqué, and others. 2018. A marine heatwave drives massive losses from the world's largest seagrass carbon stocks. *Nat. Clim. Chang.* doi:10.1038/s41558-018-0096-y

Armitage, A. R., and J. W. Fourqurean. 2016. Carbon storage in seagrass soils: Long-term nutrient history exceeds the effects of near-term nutrient enrichment. *Biogeosciences* **13**: 313–321. doi:10.5194/bg-13-313-2016

Berg, P., M. L. Delgard, P. Polsenaere, K. J. McGlathery, S. C. Doney, and A. C. Berger. 2019. Dynamics of benthic metabolism, O₂, and pCO₂ in a temperate seagrass meadow. *Limnol. Oceanogr.* Ino.11236. doi:10.1002/lno.11236

Berger, A. C., P. Berg, K. J. McGlathery, and M. L. Delgard. 2020. Long-term trends and resilience of seagrass metabolism: A decadal aquatic eddy covariance study. *Limnol. Oceanogr.* 1–16. doi:10.1002/lno.11397

Borum, J., O. Pedersen, T. M. Greve, T. A. Frankovich, J. C. Zieman, J. W. Fourqurean, and C. J. Madden. 2005. The potential role of plant oxygen and sulphide dynamics in die-off events

of the tropical seagrass, *Thalassia testudinum*. *J. Ecol.* **93**: 148–158. doi:10.1111/j.1365-2745.2004.00943.x

Böttcher, M. E., B.-K. Khim, A. Suzuki, M. Gehre, U. G. Wortmann, and H.-J. Brumsack. 2004. Microbial sulfate reduction in deep sediments of the Southwest Pacific (ODP Leg 181, Sites 1119–1125): evidence from stable sulfur isotope fractionation and pore water modeling. *Mar. Geol.* **205**: 249–260. doi:10.1016/S0025-3227(04)00026-X

Calleja, M. L., N. Marbá, and C. M. Duarte. 2007. The relationship between seagrass (*Posidonia oceanica*) decline and sulfide porewater concentration in carbonate sediments. *Estuar. Coast. Shelf Sci.* **73**: 583–588. doi:10.1016/j.ecss.2007.02.016

Canfield, D. E. 2001. Biogeochemistry of Sulfur Isotopes. *Rev. Mineral. Geochemistry* **43**: 607–636. doi:10.2138/gsrmg.43.1.607

Collier, C. J., S. Uthicke, and M. Waycott. 2011. Thermal tolerance of two seagrass species at contrasting light levels: Implications for future distribution in the Great Barrier Reef. *Limnol. Oceanogr.* **56**: 2200–2210. doi:10.4319/lo.2011.56.6.2200

Costanza, R., R. Arge, R. De Groot, and others. 1997. The value of the world's ecosystem services and natural capital. *Nature* **387**: 253–260. doi:10.1038/387253a0

Duarte, G. A. S., H. D. M. Villela, M. Deocleciano, and others. 2020. Heat Waves Are a Major Threat to Turbid Coral Reefs in Brazil. **7**: 1–8. doi:10.3389/fmars.2020.00179

Ehlers, A., B. Worm, and T. B. H. Reusch. 2008. Importance of genetic diversity in eelgrass *Zostera marina* for its resilience to global warming. *Mar. Ecol. Prog. Ser.* **355**: 1–7. doi:10.3354/meps07369

Ewers, C. J. 2013. Assessing physiological thresholds for eelgrass (*Zostera marina* L.) survival in the face of climate change. *Biol. Sci.* doi:https://doi.org/10.15368/theses.2013.126

Fourqurean, J. W., C. M. Duarte, H. A. Kennedy, and others. 2012. Seagrass ecosystems as a globally significant carbon stock. *Nat. Geosci.* **5**: 505–509. doi:10.1038/ngeo1477

Frederiksen, M. S., and R. N. Glud. 2006. Oxygen dynamics in the rhizosphere of *Zostera marina*: A two-dimensional planar optode study. *Limnol. Oceanogr.* **51**: 1072–1083. doi:10.4319/lo.2006.51.2.1072

Frederiksen, M. S., M. Holmer, J. Borum, and H. A. Kennedy. 2006. Temporal and spatial variation of sulfide invasion in eelgrass (*Zostera marina*) as reflected by its sulfur isotopic composition. *Limnol. Oceanogr.* **51**: 2308–2318. doi:10.4319/lo.2006.51.5.2308

Frölicher, T. L., E. M. Fischer, and N. Gruber. 2018. Marine heatwaves under global warming. *Nature* **560**: 360–364. doi:10.1038/s41586-018-0383-9

Greve, T. M., J. Borum, and O. Pedersen. 2003. Meristematic oxygen variability in eelgrass (*Zostera marina*). *Limnol. Oceanogr.* **48**: 210–216. doi:10.4319/lo.2003.48.1.0210

Hobday, A. J., L. V. Alexander, S. E. Perkins, and others. 2016. A hierarchical approach to defining marine heatwaves. *Prog. Oceanogr.* **141**: 227–238. doi:10.1016/j.pocean.2015.12.014

Holmer, M., M. S. Frederiksen, and H. Møllegaard. 2005. Sulfur accumulation in eelgrass (*Zostera marina*) and effect of sulfur on eelgrass growth. *Aquat. Bot.* **81**: 367–379. doi:10.1016/j.aquabot.2004.12.006

Holmer, M., and S. L. Nielsen. 1997. Sediment sulfur dynamics related to biomass-density patterns in *Zostera marina* (eelgrass) beds. *Mar. Ecol. Prog. Ser.* **146**: 163–171. doi:10.3354/meps146163

Hughes, T. P., J. T. Kerry, M. Álvarez-Noriega, and others. 2017. Global warming and recurrent mass bleaching of corals. *Nature* **543**: 373–377. doi:10.1038/nature21707

Koch, E. W., E. B. Barbier, B. R. Silliman, and others. 2009. Non-linearity in ecosystem services: Temporal and spatial variability in coastal protection. *Front. Ecol. Environ.* **7**: 29–37. doi:10.1890/080126

Lawson, S. E., P. L. Wiberg, K. J. McGlathery, and D. C. Fugate. 2007. Wind-driven sediment suspension controls light availability in a shallow coastal lagoon. *Estuaries and Coasts* **30**: 102–112. doi:10.1007/BF02782971

Lee, K.-S., S. R. Park, and Y. K. Kim. 2007. Effects of irradiance, temperature, and nutrients on growth dynamics of seagrasses: A review. *J. Exp. Mar. Bio. Ecol.* **350**: 144–175. doi:10.1016/j.jembe.2007.06.016

Liu, G., S. Heron, C. Eakin, and others. 2014. Reef-Scale Thermal Stress Monitoring of Coral Ecosystems: New 5-km Global Products from NOAA Coral Reef Watch. *Remote Sens.* **6**: 11579–11606. doi:10.3390/rs61111579

Macreadie, P. I., A. Anton, J. A. Raven, and others. 2019. The future of Blue Carbon science. *Nat. Commun.* **10**: 1–13. doi:10.1038/s41467-019-11693-w

Marbá, N., and C. M. Duarte. 2010. Mediterranean warming triggers seagrass (*Posidonia oceanica*) shoot mortality. *Glob. Chang. Biol.* **16**: 2366–2375. doi:10.1111/j.1365-2486.2009.02130.x

Mateo, M. Á., J. L. Sánchez-Lizaso, and J. Romero. 2003. *Posidonia oceanica* “banquettes”: A preliminary assessment of the relevance for meadow carbon and nutrients budget. *Estuar. Coast. Shelf Sci.* **56**: 85–90. doi:10.1016/S0272-7714(02)00123-3

Moore, K. A., and J. C. Jarvis. 2008. Eelgrass Diebacks in the Lower Chesapeake Bay : Implications for Long-term Persistence. *J. Coast. Res.* **55**: 135–147. doi:10.2112/S155-014.acteristics

Moore, K. A., F. T. Short, R. J. Orth, and C. M. Duarte. 2006. *Zostera : Biology , Ecology , and Management.*

Moreno-Marín, F., F. G. Brun, and M. F. Pedersen. 2018. Additive response to multiple environmental stressors in the seagrass *Zostera marina* L. *Limnol. Oceanogr.* **63**: 1528–1544. doi:10.1002/lno.10789

Nagelkerken, I., G. van der Velde, M. W. Gorissen, G. J. Meijer, T. Van't Hof, and C. den Hartog. 2000. Importance of Mangroves, Seagrass Beds and the Shallow Coral Reef as a Nursery for Important Coral Reef Fishes, Using a Visual Census Technique. *Estuar. Coast. Shelf Sci.* **51**: 31–44. doi:10.1006/ecss.2000.0617

Oliver, E. C. J., M. T. Burrows, M. G. Donat, and others. 2019. Projected Marine Heatwaves in the 21st Century and the Potential for Ecological Impact. *Front. Mar. Sci.* **6**: 1–12. doi:10.3389/fmars.2019.00734

Oreska, M. P. J., K. J. McGlathery, J. H. Porter, H. Asmus, R. M. Asmus, and A. Vaquer. 2017. Seagrass blue carbon spatial patterns at the meadow-scale J. Cebrian [ed.]. *PLoS One* **12**: e0176630. doi:10.1371/journal.pone.0176630

Oreska, M. P. J., K. J. McGlathery, P. L. Wiberg, R. J. Orth, and D. J. Wilcox. 2021. Defining the *Zostera marina* (Eelgrass) Niche from Long-Term Success of Restored and Naturally Colonized Meadows: Implications for Seagrass Restoration. *Estuaries and Coasts* **44**: 396–411. doi:10.1007/s12237-020-00881-3

Orth, R. J., J. S. Lefcheck, K. S. McGlathery, and others. 2020. Restoration of seagrass habitat leads to rapid recovery of coastal ecosystem services. *Sci. Adv.* **6**: eabc6434. doi:10.1126/sciadv.abc6434

Orth, R. J., M. L. Luckenbach, S. R. Marion, K. A. Moore, and D. J. Wilcox. 2006. Seagrass recovery in the Delmarva Coastal Bays, USA. *Aquat. Bot.* **84**: 26–36. doi:10.1016/j.aquabot.2005.07.007

Orth, R. J., and K. J. McGlathery. 2012. Eelgrass recovery in the coastal bays of the Virginia Coast Reserve, USA. *Mar. Ecol. Prog. Ser.* **448**: 173–176. doi:10.3354/meps09596

Orth, R. J., and K. A. Moore. 1986. Seasonal and Year-to Year Variations in the Growth of *Zostera marina* L.(Eelgrass) in the Lower Chesapeake Bay. *Aquat. Botany* **24**: 335–341. doi:10.1017/CBO9781107415324.004

Pedersen, O., T. Binzer, and J. Borum. 2004. Sulphide intrusion in eelgrass (*Zostera marina* L.). *Plant. Cell Environ.* **27**: 595–602. doi:doi: 10.1111/j.1365-3040.2004.01173.x

Pendleton, L., D. C. Donato, B. C. Murray, and others. 2012. Estimating Global “Blue Carbon” Emissions from Conversion and Degradation of Vegetated Coastal Ecosystems. *PLoS One* **7**. doi:10.1371/journal.pone.0043542

Rees, C. E., W. J. Jenkins, and J. Monster. 1978. The sulphur isotopic composition of ocean water sulphate. *Geochim. Cosmochim. Acta* **42**: 377–381. doi:10.1016/0016-7037(78)90268-5

Rees, S. E., L. D. Rodwell, M. J. Attrill, M. C. Austen, and S. C. Mangi. 2010. The value of marine biodiversity to the leisure and recreation industry and its application to marine spatial planning. *Mar. Policy* **34**: 868–875. doi:10.1016/j.marpol.2010.01.009

Skirving, W. J., S. F. Heron, B. L. Marsh, G. Liu, J. L. De La Cour, E. F. Geiger, and C. M. Eakin. 2019. The relentless march of mass coral bleaching: a global perspective of changing heat stress. *Coral Reefs* **38**: 547–557. doi:10.1007/s00338-019-01799-4

Smale, D. A., T. Wernberg, E. C. J. Oliver, and others. 2019. Marine heatwaves threaten global biodiversity and the provision of ecosystem services. *Nat. Clim. Chang.* **9**: 306–312. doi:10.1038/s41558-019-0412-1

Strydom, S., K. Murray, S. Wilson, and others. 2020. Too hot to handle: Unprecedented seagrass death driven by marine heatwave in a World Heritage Area. *Glob. Chang. Biol.* **26**: 3525–3538. doi:10.1111/gcb.15065

Storlazzi, C.D., Cheriton, O.M., van Hooonk, R., and others. 2020. Internal tides can provide thermal refugia that will buffer some coral reefs from future global warming. *Sci Rep* **10**, 13435. <https://doi.org/10.1038/s41598-020-70372-9>

Thomsen, M. S., L. Mondardini, T. Alestra, and others. 2019. Local Extinction of Bull Kelp (*Durvillaea* spp.) Due to a Marine Heatwave. *Front. Mar. Sci.* **6**: 1–10. doi:10.3389/fmars.2019.00084

Thomson, J. A., D. A. Burkholder, M. R. Heithaus, J. W. Fourqurean, M. W. Fraser, J. Statton, and G. A. Kendrick. 2015. Extreme temperatures, foundation species, and abrupt ecosystem change: an example from an iconic seagrass ecosystem. *Glob. Chang. Biol.* **21**: 1463–1474. doi:10.1111/gcb.12694

Wahid, A., S. Gelani, M. Ashraf, and M. R. Foolad. 2007. Heat tolerance in plants: An overview. *Environ. Exp. Bot.* **61**: 199–223. doi:10.1016/j.envexpbot.2007.05.011

Wernberg, T., S. Bennett, R. C. Babcock, and others. 2016a. Climate-driven regime shift of a temperate marine ecosystem. *Science* (80-.). **353**: 169–172. doi:10.1126/science.aad8745

Wernberg, T., T. de Bettignies, B. A. Joy, and P. M. Finnegan. 2016b. Physiological responses of habitat-forming seaweeds to increasing temperatures. *Limnol. Oceanogr.* **61**: 2180–2190. doi:10.1002/lno.10362

York, P. H., R. K. Gruber, R. Hill, P. J. Ralph, D. J. Booth, and P. I. Macreadie. 2013. Physiological and Morphological Responses of the Temperate Seagrass *Zostera muelleri* to Multiple Stressors : Investigating the Interactive Effects of Light and Temperature. **8**: 1–12. doi:10.1371/journal.pone.0076377

CHAPTER 4: SEAGRASS MEADOW (*ZOSTERA MARINA*) LIGHT-USE EFFICIENCY MEASURED BY AQUATIC EDDY COVARIANCE.

Amelie C. Berger, Peter Berg

Abstract

Light-use efficiency (LUE) describes the ability of primary producers to convert sunlight energy into primary production, and has been widely used in terrestrial systems to assess crop yields and resource-use efficiency. In benthic marine ecosystems such as seagrass meadows, LUE can be a useful metric to assess how much light is needed to sustain a healthy ecosystem and how seagrasses might respond to future changes in light availability, caused for example by sea level rise and more frequently reduced water clarity due to storms. LUE is computed as the ratio between gross primary production (GPP) and the absorbed photosynthetically active radiation (PAR). Most studies estimating LUE for seagrass species have done so based on metabolism measurements on leaf fragments incubated under controlled conditions. In this study, we use 106 days (2115 hours) of high-quality in situ seagrass metabolism data measured via aquatic eddy covariance (AEC) to estimate, for the first time, eelgrass (*Zostera marina*) LUE at the ecosystem-scale and under naturally varying environmental conditions. Average LUE was 0.004–0.005 O₂ photon⁻¹, which is ~an order of magnitude lower than previous LUE estimates for eelgrass, and far below the theoretical maximum of 0.125 O₂ photon⁻¹. These results reflect the importance of including all ecosystem components in metabolic measurements to better assess the photosynthetic efficiency of seagrass at the meadow-scale. Patterns in hourly LUE revealed maximum LUE (0.01 O₂ photon⁻¹) under light-limiting conditions during the first and last light hour of the day, and minimum LUE (0.0030 O₂ photon⁻¹) under high midday irradiances. This reflects the ability of eelgrass to regulate photosynthesis in response to low light availability and potentially damaging high irradiances. Daily LUE was highly variable (CV = 69%) over the 8-year record, and no seasonal trends were observed. These results may reflect the highly dynamic nature of seagrass metabolism and its environmental drivers, and perhaps reduction of GPP from nutrient-limitation.

Introduction

Seagrass meadows are highly productive ecosystems that inhabit shallow coastal waters worldwide. Their high rates of primary production play a key part in their ability to sequester and store ‘blue carbon’ (Duarte et al. 2010), as well as to provide food and habitat for many marine species (e.g. Costanza et al. 1997; Nagelkerken et al. 2000; Beck et al. 2001). While seagrasses, particularly eelgrass (*Zostera marina*), have shown acclimation to variations in environmental conditions (light and temperature) (e.g. Moore et al. 1997; Staehr and Borum 2011), they remain threatened by future climate change scenarios of increased water temperatures (e.g. Ehlers et al. 2008; Smale et al. 2019; Berger et al. *in prep*) and decreased light availability due to sea level rise and changes in storm frequency (e.g. Lencart e Silva et al. 2013; Davis et al. 2016; Saunders et al. 2017). For this reason, and because light is the dominant driver of seagrass primary production (Hume et al. 2011; Berg et al. 2013; Rheuban et al. 2014; Berger et al. 2020), it is important to enhance our understanding of the light requirements for seagrass ecosystem growth.

Light-use efficiency (LUE) is a useful measure of ecosystem function, describing the efficiency with which absorbed photosynthetically active radiation (PAR) is converted into primary production. It is computed as $LUE = \text{gross primary production (GPP)} / (\text{PAR} * fAPAR)$ ($fAPAR = \text{the fraction of absorbed PAR}$) (Monteith 1977), and has units of mol O₂ evolved per mol photon absorbed (O₂ photon⁻¹). This measure is commonly used to assess crop yield and productivity in terrestrial ecosystems (e.g. Stocker et al. 2018; Hemes et al. 2020), but has not been applied widely to aquatic ecosystems. LUE has mostly been used to understand the energy budgets of microbial mats and corals (Al-Najjar et al. 2010, 2012; Brodersen et al. 2014) and has been employed recently to investigate the benthic primary production of algal mats and mussel beds (Attard and Glud 2020). A number of studies have estimated the LUE of seagrasses by measuring photosynthesis and respiration of seagrass leaf fragments incubated in the lab under controlled light conditions (e.g. Major and Dunton 2000; Enríquez et al. 2002; Staehr and Borum 2011). In these studies, LUE is determined from the initial slope of the photosynthesis-irradiance (PI) curve and represents the minimum amount of PAR required for leaf photosynthesis under sub-saturated light conditions (e.g. Frost-Christensen and Sand-Jensen 1992; Staehr and Borum 2011). This approach to estimating LUE, however, focuses on the leaves and thus does not provide a realistic idea of the minimum light requirements for eelgrass growth at the ecosystem scale, where, for example, below-ground biomass is a significant contributor to ecosystem respiration (Cayabyab

and Enríquez 2007; Ralph et al. 2007; Staehr and Borum 2011). The light requirements for maintaining an eelgrass meadow—i.e., maintaining a carbon balance ≥ 0 , all ecosystem components considered—are thus likely much higher than previously determined. LUE estimates derived from past studies therefore offer little insights into potential for survival of eelgrass ecosystems under future changes in light availability.

There are currently no estimates for the LUE of seagrasses at the ecosystem scale. In this study, we used in situ seagrass (*Z. marina*) metabolism data measured via aquatic eddy covariance (AEC) to estimate seagrass LUE under naturally varying environmental conditions. The AEC technique generates benthic O₂ fluxes at a high temporal resolution (15 min), over multiple days, and over a large benthic area (10–100 m²) — therefore integrating over landscape heterogeneity (e.g. seagrass patchiness) and accurately capturing the dynamic response of seagrass metabolism to its environmental drivers at the ecosystem scale (Berg et al. 2007). The results from this study will provide insights into the efficiency of eelgrass ecosystems to convert solar energy into GPP, and their potential response to lower light conditions in the future.

Methods

Study Site

South Bay contains a previously restored eelgrass meadow that was seeded in 2001, and reached maturity around 2010 (Orth et al. 2006; Orth and McGlathery 2012). It is located at the Virginia Coast Reserve, on the Atlantic side of the Delmarva Peninsula. The shallow, oligotrophic waters of this coastal bay are sheltered by a barrier island, which provides a calm, light-filled environment suitable for eelgrass growth (Lawson et al. 2007). This study uses eelgrass metabolism data measured between 2011–2019 at a long-term study site near the center of the 7-km² meadow (37°15'43.6356"N, 75°48'54.547"W) (Rheuban et al. 2014; Berg et al. 2017; Berger et al. 2020, “center site” in chapters 2 and 3). Mean water depth at this site is 1.2 m with a tidal range of 1 m and current speeds ranging from 0.3 to 21.5 cm s⁻¹.

Data collection and light-use efficiency calculations

Seagrass metabolism data were collected using the AEC technique and processed as described in Berger et al. (2020), Berg et al. (2019), and Berg et al. (2017). The hourly benthic O₂ fluxes derived from this approach were aligned with corresponding PAR, which was recorded every 5 min by planar 2 π Odyssey PAR loggers deployed at canopy height (30 cm above the

seafloor), and cumulated on an hourly basis. All hourly PAR and O₂ flux values obtained between March and October 2011–2019 (n = 2,115 hours) were binned by hour of day to represent a typical 24-hour cycle during the most productive months, as in Juska and Berg (*in prep*). Because high temperatures have negative effects on seagrass photosynthesis (e.g. Staehr and Borum 2011; Rasmussen et al. 2020; Berger et al. *in prep*), this dataset excludes daytime O₂ fluxes where water temperatures reach or exceed 28°C (Juska and Berg, *in prep*).

The daytime O₂ fluxes measured by AEC represent the balance between ecosystem GPP and respiration (R) during light hours (when PAR > 1% max daily irradiance). LUE calculations require GPP instead of the net primary production that we measured directly. It is therefore necessary to add daytime hourly R to our hourly O₂ fluxes to calculate GPP (GPP_{hourly}). This was done as described in (Juska and Berg, *in prep*). After converting GPP_{hourly} from units of mmol O₂ m⁻² d⁻¹ to units of μmol O₂ m⁻² s⁻¹ (matching PAR units of μmol photon m⁻² s⁻¹), hourly LUE was computed as:

$$LUE_{hourly} = \frac{GPP_{hourly}}{PAR_{hourly} \times fAPAR} \quad (1)$$

where fAPAR—the fraction of incident PAR absorbed—was assumed to equal 1.0, as in Attard and Glud (2020). The fraction of incident PAR absorbed is typically between 80–100% in benthic environments, and reaches its maximum in environments such as seagrass beds where greater structural complexity leads to higher light scattering (Al-Najjar et al., 2012; Zimmerman, 2003). In the absence of direct field measurements of fAPAR for this study, we assume fAPAR = 1.0, which could lead to slightly underestimated LUE values.

To compute daily LUE (LUE_{daily}), hourly PAR values were converted to mmol photons m⁻² h⁻¹ and summed to obtain daily integrated PAR in mmol photons m⁻² d⁻¹ (PAR_{daily}). Daily GPP (GPP_{daily}) was calculated for each 24 h period as in Hume et al. (2011) and Berger et a. (2020) following the equation:

$$GPP_{daily} = \frac{1}{24} \left(\sum flux_{light} + \frac{|\sum flux_{dark}|}{h_{dark}} h_{light} \right) \quad (2)$$

where flux_{light} are the hourly O₂ fluxes during the day (during light hours, h_{light}), and flux_{dark} are the nighttime O₂ fluxes (during dark hours, h_{dark}) based on a light/dark threshold of 1% max

daily PAR. Daily LUE was then computed as $LUE_{\text{daily}} = GPP_{\text{daily}} / PAR_{\text{daily}}$, with GPP and PAR_{daily} in $\text{mmol O}_2 \text{ m}^{-2} \text{ d}^{-1}$ and $\text{mmol photon m}^{-2} \text{ d}^{-1}$, respectively, and LUE_{daily} in $\text{O}_2 \text{ photon}^{-1}$. LUE_{daily} was computed for a total of 106 days. For 2011–2012 data, hourly O_2 flux and PAR data were binned by hour of day for each field campaign, to produce one representative 24-hr period for each sampled month. These 4 representative days were then treated as the other 24-hr periods for GPP_{daily} and LUE_{daily} calculations.

Finally, we examined seasonal variations in eelgrass LUE by computing LUE from daily GPP and PAR data binned by month of year, as in Berger et al. (2020). No data were collected during September or December, so GPP, R, and PAR values were interpolated based on the adjacent months.

Results

Hourly light-use efficiency

Hourly LUE averaged $0.0049 \pm 0.0007 \text{ O}_2 \text{ photon}^{-1}$ (all results are reported as mean \pm SE) ($n = 14$) and was at its highest during the first and last light hours ($LUE_{\text{hourly}} = 0.0095 \text{ O}_2 \text{ photon}^{-1}$ at 6:00 and 0.0109 at 19:00, respectively) (Fig. 1). LUE_{hourly} decreased rapidly after sunrise to a minimum of $0.0030 \text{ O}_2 \text{ photon}^{-1}$ at midday (12:00–15:00), corresponding to peak irradiance (average $PAR_{\text{hourly}} = 1407 \mu\text{mol photon m}^{-2} \text{ s}^{-1}$ during those 3 midday hours).

Daily light-use efficiency

Daily LUE averaged $0.0037 \pm 0.00025 \text{ O}_2 \text{ photon}^{-1}$ ($n = 106$) between 2011–2019 (Fig. 2), and varied between 0.000039 and $0.0165 \text{ O}_2 \text{ photon}^{-1}$. LUE_{daily}

was highly variable, with a coefficient of variation (CV) of 69%. Highest LUE_{daily} was observed in 2011 and 2012 (mean $LUE_{\text{daily}} = 0.0117 \pm 0.002 \text{ O}_2 \text{ photon}^{-1}$, $n = 4$). In comparison, average

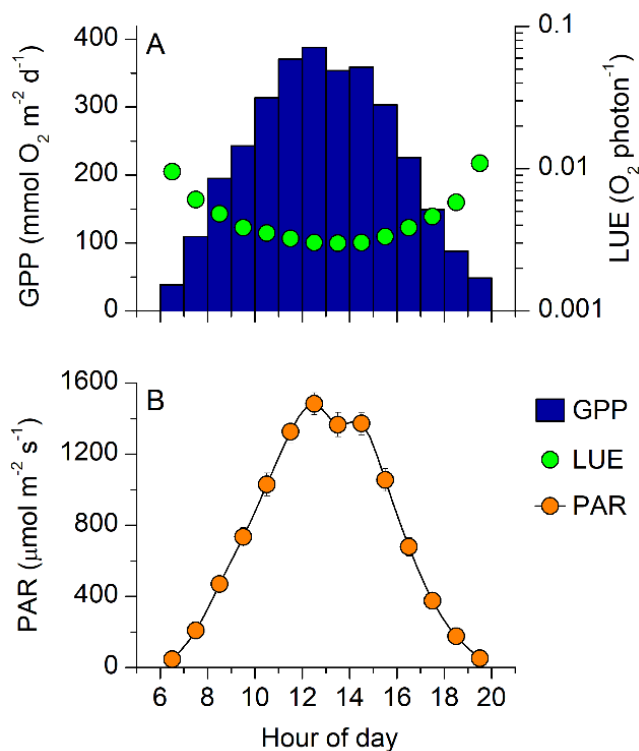


Fig. 1: A) Hourly gross primary production (GPP, blue) and light-use efficiency (LUE, green) during light hours. B) Photosynthetically active radiation (PAR, orange) binned by hour of day. Error bars are \pm SE, $n = 64$ –92.

LUE_{daily} during 2014–2019 was 0.0033 ± 0.0002 O₂ photon⁻¹ (n = 102). Lowest LUE_{daily} occurred in January 2015, when R and GPP were -34 and 1.8 mmol O₂ m⁻² d⁻¹, respectively. Over the entire 8-year period, R averaged -122 ± 7 mmol O₂ m⁻² d⁻¹, GPP averaged 119 ± 7 mmol O₂ m⁻² d⁻¹, and PAR averaged $34,945 \pm 1,355$ mmol photon m⁻² d⁻¹ (n = 106).

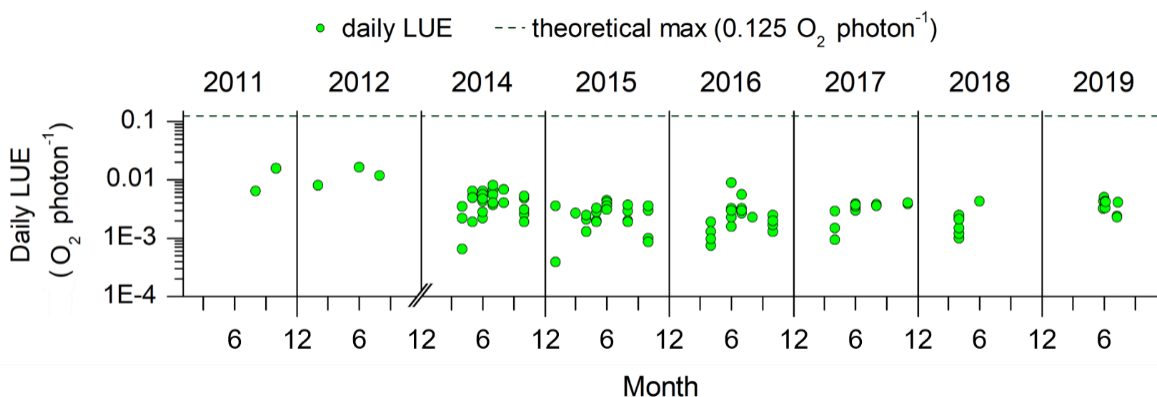


Fig. 2: Daily light-use efficiency (LUE, green) for n = 106 days between July 2011 and August 2019, relative to the theoretical maximum LUE of 0.125 O₂ photon⁻¹ (Godvinjee, 1999).

Seasonal variations in light-use efficiency

Monthly LUE averaged 0.0037 ± 0.0004 O₂ photon⁻¹ and varied between 0.0017–0.0073 O₂ photon⁻¹ throughout the year (Fig. 3). Monthly LUE was variable (CV = 39%) and did not exhibit any seasonal patterns.

Discussion

This study provides the first estimates of seagrass LUE under naturally varying environmental conditions and at the ecosystem scale, using robust AEC data. Previous estimates of LUE for *Z. marina* leaves based on PI curves averaged 0.05 O₂ photon⁻¹ and have reached the theoretical maximum of 0.125 O₂ photon⁻¹ (Frost-Christensen and Sand-Jensen 1992; Govindjee 1999; Enríquez et al.

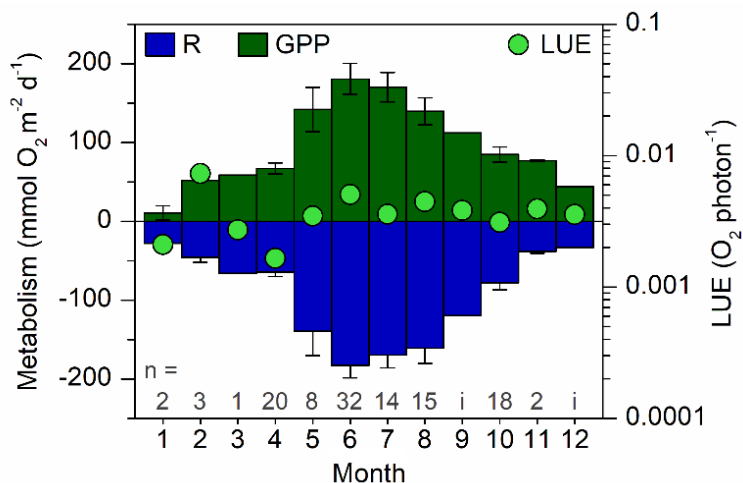


Fig. 3: Annual oxygen budget in South Bay from Berger et al. (2020), with seasonal measurements of gross primary production (GPP, dark green) and respiration (R, blue) (n = 2–32, i = interpolated values). Monthly light-use efficiency (LUE, light green) was calculated for each month based on the binned and interpolated GPP and photosynthetically active radiation (PAR) measurements.

2002; Staehr and Borum 2011). This theoretical maximum provides an upper constraint for the GPP that is possible for a given PAR level, and also indicates that a minimum of 8 photons must be absorbed for a plant to synthesize one molecule of O₂. On an hourly scale, we found that LUE averaged 0.0049 O₂ photon⁻¹, which is an order of magnitude lower than these estimates (Table 1) and far below the theoretical maximum. Average daily LUE (0.0037 O₂ photon⁻¹) was similarly low, reaching at most ~one-tenth of the theoretical maximum during our 8-year measurement period (Fig. 2). This is not surprising, however, given that previous studies based their LUE estimates on the metabolism of seagrass leaf fragments, which ignores ecosystem-scale dynamics and whole plant respiratory demands that include below-ground plant biomass (Cayabyab and Enríquez 2007; Ralph et al. 2007; Staehr and Borum 2011). GPP estimates for seagrass ecosystems measured via AEC include the respiratory demands of above and below-ground seagrass biomass as well as other primary producers and autotrophs, and therefore include higher R compared to studies that only measure seagrass leaf respiration, resulting in ~40% higher GPP estimates, and therefore lower LUE values (Table 1). The LUE values reported in this study are within the range of those in Attard and Glud (2020), another ecosystem-scale AEC study over algal mats and mussel reefs.

Table 1: Comparison of mean, minimum, and maximum hourly light-use efficiency (LUE_{hourly}, in O₂ photon⁻¹) in comparable studies on benthic ecosystems. Peak daily irradiance (PAR in μmol m⁻² s⁻¹) and the ratio between mean hourly dark respiration and maximum net photosynthetic rate (R/NP_{max}, unitless) were also compared where data were available.

	mean LUE _{hourly}	min LUE _{hourly}	max LUE _{hourly}	R/NP _{max}	max PAR	system	method
This study	0.0049	0.003	0.011	0.54	1483	<i>Zostera marina</i> (VCR)	AEC
Attard and Glud (2020)		0.008	0.013	0.51	500	benthic algae	AEC
Attard and Glud (2020)		0.006	0.007		500	mussel reef	AEC
Staehr and Borum (2011)		0.042	0.125	0.15	410	<i>Zostera marina</i> (Denmark)	leaf fragment incubations - PI curve
Frost-Christensen and Sand-Jensen (1992)	0.049					submerged angiosperms	leaf fragment incubations - PI curve
Enriquez et al. (2002)	0.045			0.08	2075	<i>Thalassia testudinum</i>	leaf fragment incubations - PI curve

Results from leaf incubation studies are also difficult to translate to in situ conditions because they do not reflect the natural light environment within the seagrass canopy (e.g. Enríquez et al. 2002), with large differences in light exposure between self-shading and light flecks. Instead, laboratory studies rely on homogeneous tissue illumination from experimental light sources (Staehr and Borum 2011).

The LUE values reported in this study may also be slightly underestimated given our assumption that all incident PAR is absorbed by the seabed ($fAPAR = 1.0$), when in reality a fraction of incident PAR is reflected and not available for photosynthesis. Studies have found that seagrass leaf reflectance falls between 4–9% of incident PAR (Runcie and Durako, 2004; Enríquez, 2005; Thorhaug et al., 2006; Durako, in press), and thus our LUE estimates are therefore likely underestimated by $< 10\%$. It is also unclear how the presence of epiphytes on the seagrass leaves may have impacted our LUE estimates. In our study system, seagrass is the main driver of ecosystem metabolism (70–75%, Berger et al. 2020), yet in the late summer, seagrass leaves become covered by epiphytes, which most likely intercept a higher proportion of incident PAR. This changes the distribution of available PAR between primary producers in the system, and it is uncertain what affect this might have on LUE.

Patterns in daily light-use efficiency

While no striking interannual trends in LUE_{daily} was observed (Fig. 2), this study found that on average, LUE_{daily} values from 2011 and 2012 were ~ 3.5 times higher than average LUE_{daily} values from 2014–2019. This pattern matches that observed in the nitrogen content (%N) of eelgrass leaves collected in South Bay every summer from 2010–2018 (Fig. 4), which suggests eelgrass at our study site experienced

nitrogen limitation ($\%N < 1.8\%$, Duarte 1990) between 2014–2018. Mean %N for 2010–2012 was 1.84 ± 0.04 ($n = 8$). While marginally above the 1.8% threshold for nitrogen limitation (Duarte 1990), this suggests GPP in 2011 and 2012 may have been stimulated by slightly higher nutrient availability. Nitrogen-limited conditions throughout most of our AEC record (2014–2019) may also partially explain why GPP was not higher given our high PAR values, and why our LUE values might be considered low.

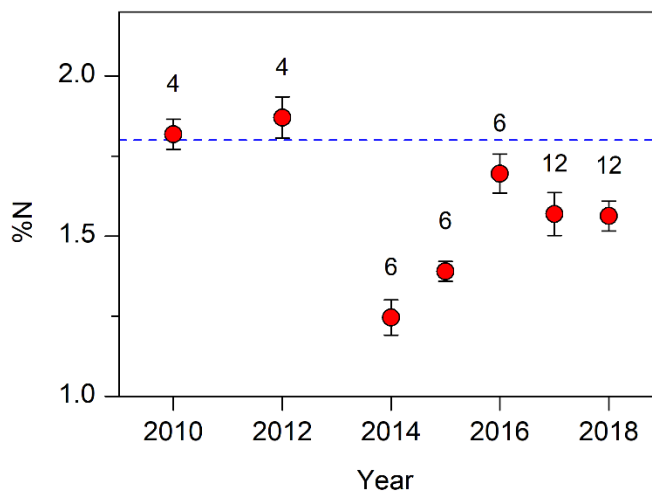


Fig. 4: Nitrogen content (%N) of eelgrass leaves collected in South Bay each summer (June or July) between 2010 and 2018. Means \pm SE (n displayed above symbols) are shown in comparison to the nitrogen limitation threshold of 1.8%N (dashed line) (Duarte, 1990)

Patterns in hourly light-use efficiency

This study found that LUE_{hourly} was highest under low-light conditions ($< 50 \mu\text{mol photon m}^{-2} \text{ s}^{-1}$) after sunrise and before sunset (Fig. 1), and lowest under high midday irradiance levels (reaching ~one-tenth of maximum LUE_{hourly}). This pattern is consistent with the findings from other studies (e.g. Al-Najjar et al. 2012; Brodersen et al. 2014; Attard and Glud 2020). Seagrasses have been found to acclimate to changes in light by modifying their photosynthetic efficiency as well as pigment concentrations in their tissues (e.g. Abal et al. 1994; Masini and Manning 1997; Major and Dunton 2002). While structural changes tend to occur over longer timescales (monthly to seasonal), seagrasses are able to downregulate photosynthesis during the day to avoid photodamage from high midday irradiances, and conversely, increase the photon yield of photosynthesis when light becomes limiting (Major and Dunton 2000; Staehr and Borum 2011).

Seasonal trends in light-use efficiency

While Staehr and Borum (2011) found higher eelgrass LUE in the winter (February) than in the summer (August), we did not observe any clear seasonal trends in LUE (Fig. 3). In fact, the difference in LUE between our minimum and maximum LUE values was $\sim 0.006 \text{ O}_2 \text{ photon}^{-1}$, which is over an order of magnitude lower than the difference in LUE found in that study (difference of $0.085 \text{ O}_2 \text{ photon}^{-1}$). It is likely that the dynamic and variable nature of the factors going into LUE estimates may not be properly captured in lab incubations. These factors include seasonal changes in light levels (not only due to changes in incoming solar irradiance, but also the seasonality of storms), changes in aboveground to belowground seagrass biomass ratios—which in turn affects R and GPP—changes in temperature, with potential limitation of photosynthesis under very low or very high temperatures ($>28.6^\circ\text{C}$, Berger et al. *in prep*), and other changes in the structural and functional response of the plants to environmental change. Additionally, nutrient-limited conditions may prevent us from observing certain trends under increasing light conditions throughout the year.

Conclusion

The LUE approach provided some insights into the photosynthetic performance of eelgrass at the ecosystem scale and on multiple timescales. We found evidence of short-term acclimation to high midday irradiances, and high variability in LUE on daily to monthly timescales. This high variability highlights the dynamic nature of seagrass metabolism and its environmental drivers. It

is also possible that nutrient limitation in our study system may impose a cap on the GPP that is possible given high PAR levels. More detailed and targeted studies of LUE in seagrass environments would be useful in formulating hypotheses about the response of seagrasses to future environmental change.

Literature Cited

- Abal, E. G., N. Loneragan, P. Bowen, C. J. Perry, J. W. Udy, and W. C. Dennison. 1994. Physiological and morphological responses of the seagrass *Zostera capricorni* Aschers, to light intensity. *J. Exp. Mar. Bio. Ecol.* **178**: 113–129. doi:10.1016/0022-0981(94)90228-3
- Al-Najjar, M. A. A., D. De Beer, B. B. Jørgensen, M. Kühl, and L. Polerecky. 2010. Conversion and conservation of light energy in a photosynthetic microbial mat ecosystem. *ISME J.* **4**: 440–449. doi:10.1038/ismej.2009.121
- Al-Najjar, M. A. A., D. de Beer, M. Kühl, and L. Polerecky. 2012. Light utilization efficiency in photosynthetic microbial mats. *Environ. Microbiol.* **14**: 982–992. doi:10.1111/j.1462-2920.2011.02676.x
- Attard, K. M., and R. N. Glud. 2020. Technical Note: Estimating light-use efficiency of benthic habitats using underwater O₂ eddy covariance. *Biogeosciences* **17**: 4343–4353. doi:10.5194/bg-17-4343-2020
- Beck, M. W., K. L. Heck, K. W. Able, and others. 2001. The Identification, Conservation, and Management of Estuarine and Marine Nurseries for Fish and Invertebrates. *Bioscience* **51**: 633. doi:10.1641/0006-3568(2001)051[0633:TICAMO]2.0.CO;2
- Berg, P., M. L. Delgard, R. N. Glud, M. Huettel, C. E. Reimers, and M. L. Pace. 2017. Non-invasive flux Measurements at the Benthic Interface: The Aquatic Eddy Covariance Technique. *Limnol. Oceanogr. e-Lectures* **7**: 1–50. doi:10.1002/loe2.10005
- Berg, P., M. H. Long, M. Huettel, and others. 2013. Eddy correlation measurements of oxygen fluxes in permeable sediments exposed to varying current flow and light. *Limnol. Oceanogr.* **58**: 1329–1343. doi:10.4319/lo.2013.58.4.1329
- Berg, P., H. Røy, and P. L. Wiberg. 2007. Eddy correlation flux measurements: The sediment surface area that contributes to the flux. *Limnol. Oceanogr.* **52**: 1672–1684. doi:10.4319/lo.2007.52.4.1672
- Berger, A. C., P. Berg, K. J. McGlathery, and M. L. Delgard. 2020. Long-term trends and resilience of seagrass metabolism: A decadal aquatic eddy covariance study. *Limnol. Oceanogr.* 1–16. doi:10.1002/lno.11397
- Brodersen, K. E., M. Lichtenberg, P. J. Ralph, M. Kühl, and D. Wangpraseurt. 2014. Radiative energy budget reveals high photosynthetic efficiency in symbiont-bearing corals. *J. R. Soc. Interface* **11**. doi:10.1098/rsif.2013.0997
- Cayabyab, N. M., and S. Enríquez. 2007. Leaf photoacclimatory responses of the tropical seagrass *Thalassia testudinum* under mesocosm conditions: A mechanistic scaling-up study. *New Phytol.* **176**: 108–123. doi:10.1111/j.1469-8137.2007.02147.x
- Costanza, R., R. Arge, R. De Groot, and others. 1997. The value of the world's ecosystem services and natural capital. *Nature* **387**: 253–260. doi:10.1038/387253a0

- Davis, T. R., D. Harasti, S. D. A. Smith, and B. P. Kelaher. 2016. Using modelling to predict impacts of sea level rise and increased turbidity on seagrass distributions in estuarine embayments. *Estuar. Coast. Shelf Sci.* **181**: 294–301. doi:10.1016/j.ecss.2016.09.005
- Duarte, C. M. 1990. Seagrass nutrient content. *Mar. Ecol. Prog. Ser.* **67**: 201–207–207. doi:10.3354/meps067201
- Duarte, C. M., N. Marbá, E. Gacia, J. W. Fourqurean, J. Beggins, C. Barrón, and E. T. Apostolaki. 2010. Seagrass community metabolism: Assessing the carbon sink capacity of seagrass meadows. *Global Biogeochem. Cycles* **24**: 1–8. doi:10.1029/2010GB003793
- Ehlers, A., B. Worm, and T. B. H. Reusch. 2008. Importance of genetic diversity in eelgrass *Zostera marina* for its resilience to global warming. *Mar. Ecol. Prog. Ser.* **355**: 1–7. doi:10.3354/meps07369
- Enríquez, S., M. Merino, and R. Iglesias-Prieto. 2002. Variations in the photosynthetic performance along the leaves of the tropical seagrass *Thalassia testudinum*. *Mar. Biol.* **140**: 891–900. doi:10.1007/s00227-001-0760-y
- Frost-Christensen, H., and K. Sand-Jensen. 1992. The quantum efficiency of photosynthesis in macroalgae and submerged angiosperms. *Oecologia* **91**: 377–384. doi:10.1007/BF00317627
- Govindjee, A. 1999. On the requirement of minimum number of four versus eight quanta of light for the evolution of one molecule of oxygen in photosynthesis: A historical note. *Photosynth. Res.* **59**: 249–254. doi:10.1023/A:1006122501487
- Hemes, K. S., J. Verfaillie, and D. D. Baldocchi. 2020. Wildfire-Smoke Aerosols Lead to Increased Light Use Efficiency Among Agricultural and Restored Wetland Land Uses in California's Central Valley. *J. Geophys. Res. Biogeosciences* **125**: e2019JG005380. doi:10.1029/2019JG005380
- Hume, A. C., P. Berg, and K. J. McGlathery. 2011. Dissolved oxygen fluxes and ecosystem metabolism in an eelgrass (*Zostera marina*) meadow measured with the eddy correlation technique. *Limnol. Oceanogr.* **56**: 86–96. doi:10.4319/lo.2011.56.1.0086
- Juska, I. and P. Berg. *In prep.* Variation in seagrass meadow respiration measured by aquatic eddy covariance.
- Lawson, S. E., P. L. Wiberg, K. J. McGlathery, and D. C. Fugate. 2007. Wind-driven sediment suspension controls light availability in a shallow coastal lagoon. *Estuaries and Coasts* **30**: 102–112. doi:10.1007/BF02782971
- Lencart e Silva, J. D., A. Azevedo, A. I. Lillebø, and J. M. Dias. 2013. Turbidity under changing physical forcing over two contrasting locations of seagrass meadows. *J. Coast. Res.* **165**: 2023–2028. doi:10.2112/si65-342.1
- Major, K. M., and K. H. Dunton. 2000. Photosynthetic performance in *Syringodium filiforme*: Seasonal variation in light-harvesting characteristics. *Aquat. Bot.* **68**: 249–264. doi:10.1016/S0304-3770(00)00115-7
- Major, K. M., and K. H. Dunton. 2002. Variations in light-harvesting characteristics of the seagrass, *Thalassia testudinum*: Evidence for photoacclimation. *J. Exp. Mar. Bio. Ecol.* **275**: 173–189. doi:10.1016/S0022-0981(02)00212-5

- Masini, R. J., and C. R. Manning. 1997. The photosynthetic responses to irradiance and temperature of four meadow-forming seagrasses. *Aquat. Bot.* **58**: 21–36. doi:10.1016/S0304-3770(97)00008-9
- Monteith, J. L. 1977. Climate and the efficiency of crop production in Britain. *Philos. Trans. R. Soc. London. B, Biol. Sci.* **281**: 277–294. doi:10.1098/rstb.1977.0140
- Moore, K. A., R. L. Wetzel, and R. J. Orth. 1997. Seasonal pulses of turbidity and their relations to eelgrass (*Zostera marina* L.) survival in an estuary. **215**: 115–134.
- Nagelkerken, I., G. van der Velde, M. W. Gorissen, G. J. Meijer, T. Van't Hof, and C. den Hartog. 2000. Importance of Mangroves, Seagrass Beds and the Shallow Coral Reef as a Nursery for Important Coral Reef Fishes, Using a Visual Census Technique. *Estuar. Coast. Shelf Sci.* **51**: 31–44. doi:10.1006/ecss.2000.0617
- Orth, R. J., M. L. Luckenbach, S. R. Marion, K. A. Moore, and D. J. Wilcox. 2006. Seagrass recovery in the Delmarva Coastal Bays, USA. *Aquat. Bot.* **84**: 26–36. doi:10.1016/j.aquabot.2005.07.007
- Orth, R. J., and K. J. McGlathery. 2012. Eelgrass recovery in the coastal bays of the Virginia Coast Reserve, USA. *Mar. Ecol. Prog. Ser.* **448**: 173–176. doi:10.3354/meps09596
- Ralph, P. J., M. J. Durako, S. Enríquez, C. J. Collier, and M. A. Doblin. 2007. Impact of light limitation on seagrasses. **350**: 176–193. doi:10.1016/j.jembe.2007.06.017
- Rasmusson, L. M., P. Buapet, R. George, M. Gullström, P. C. B. Gunnarsson, and M. Björk. 2020. Effects of temperature and hypoxia on respiration, photorespiration, and photosynthesis of seagrass leaves from contrasting temperature regimes. *ICES J. Mar. Sci.* doi:10.1093/icesjms/fsaa093
- Rheuban, J. E., P. Berg, and K. J. McGlathery. 2014. Multiple timescale processes drive ecosystem metabolism in eelgrass (*Zostera marina*) meadows. *Mar. Ecol. Prog. Ser.* **507**: 1–13. doi:10.3354/meps10843
- Saunders, M. I., S. Atkinson, C. J. Klein, T. Weber, and H. P. Possingham. 2017. Increased sediment loads cause non-linear decreases in seagrass suitable habitat extent R. Coleman [ed.]. *PLoS One* **12**: e0187284. doi:10.1371/journal.pone.0187284
- Smale, D. A., T. Wernberg, E. C. J. Oliver, and others. 2019. Marine heatwaves threaten global biodiversity and the provision of ecosystem services. *Nat. Clim. Chang.* **9**: 306–312. doi:10.1038/s41558-019-0412-1
- Staehr, P. A., and J. Borum. 2011. Seasonal acclimation in metabolism reduces light requirements of eelgrass (*Zostera marina*). *J. Exp. Mar. Bio. Ecol.* **407**: 139–146. doi:10.1016/j.jembe.2011.05.031
- Stocker, B. D., J. Zscheischler, T. F. Keenan, I. C. Prentice, J. Peñuelas, and S. I. Seneviratne. 2018. Quantifying soil moisture impacts on light use efficiency across biomes. *New Phytol.* **218**: 1430–1449. doi:10.1111/nph.15123

CONCLUSIONS

Seagrass meadows and other coastal ecosystems worldwide are increasingly threatened by climate change. While sea level rise and increased storm frequencies may lead to decreased light availability in the future (e.g. Lencart e Silva et al. 2013; Davis et al. 2016; Saunders et al. 2017), rising water temperatures and severe heating events such as marine heatwaves have already been shown to cause seagrass die-off events worldwide (e.g. Marbá and Duarte 2010; Arias-Ortiz et al. 2018). Based on a recent high-temperature-related eelgrass die-off event at the Virginia Coast Reserve (VCR) and long-term in situ data collected via innovative technology, this dissertation provides insights into how such mortality events affect ecosystem function (carbon sequestration, metabolism) in the long-term, and how thermal stress can lead to such events.

Encompassing the work of past students and postdocs (Hume et al. 2011; Rheuban et al. 2014; Berg et al. 2019), this dissertation represents the largest dataset for in situ seagrass ecosystem metabolism measured by aquatic eddy covariance (AEC). On average, seagrass metabolism was found to be balanced over the 11-year measurement period analyzed in Chapter 1. The die-off event shifted ecosystem metabolism from balanced to net heterotrophy when it occurred in 2015, then to net autotrophy as the meadow recovered. These results highlighted the resilience of seagrass metabolism to disturbance events on an interannual scale. Chapter 1 highlighted the benefits of frequent and long-term measurements of in situ seagrass metabolism. Our measurements not only allowed us to capture a seagrass die-off event, they demonstrated the highly dynamic and variable nature of seagrass ecosystem metabolism. With day-to-day variability as high as seasonal variability, we highlighted the importance of using frequent measurements throughout the year and under a wide range of environmental conditions to correctly estimate trophic status in seagrass meadows.

This dissertation also provides a new framework for quantifying heat stress in marine ecosystems. Using a modeling approach on our measured oxygen fluxes, we were able to determine, for the first time, the temperature threshold above which seagrass metabolism was negatively affected in our study system (28.6°C, Chapter 2). While this approach required a lot of data to tease out the effects of high temperature compared studies relying on lab experiments (e.g. Marsh et al. 1986; Nejrup and Pedersen 2008; Rasmusson et al. 2020), the threshold we derived was based on in situ measurements of seagrass metabolism at the ecosystem scale. The AEC

technique includes all components of seagrass ecosystems (other autotrophs, below-ground biomass, heterotrophic communities) and captures a wide range of unaltered environmental conditions. Therefore, our results are more likely to be ecologically relevant in addressing questions about seagrass ecosystem response to changes in environmental conditions under future climate change scenarios. The two thermal stress metrics developed in Chapter 3—heating and cooling degree-hours (HDH and CDH, respectively)—were also useful in quantifying thermal stress in our study system based on its physiological vulnerability (metabolic temperature threshold) and the intensity and duration of heating and cooling. Considering all these factors in quantifying heat stress may be more helpful in identifying potentially “harmful” heating events to seagrass ecosystems compared to traditional approaches that rely only on climatological data. We found that local hydrodynamics played an important role in seagrass thermal stress, with the cooling effect of incoming tides during warm events helped maintain high shoot density and shoot length at sites that were closer to the ocean inlet. In comparison, sites closer to the center of the meadow that did not benefit from this thermal relief saw shorter shoots and lower shoot densities. In terms of impacts of thermal stress, we found a 50% reduction in net primary production during afternoons where the temperature threshold was exceeded by $\sim 2^{\circ}\text{C}$ (Chapter 2), and a heat stress of $\sim 100\text{--}200^{\circ}\text{C}\text{-hours}$ during the growing season is enough to trigger a die-off event (Chapter 3). Being aware of these metrics, and calculating them for other ecosystems, may enable coastal scientists and managers to identify signs of heat stress before a collapse, determine the suitability of potential restoration and conservation sites, and better predict future ecosystem trajectories in response to climate change.

This dissertation demonstrates the vulnerability of the eelgrass meadows to future warming at the VCR. While the eelgrass in our study system recovered from the die-off event in 2015, and has shown some level of adaptability to changes in environmental conditions (e.g. light, as determined in Chapter 4), eelgrass at the VCR is already growing at the southern thermal boundary of the species’ geographic range (Moore and Jarvis 2008). Water temperatures at the VCR frequently exceed 28.6°C , and thermal stress is expected to increase as extreme heating events become more frequent and severe on top of background ocean warming (Oliver et al. 2019). Eelgrass is projected to shift $1.4\text{--}6.5^{\circ}\text{N}$ by 2100 under future warming scenarios (Wilson and Lotze 2019), which would signify complete loss of eelgrass in the VCR and Chesapeake Bay region, with a potential community shift to more heat tolerant seagrass species (Moreno-Marín et al. 2018;

Shields et al. 2019). The consequences of this are uncertain, and warrant continued long-term monitoring of temperature and benthic metabolism at the VCR, particularly during the summer.

Future studies in this system are encouraged to incorporate thermal stress and relief parameters in habitat suitability models for eelgrass at the VCR (Oreska et al. 2021), to maximize the extent of eelgrass in the region. In addition, estimates for thermal stress at the VCR throughout the rest of the century based on climatological projections of temperature—paired with further investigation into the effects of heat stress on ecosystem metabolism—could inform our expectations of future eelgrass cover in the area. Investigating the effects of sediment temperatures on eelgrass below-ground biomass would also enhance our understanding of seagrass plant response to warming.

Literature cited

- Arias-Ortiz, A., O. Serrano, P. Masqué, and others. 2018. A marine heatwave drives massive losses from the world's largest seagrass carbon stocks. *Nat. Clim. Chang.* doi:10.1038/s41558-018-0096-y
- Berg, P., M. L. Delgard, P. Polsenaere, K. J. McGlathery, S. C. Doney, and A. C. Berger. 2019. Dynamics of benthic metabolism, O₂, and pCO₂ in a temperate seagrass meadow. *Limnol. Oceanogr.* Ino.11236. doi:10.1002/Ino.11236
- Davis, T. R., D. Harasti, S. D. A. Smith, and B. P. Kelaher. 2016. Using modelling to predict impacts of sea level rise and increased turbidity on seagrass distributions in estuarine embayments. *Estuar. Coast. Shelf Sci.* **181**: 294–301. doi:10.1016/j.ecss.2016.09.005
- Hume, A. C., P. Berg, and K. J. McGlathery. 2011. Dissolved oxygen fluxes and ecosystem metabolism in an eelgrass (*Zostera marina*) meadow measured with the eddy correlation technique. *Limnol. Oceanogr.* **56**: 86–96. doi:10.4319/lo.2011.56.1.0086
- Lencart e Silva, J. D., A. Azevedo, A. I. Lillebø, and J. M. Dias. 2013. Turbidity under changing physical forcing over two contrasting locations of seagrass meadows. *J. Coast. Res.* **165**: 2023–2028. doi:10.2112/si65-342.1
- Marbá, N., and C. M. Duarte. 2010. Mediterranean warming triggers seagrass (*Posidonia oceanica*) shoot mortality. *Glob. Chang. Biol.* **16**: 2366–2375. doi:10.1111/j.1365-2486.2009.02130.x
- Marsh, J. a, W. C. Dennison, R. S. Alberte, and S. Alberte. 1986. Effects of temperature on photosynthesis and respiration in eelgrass (*Zostera marina* L.). *J. Exp. Mar. Bio. Ecol.* **101**: 257–267. doi:10.1016/0022-0981(86)90267-4
- Moore, K. A., and J. C. Jarvis. 2008. Eelgrass Diebacks in the Lower Chesapeake Bay : Implications for Long-term Persistence. *J. Coast. Res.* **55**: 135–147. doi:10.2112/SI55-014.acteristics
- Moreno-Marín, F., F. G. Brun, and M. F. Pedersen. 2018. Additive response to multiple environmental stressors in the seagrass *Zostera marina* L. *Limnol. Oceanogr.* **63**: 1528–1544. doi:10.1002/Ino.10789

- Nejrup, L. B., and M. F. Pedersen. 2008. Effects of salinity and water temperature on the ecological performance of *Zostera marina*. *Aquat. Bot.* **88**: 239–246. doi:10.1016/j.aquabot.2007.10.006
- Oliver, E. C. J., M. T. Burrows, M. G. Donat, and others. 2019. Projected Marine Heatwaves in the 21st Century and the Potential for Ecological Impact. *Front. Mar. Sci.* **6**: 1–12. doi:10.3389/fmars.2019.00734
- Rasmusson, L. M., P. Buapet, R. George, M. Gullström, P. C. B. Gunnarsson, and M. Björk. 2020. Effects of temperature and hypoxia on respiration, photorespiration, and photosynthesis of seagrass leaves from contrasting temperature regimes. *ICES J. Mar. Sci.* doi:10.1093/icesjms/fsaa093
- Rheuban, J. E., P. Berg, and K. J. McGlathery. 2014. Multiple timescale processes drive ecosystem metabolism in eelgrass (*Zostera marina*) meadows. *Mar. Ecol. Prog. Ser.* **507**: 1–13. doi:10.3354/meps10843
- Saunders, M. I., S. Atkinson, C. J. Klein, T. Weber, and H. P. Possingham. 2017. Increased sediment loads cause non-linear decreases in seagrass suitable habitat extent R. Coleman [ed.]. *PLoS One* **12**: e0187284. doi:10.1371/journal.pone.0187284
- Shields, E. C., D. Parrish, and K. A. Moore. 2019. Short-Term Temperature Stress Results in Seagrass Community Shift in a Temperate Estuary. *Estuaries and Coasts* **42**: 755–764. doi:10.1007/s12237-019-00517-1
- Wilson, K., and H. K. Lotze. 2019. Projected range shift of eelgrass *Zostera marina* in the Northwest Atlantic with climate change. *Mar. Ecol. Prog. Ser.* **620**: 47–62. doi:10.3354/meps12973

FUNDING ACKNOWLEDGMENT

Support for this study was provided by the University of Virginia, the National Science Foundation through grants to Peter Berg from Chemical Oceanography (OCE-1851424) and Ocean Technology and Interdisciplinary Coordination (OCE-1824144), from the Division of Environmental Biology to the Virginia Coast Reserve Long Term Ecological Research Program (DEB-1237733 and DEB-1832221).